Universitetet i Stavanger

FACULTY OF SCIENCE AND TECHNOLOGY

MASTER'S THESIS

Study programme/specialisation: Mechanical and Structural Engineering and Materials Science / Civil Engineering Structures	Spring semester, 2019 Open
Author: Stina Selstø Greve	
Programme coordinator: Sudath Siriwardane Supervisor(s): Samindi Samarakoon Arnt Egil Rørtvedt (external), Statens Vegvesen	
Title of master's thesis: Analysis of post-tensioned concrete bridge constructed using incremental launching method	
Credits: 30	
Keywords: Concrete Prestressing Post-tensioning Box-girder bridge Bridge Incremental launching method	Number of pages: 92 + Attachments: 75 Stavanger,14.06.2019

PREFACE

This thesis is written as a finishing part of a two-year master´s degree in constructions and materials at the University of Stavanger. The thesis was carried out during the spring of 2019 and represent 30 study points.

I would like to give thanks to my main supervisor, Associate Professor Samindi Samarakoon, for her guidance and invaluable help during this process. Furthermore, I would like to thank my external supervisor at the Norwegian public road administration, Arnt Egil Rørtvedt, for helping me formulate the topic question and for his help especially in regard to the software NovaFrame.

Finally, I would like to thank my family for all the support during my studies and all my friends here at UiS whom have made these 5 years the absolute best!

Stina Selstø Greve

Stavanger, 14.06.2019

ABSTRACT

The aim of this thesis is to gain a broader understanding of bridge construction methods and to analyse a bridge constructed in stages. To do so, a model is created for analyses in the frame software NovaFrame.

The bridge which is to be analysed in this thesis is Bagn bridge, a three-span bridge which is already constructed using the movable scaffolding system. In cooperation with the Norwegian public road administration, the bridge is to be analysed by using the incremental launching method (ILM).

First, a literature review is performed to collect relevant information about the project, relevant regulations, materials, construction method and methods for analysis.

When using ILM, the bridge is casted in segments in a casting yard at one end of the bridge and is launched after the concrete has reached satisfying strength. Due to the fact that the casting is done in a casting yard and that the bridge is launched over pre-casted piers, this method has little effect on the surrounding environments. This makes this method highly efficient when casting over for example highways and railroads.

One of the mayor parts of this thesis was to create analytical models in NovaFrame. The models were based on detail drawings handed out by the Norwegian Public Road Administration (SVV) but were adjusted to be suitable for ILM. Two models were made, one model for the bridge during launching and one model for the final bridge construction. The reason for this is to have full control of loads and load combinations, as the launching stages requires many load-cases.

22 centric pre-stressing tendons were used during launching, whereas 14 were placed in the top flange of the box girder and 8 were placed in the bottom. Two pre-stressing tendons were placed in each web to be post-tensioned after the final launch.

Capacity controls were performed at ultimate limit state (ULS) and serviceability limit state (SLS) for both the launching stages and the final construction. Simplified load combinations were used for the launching stages, as most of the variable loads were neglected due to the fact that most of the variable loads would have small effects on the structure.

Results from calculations at ULS for the launching stages showed that the predefined number of prestressing tendons were sufficient with additional reinforcement over supports. Additional shear reinforcement was also necessary. At SLS, the section was found to be uncracked. Stress limitations were neglected for the launching stages. The stress limitations are performed to at

construction stages to limit cracks and large deformations due to creep. As the stress limitations are valid for cracks which are smaller than the allowable cracks during constriction, they are not considered relevant during launching.

For the final construction, more load cases were introduced. Variable loads such as wind, traffic and creep were included in this analysis. For ULS, calculations showed that excessive reinforcement was needed in span. From shear calculations, additional shear reinforcement was required. A more excessive control at SLS were performed, and in addition to the crack control, decompression, stress limitation and deflection control were done. The analysis of cracked section proved that the section was to be considered as uncracked. Therefore, stresses taken directly from NovaFrame were sufficient for further analysis. Decompressions gave satisfying results, but for the stress limitations for quasi permanent load combination showed that extra reinforcement over support 2 were necessary.

Resulting additional reinforcement from calculations ULS for both launching stages and the final construction is represented in Table 0. As one can see from Table 0, the reinforcement needed for the final construction is sufficient for the launching stages as well.

Table 0 Results - Reinforcement

Launching stages		
	Span	Support
Longitudinal reinforcement	15Ø25c330	-
Shear reinforcement	8Ø12c250	
Final construction		
Longitudinal reinforcement	**33Ø25s150**	**-**
Shear reinforcement	**12Ø12c220**	

INNHOLDSFORTEGNELSE

PREFACE ..... **I**

ABSTRACT ..... **II**

LIST OF FIGURES ..... **VII**

LIST OF TABLES ..... **IX**

ABBREVIATIONS ..... **XI**

1 INTRODUCTION **1**

1.1 BACKGROUND 1

1.2 AIM AND SCOPE 2

1.3 LIMITATIONS 2

1.4 BRIEF OVERVIEW OF THE PROJECT 3

2 LITERATURE REVIEW **4**

2.1 REGULATIONS 4

2.2 PARTS OF BRIDGES 4

2.2.1 Substructure *4*

2.2.2 Superstructure *5*

2.3 INCREMENTAL LAUNCHING METHOD (ILM) 6

2.3.1 General principles *6*

2.3.2 Advantages and inconveniences of ILM *8*

2.4 PRE-STRESSING CONCRETE 10

2.4.1 Post-tensioned concrete *10*

2.4.2 Load balancing *12*

2.4.3 Tendon profile *16*

2.5 LOSS OF PRESTRESSING FORCE 17

2.5.1 Intermediate loss of prestress *17*

2.5.2 Time-dependent losses *20*

2.6 LOAD COMBINATIONS 21

2.6.1 Ultimate limit state *21*

2.6.2 Serviceability Limit State *23*

3 MATERIAL PROPERTIES **25**

3.1 CONCRETE 25

3.1.1 Compressive strength *25*

3.1.2 Tensile strength *27*

3.1.3 Deformational properties *28*

3.1.4 Material parameters *30*

3.2 PRESTRESSING STEEL 31

3.2.1 Strength and ductility ... *32*
3.2.2 Elastic modulus ... *33*
3.2.3 Steel relaxation ... *33*
3.2.4 Material properties ... *34*
3.3 STEEL REINFORCEMENT ... 35
3.3.1 Strength and ductility ... *35*
3.3.2 Elastic modulus ... *35*
3.3.3 Material properties ... *36*
3.4 DURABILITY AND COVER TO REINFORCEMENT ... 37
4 MODELLING IN NOVAFRAME ... 39
4.1 COORDINATE SYSTEM ... 39
4.2 REFERENCE LINES AND CROSS-SECTION ... 40
4.3 NODES AND ELEMENTS AND BOUNDARY CONDITIONS ... 40
4.4 MODELS ... 41
4.5 LOADS ... 41
4.5.1 Permanent loads ... *41*
4.5.2 Variable loads ... *42*
4.5.3 Creep ... *44*
4.5.4 Shrinkage ... *44*
4.6 PRESTRESSING ... 45
4.6.1 Prestressing during launching ... *45*
4.6.2 Prestressing for final construction ... *47*
4.6.3 Loss of prestresses ... *53*
4.7 VERIFICATION OF MODEL IN NOVAFRAME ... 55
4.7.1 Control of cross-sectional parameters ... *55*
4.7.2 Control of self-weight ... *56*
4.7.3 Summary ... *57*
5 ANALYSIS OF STAGE CONSTRUCTION ... 58
5.1 ULS ... 60
5.1.1 Ultimate moment capacity ... *60*
5.1.2 Shear resistance ... *65*
5.2 SLS ... 68
5.2.1 Crack control ... *69*
6 ANALYSIS OF FINAL CONSTRUCTION ... 73
6.1 ULS ... 73
6.1.1 Design forces in ULS ... *73*
6.1.2 Ultimate moment capacity ... *74*
6.1.3 Shear resistance ... *76*

6.2 SLS 78
6.2.1 Design moments in SLS 78
6.2.2 Crack control 79
6.2.3 Stress limitations 81
6.27.2 Deflection control 84
7 DISCUSSION AND CONCLUSION 85
8 REFERENCE LIST 90
9 APPENDIX 92

LIST OF FIGURES

Figure 1.1 3D-illustration of bridge over Begna [1] 3

Figure 2.1 Illustration of Bagn bridge substructure (dimensions in meters) 4

Figure 2.2 Different geometries of bridge superstructure [5] 5

Figure 2.3 Typical box-girder cross-section [5] 6

Figure 2.4 Evolution of ILM 7

Figure 2.5 General arrangement of ILM [7] 8

Figure 2.6 Lifting jack 8

Figure 2.7 Post-tensioning procedure [11] 11

Figure 2.8 Load balancing design of prestressed concrete [12] 12

Figure 2.9 Equivalent loads from pre-stressing [10] 13

Figure 2.10 Anchoring of prestressing steel [10] 14

Figure 2.11 Determination of secondary moment 15

Figure 2.12 Tendon profile for both launching and final state 16

Figure 2.13 Losses of prestress in the tendons [11] 18

Figure 3.1 Strength and deformation characteristics for concrete [11] 27

Figure 3.2 Idealised stress-strain relationship for concrete in uniaxial compression [11] 28

Figure 3.3 Cross-section of a standard and drawn strand [15] 31

Figure 3.4 Stress-strain curve for prestressing steel [13] 32

Figure 3.5 Stress-strain diagrams for typical reinforcing steel [11] 35

Figure 3.6 Minimum clear spacing between ducts 38

Figure 4.1 Local and global coordinate system in NovaFrame 39

Figure 4.2 Cross-section in NovaFrame (dimensions are given in mm) 40

Figure 4.3 Nodes and boundary conditions for the final bridge model in NovaFrame 40

Figure 4.4 Bridge model 1 41

Figure 4.5 Arrangement of pre-stressing tendons during launching (Dimensions given in mm) 46
Figure 4.6 Arrangement of tendons for the final construction (Dimensions given in mm) 47
Figure 4.7 Idealized tendon profile for Bagn bridge 47
Figure 4.8 Realistic tendon profile for span 1-2 48
Figure 4.9 Realistic tendon profile for span 2-3 50
Figure 4.10 Realistic tendon profile for span 3-4 51
Figure 4.11 Explanation of tendon curve types in NovaFrame [16] 52
Figure 4.12 Simplified cross-section (Dimensions given in mm) 55
Figure 4.13 Static model of Bagn bridge (Dimensions given in m) 56
Figure 5.1 Illustration of selected models 58
Figure 5.2 Variation of moments for all 136 models at distance x [m] from support 1 59
Figure 5.3 Cross-section with prestressing steel in tensile zone [10] 60
Figure 5.4 Strains at fracture for balanced prestressed cross-section [10] 62
Figure 5.5 (A) Tendon layout and (B) moment diagram for model 62 62
Figure 5.6 (A) Tendon layout and (B) Moment diagram for model 92 64
Figure 5.7 Shear force for model 93 65
Figure 5.8 Limiting values of w_{max}(mm) [13] 69
Figure 5.9 Cross-section with moment and axial force [8] 70
Figure 5.10 Total moment due to prestress for model 92 71
Figure 6.1 Moment diagram for ULS 73
Figure 6.2 Shear force diagram for ULS 73
Figure 6.3 Moment diagram for SLS 78
Figure 6.4 Moment diagram for characteristic load combination 82
Figure 6.5 Moment diagram for quasi-permanent load combination 82

LIST OF TABLES

Table 2.1 Load combinations at ULS (STR) 22

Table 2.2 Load combinations in SLS 24

Table 3.1 Material properties for concrete 30

Table 3.2 Material properties for prestressing steel 34

Table 3.3 Material properties for reinforcement 36

Table 3.4 Construction measurements for steel reinforcement 36

Table 3.5 Exposure classes [13] 37

Table 3.6 Chosen exposure classes and corresponding cover values 38

Table 4.1 Traffic loads in NovaFrame 42

Table 4.2 Wind loads 42

Table 4.3 Temperature loads in NovaFrame 43

Table 4.4 Tendon geometry in N-direction 52

Table 4.5 Loss of prestress due to creep – FINAL CONSTRUCTION 53

Table 4.6 Loss of prestress due to creep – LAUNCHING STAGES 54

Table 4.7 Verification of cross-sectional parameters in NovaFrame 55

Table 4.8 Verification of moments in NovaFrame 56

Table 5.1 ULS load combinations - during launching 60

Table 5.2 Load combination at SLS - Launching stages 68

Table 5.3 Stresses - control of cracked section 72

Table 6.1 Moments in ULS 73

Table 6.2 Maximum moments for load combinations at SLS 78

Table 6.3 Stresses - control of cracked section 79

Table 6.4 Results from decompression 80

Table 6.5 Stresses in the cross-section - Characteristic 83

Table 6.6 Stresses in the cross-section - Quasi permanent 83

Table 6.7 Deflections 84

Table 7.1 Results – ULS – Launching stages..... 86

Table 7.2 Results – SLS – Constriction stages..... 87

Table 7.3 Results – ULS – Final construction 87

Table 7.4 Results – SLS – Final construction 89

ABBREVIATIONS

CoG	Centre of gravity
EC0	Eurokode: Grunnlag for prosjektering av konstruksjoner
EC1-2	Eurokode 1: Laster på konstruksjoner. Del 2: Trafikklast på bruer.
EC1-4	Eurokode 1: Laster på konstruksjoner. Del 1-4: Allmenne laster, Vindlaster
EC1-5	Eurokode 1: Laster på konstruksjoner. Del 1-5: Allmenne laster, Termiske påvirkninger
EC2	Eurocode 2: Design of concrete structures. Part 1-1 General rules and rules for buildings
EC2-2	Eurokode 2: Prosjektering av betongkonstruksjoner, Del 2: Bruer
ILM	Incremental launching method
N400	Håndbok N400 *Bruprosjektering*
SVV	Statens Vegvesen (Norwegian public road administration)
UF	Upper flange
LF	Lower flange

1 INTRODUCTION

1.1 BACKGROUND

This thesis aims to gain a broader understanding of bridge construction methods and to analyse a bridge which is constructed in stages. All humans depend on roads to be able to move around, and bridges are an important part of this. As more and more bridges are built, the need for quick, economical and safe solutions are crucial.

To optimize the construction of the bridge, the right construction method has to be selected. The incremental launching method (ILM) is a construction method that is more and more used around the world for multi-span bridges. Due to the rapid increase of this method being used, it is important to gain as much information and understanding of the method.

This thesis was formulated in cooperation with the Norwegian Public Road Administration (SVV). As ILM is a method that have been used relatively little in Norway, the need for research is crucial to make good decisions. This thesis is written as a cooperation with SVV to gain more knowledge about the method, and to provide analyses and calculations that may prove useful in later projects.

The analysis in this thesis is done for Bagn bridge, a bridge which is already built using the movable scaffolding system. The reason why this bridge is used is that even though these two construction methods are different, they cover the same span lengths. Therefore, this analysis may be used in the future to compare with the already built bridge in regard to the amount of concrete that is used, the amount of reinforcement and to compare construction costs. In reality, Bagn bridge is not really suitable for ILM as the total length is only 138 meters. As will be explained later in this thesis, the recommended lengths for using ILM are 200 to 1000 meters. This is due to economic reasons, as this method requires expensive equipment.

1.2 AIM AND SCOPE

During design and analysis process of bridges, initially the bridges are designed to carry all external loads. When the construction method is chosen for a bridge, it is important to carry out an analysis to determine necessity of extra reinforcement or pre-stressing tendons. The aim of this thesis is to determine the required prestressing when using ILM. Due to the launching of the bridge, excessive prestressing is required. A detailed model of the chosen bridge is created which is too be analysed and results are to be controlled for ULS and SLS to determine the required prestressing in both launching stages and in the final bridge construction.

1.3 LIMITATIONS

Bagn bridge has, as shown in Appendix A, a curvature with a radius of 750 meters. XX states that bridges which has a central angle smaller than or equal to 12 degrees may be designed as a straight bridge. Further, the limit in equation 1.1 is given [1].

$$\frac{L}{R} \leq 0{,}2 \tag{1.1}$$

With the largest span being 57 meters long, L/R = 0,076 and the bridge may therefore be considered as a straight bridge.

Bagn bridge, as illustrated in Appendix A, designed with a sloped top flange in the box-girder. As this is not relevant for the analysis of ILM, the cross-section is simplified by using a horizontal top flange.

For ILM, one has to consider the friction forces caused when the superstructure is launched over the piers. To counteract this force, bracings are used. The forces caused by the launching to the columns are not relevant for this thesis, as the focus is on the prestressing of the superstructure and are not taken into account in further calculations. All analysis of columns are neglected.

1.4 BRIEF OVERVIEW OF THE PROJECT

Bagn-Bjørgo is a sub-project in the development of the new E16 going through Valdres. This road is a part of the stretch between Bergen and Oslo, and the aim is to improve the traffic safety. The development of this road includes four bridges, among them Bagn bridge [1].

The existing bridge over the river Begna, including piers and foundations, is to be demolished and replaced by a new bridge. The new bridge will be 138 meters long. The piers are placed on land to minimize the effect on the structure from the river water, yet close to the river to decrease the span length. As shown in Figure 1.1, the bridge continues into a tunnel [1].

Figure 1.1 3D-illustration of bridge over Begna [1]

2 LITERATURE REVIEW

2.1 REGULATIONS

All construction work will in some way influence the communities and is because of this regulated by laws and public regulations. The main regulating law is The Planning and Building Act which is followed by the regulations on technical requirements for construction/building works.

When it comes to the construction itself, this should be done according to *Norwegian Standard* (NS). This includes standards for products, design and execution. For concrete bridges, EC2 and EC2-2 is used [2].

N400 is used when constructing bridges, ferry piers and other load bearing structures to supplement the Eurocode with provisions for calculations and design. This manual consists of requirements for reliability and strength, durability, traffic safety, navigability and efficient maintenance [3].

2.2 PARTS OF BRIDGES

When defining the geometry of bridges, one differs between substructure and superstructure.

2.2.1 SUBSTRUCTURE

The substructure is the parts of the bridge below the bearing and includes piers, bearings, abutments, caps, wing walls and foundation structures. The usage of the substructure is to support the superstructure and transfer loads from the structure to the foundation [4].

For Bagn bridge, the substructure consists of 2 piers, as shown in Figure 2.1. Each pier is placed on land to avoid effect from the river, and the free height is circa 5 m [1]. The total length of the bridge is 138 meter and it is divided into three spans. Lengths of the spans and pier axes are also shown in Figure 2.1.

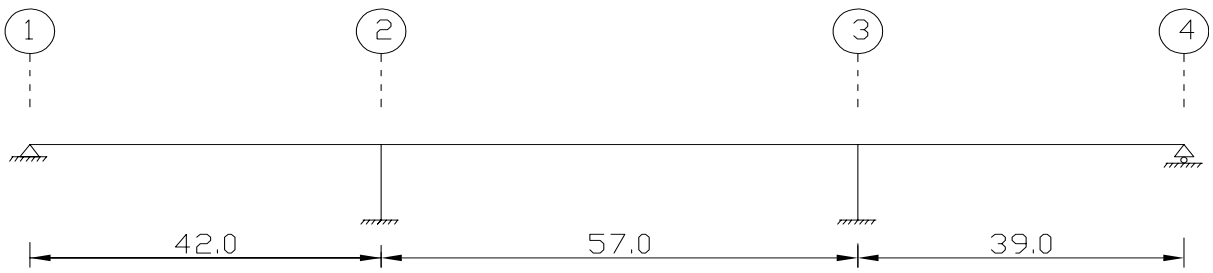

Figure 2.1 Illustration of Bagn bridge substructure (dimensions in meters)

2.2.2 SUPERSTRUCTURE

The superstructure of a bridge represents the parts of the bridge above the bearings, and includes deck, girder, truss, etc. Each part of the superstructure has a function in the final product, the bridge. The deck is the part that directly carries the traffic while other parts transmits passing loads to the substructure.

Superstructure may have different geometries, as shown in Figure 2.2. A box girder system, as shown in Figure 2.3, is used for Bagn bridge. A box girder bridge is defined as when the main load bearing system is formed as one or multiple box cross-sections.

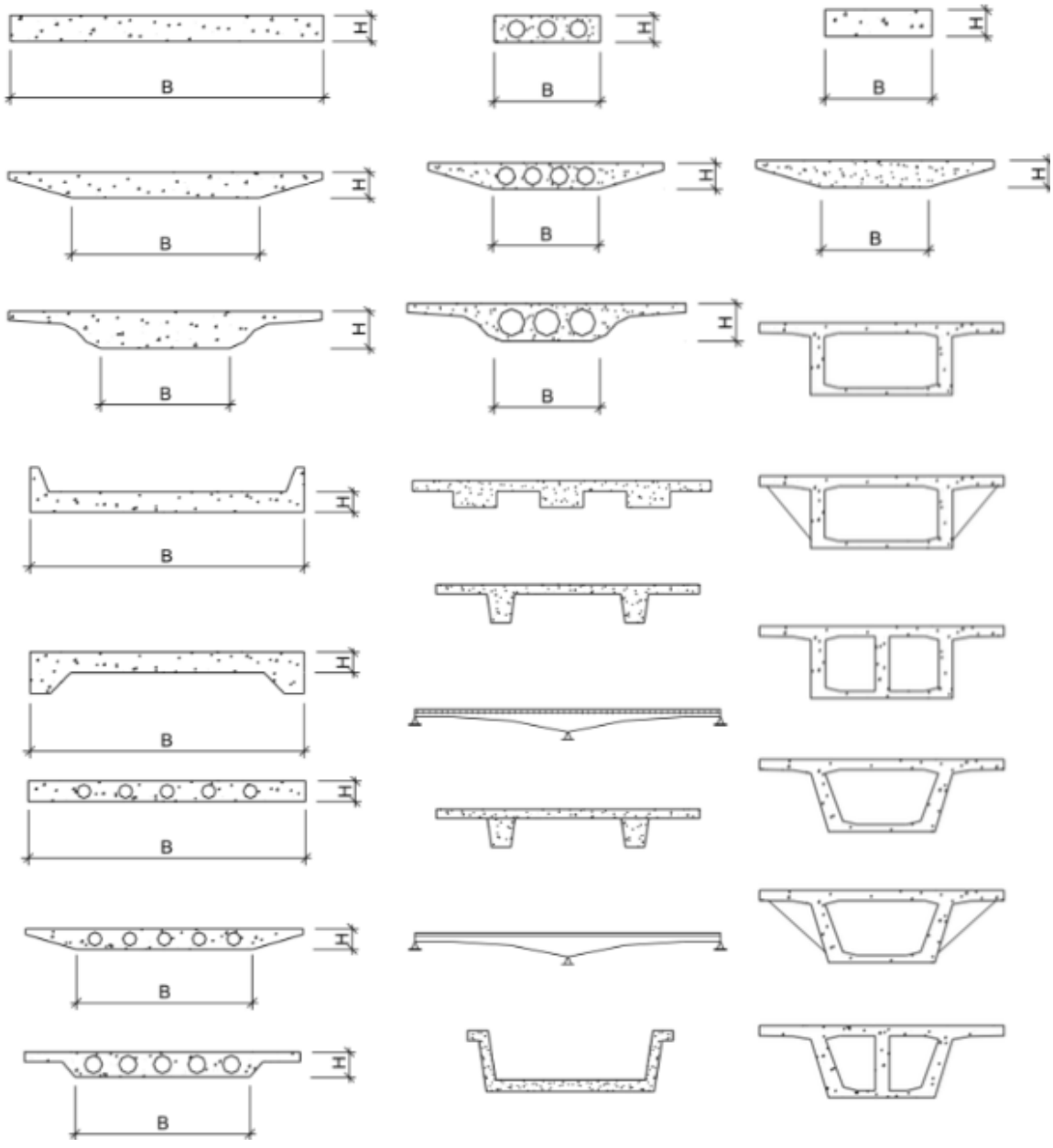

Figure 2.2 Different geometries of bridge superstructure [5]

Box-girder sections, as shown in Figure 2.3 usually consists of top deck, vertical web and bottom slab. Both top and bottom flanges are able to resist stress, which means that this cross-section can sustain positive and negative bending moments. Because of its relatively large rigidity in both bending and torsion, this box section is widely used for continuous and cantilever bridges [4].

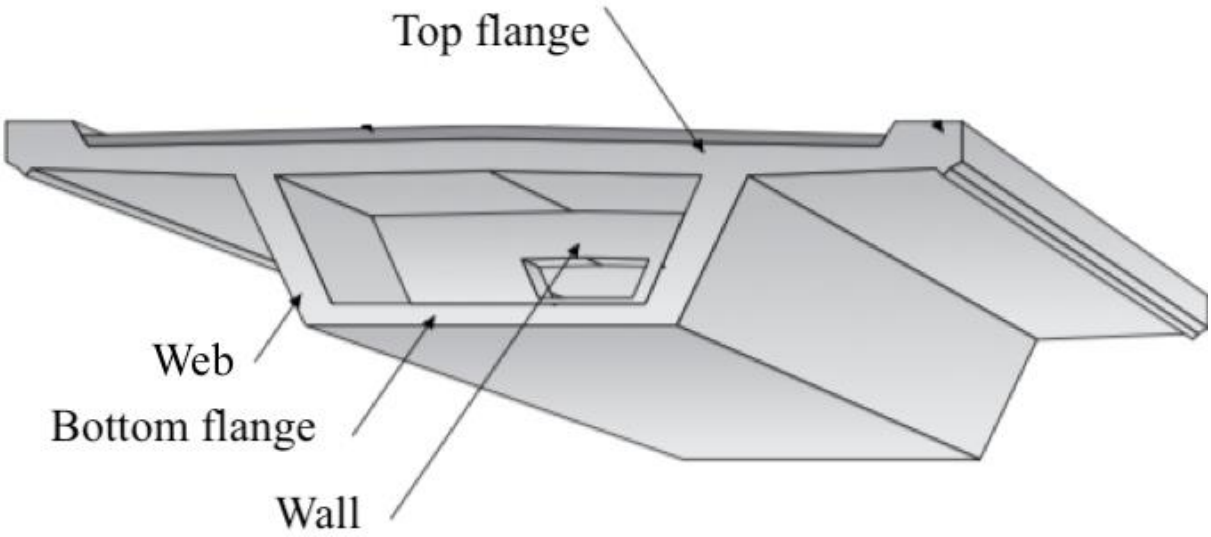

Figure 2.3 Typical box-girder cross-section [5]

2.3 INCREMENTAL LAUNCHING METHOD (ILM)

ILM has been used for many years to construct multi-span bridges. As is shown in Figure 2.4, this method was first used in the 1960´s and has since then been used on approximately 1000 bridges around the world. ILM is most suited for bridges with box girder sections. Also, it is required that the bridge is either straight or with constant curvature. The smallest radius which ILM is suitable for is set to R=300m.

2.3.1 GENERAL PRINCIPLES

Figure 2.5 shows the general arrangement of the method. At one side of the bridge, the casting yard is placed. It is here that the bridge segments are casted. Each segment is casted against the former segment, and this way creates a monolithic superstructure. As each segment is casted and connected to the former, they are launched forward using hydraulic jacks [6].

Göhler and Pearson states that the aim of ILM is to finish each segment within one week, the so-called weekly cycle, adopting as large segment length as possible. According to Göhler and Pearson, lengths up to 30 m is preferred. Segments often have a length of half of the span length.

This way, the same routines repeats themselves each week, and the production becomes a habit. The hardening of the concrete happens during the weekend and is therefore included in the weekly cycle [6]. From experience this seems to be a bit short of time, according to SVV, as the box-girder is casted in two sections; bottom flange and webs at first, then the top flange later. The concrete should stay in the scaffolding up to three days for satisfying curing conditions. The strength of the concrete shall also reach satisfying value before the prestressing. Therefore, a two-week cycle is set to be more realistic.

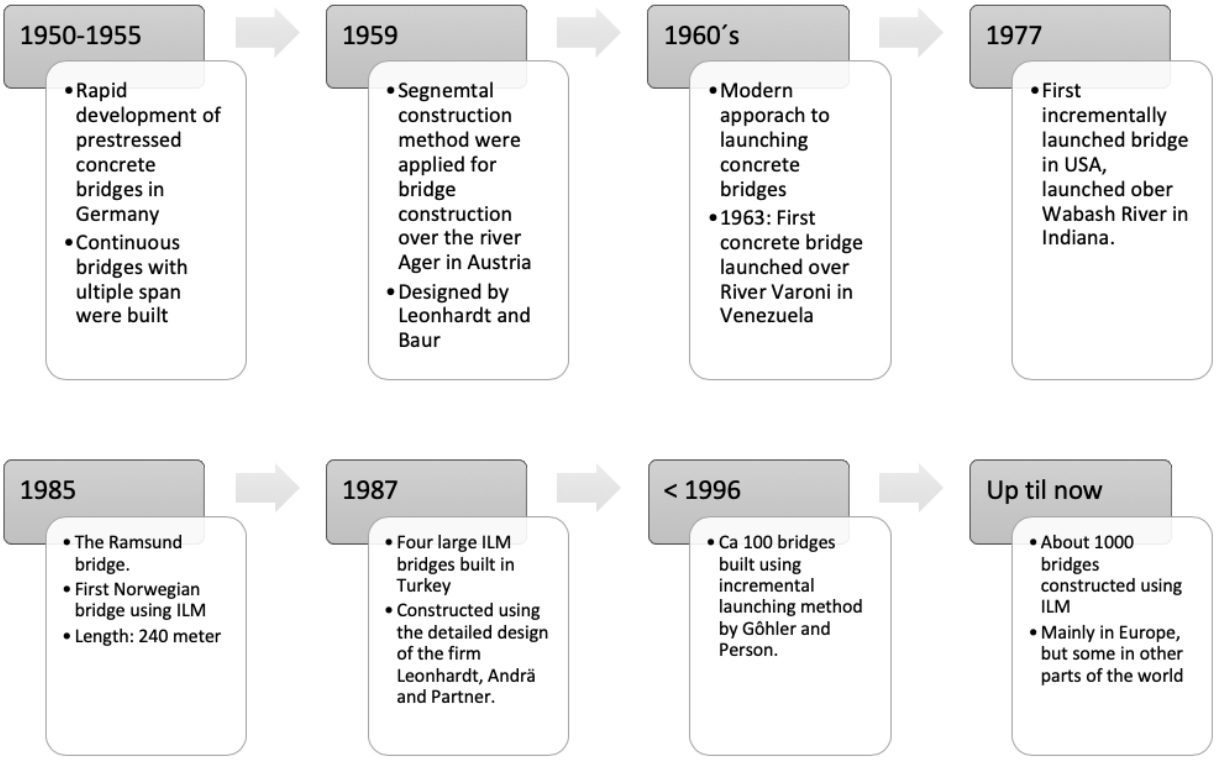

Figure 2.4 Evolution of ILM

2.3.1.1 Launching nose

A launching nose is attached in front of the first segment to reduce the high moments caused by the fact that the superstructure is a cantilever during the launching of the bridge, as shown in Figure 2.5 [6]. When considering the economical aspect of the project, the launching nose is considered as one of the largest investments besides the launching equipment and the establishment of the casting yard. Therefore, the design should allow for it to be reused without too much conversion cost [6].

For the length of the nose to be optimised, it is set to be 60% of the decisive span [6]. For Bagn bridge, this will result in a launching nose of L = 57m * 0,6 = 34,2 m. As a simplification, the launching nose used in the model is taken from another project from SVV with L=33m.

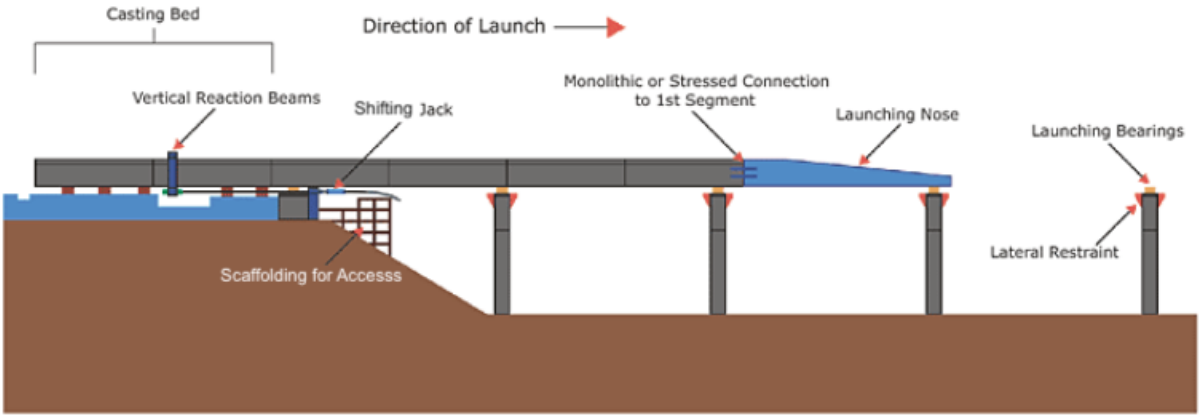

Figure 2.5 General arrangement of ILM [7]

2.3.1.2 Hydraulic device

The hydraulic device, as shown in Figure 2.6, is used to launch the bridge and consists of two launching devices which are placed below the web of the superstructure. The lifting jack raises the superstructure above the brake, as the shifting jack moves the superstructure forward. Then the lifting jack lowers the superstructure on the brake, and the shifting jacks retract to their starting position. This process is repeated till the entire bridge segment is launched. (R.SVV).

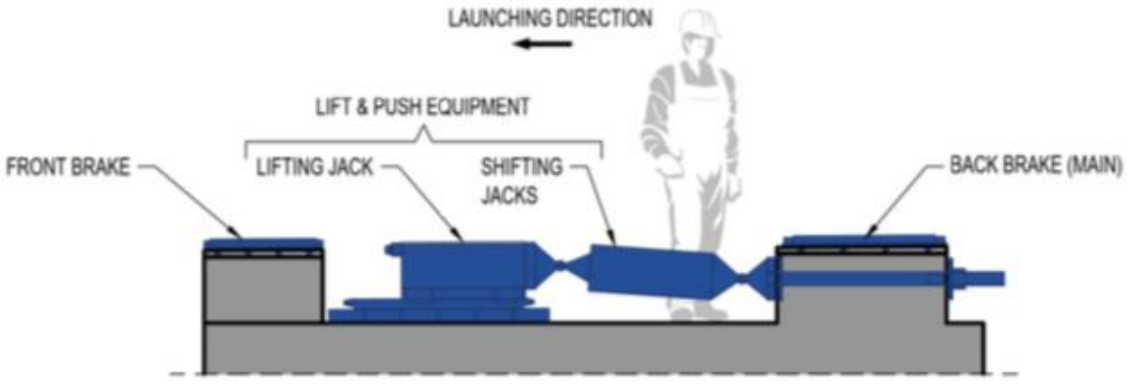

Figure 2.6 Lifting jack

2.3.2 ADVANTAGES AND INCONVENIENCES OF ILM

There are many advantages with the use of ILM. The most obvious one is the economic aspect. For bridges with lengths from 200 m to about 1000 m, this method is considered to be a good economical alternative. Another important factor when deciding between construction methods, are the effect on the surrounding environment. When using ILM, the launching can

be done over trafficked roads, railway lines, rivers and streets without interference whereas other construction methods would require traffic to stop [6].

When all the piers are constructed, there is no activity outside the casting yard. If the casting yard is located far from sensitive areas, it is possible to minimize the impact on the environment [6].

Other advantages are:

- Reinforcement- and casting work is performed in a temporary building, on land, which reduces the impact of varying weather conditions
- Secure progress, regardless of time of year
- Simpler logistics
- Positive repetition effect, the construction becomes a habit
- No traffic on the bridge during construction
- Good control of the geometry and position of the bridge during construction
- Limited construction time

There are also some disadvantages with using ILM. When casting, accuracy is crucial, and small errors in the construction of the factory will have severe consequences. Also, the bridge needs a certain size for this method to be economical advantageous. The launching nose is an expensive part and represents a significant cost which needs to be considered. By designing the nose such that it may be reused without too much conversion costs, one may look at the costs as an investment. But mostly, it is the extra reinforcement needed when launching the bridge that represents the highest costs. A 30% increase in the amount of prestressing reinforcement is required in MN, which is chargeable [9].

2.4 PRE-STRESSING CONCRETE

Since the end of the nineteenth century, reinforced concrete has been used as structural material. As concrete is a material which is low in tensile strength, steel bars are used to improve this characteristic by embedding them in the concrete. The steel bars will carry the internal tensile forces in the concrete.

One type of reinforced concrete is the so-called prestressed concrete, where there is an initial compressive load applied to the structure that to some extent will counteract the external loads [10]. This compressive load will help control or eliminate cracking by reducing and eliminating the internal tensile forces.

There are different methods of prestressing. For in-situ prestressed concrete constructions, post-tensioning is mostly used [11]. As Bagn bridge is to be constructed with ILM, which is an in-situ construction method, the focus in this thesis will be on post-tensioning.

2.4.1 POST-TENSIONED CONCRETE

When post-tensioning concrete members, steel tendons are tensioned after casting. When the formwork is in place, casting can begin. The concrete is casted around hollow ducts as shown in Figure 2.7(a). The steel ducts are fixed to the desired profile and are in most cases in place (unstressed) but can also be threaded through the duct at a later time [11].

The tendons are tensioned when the concrete is strong enough. This is done by jacking at one or both ends of the member. The stressed ends of the members are then anchored as shown in Figure 2.7(b)]. After anchoring the tendons, the ducts are injected with grout under pressure as Figure 2.7(c) shows [11].

2.4.1.1 Bonded and unbonded post-tensioned concrete

There are two ways of doing post-tensioned concrete, bonded or unbonded. As bonded post-tensioned concrete is mostly used for in-situ casted concrete bridges [10], this will be the focus in this thesis.

Bonded post-tensioned concrete is shown in Figure 2.7(c). Here there is a perfect bond between the concrete and the tendon. Bonded post-tensioned concrete is filled with grout while the tendon is under pressure. By establishing this bond, the changes in strain in both the tendons and the concrete at the same level in the cross-section will be the same. This way the post tensioned concrete will act as a pretensioned construction with the same difference in strain between concrete and reinforcement [11].

When tendons are bonded to the concrete, they will be able to control cracks and increase ultimate strength. The tendons will also withstand corrosion better than unbonded structures would [11].

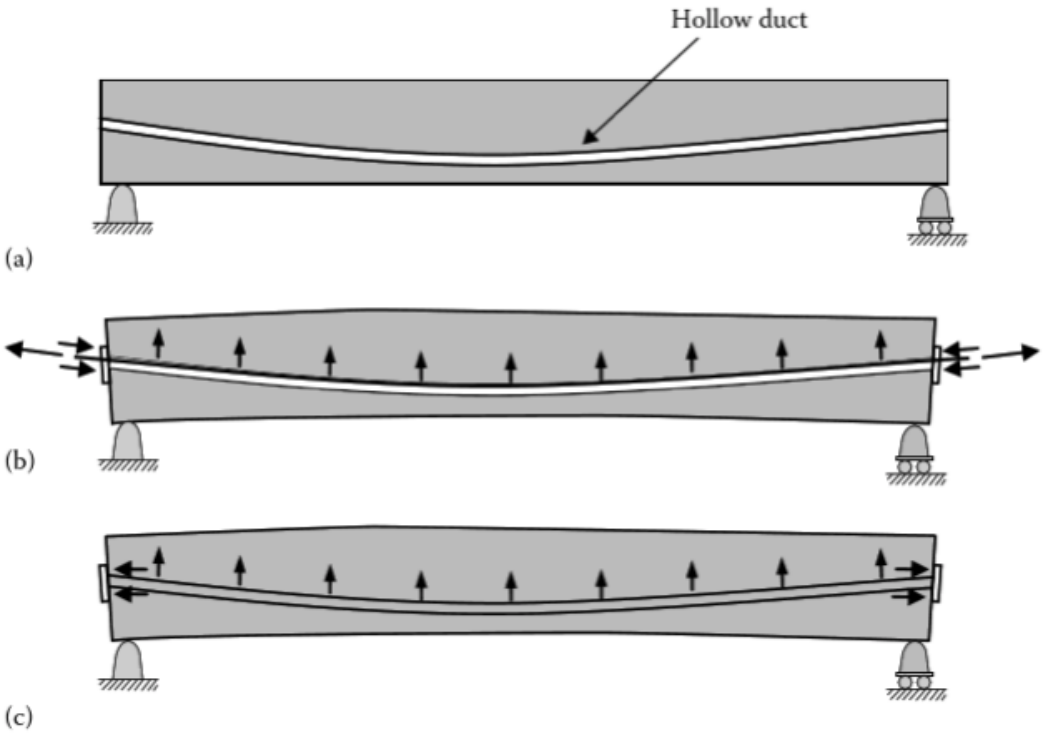

Figure 2.7 Post-tensioning procedure [11]

2.4.2 *LOAD BALANCING*

Load balancing method is a method which was introduced as a concept for design and analysis of prestressed concrete structures such as flat slabs and grid systems. This method looks at prestressing as a way to balance the loads acting on the structure. In other words, the prestressing in the steel balances or carries the loads in the concrete and the transverse loads that the structure carries are only subjected to axial stresses as shown in Figure 2.8 [12].

Load balancing is often used for post-tensioned beam design and has advantages such as being sufficient for statically in-determent structures, which the other two concepts are not [12].

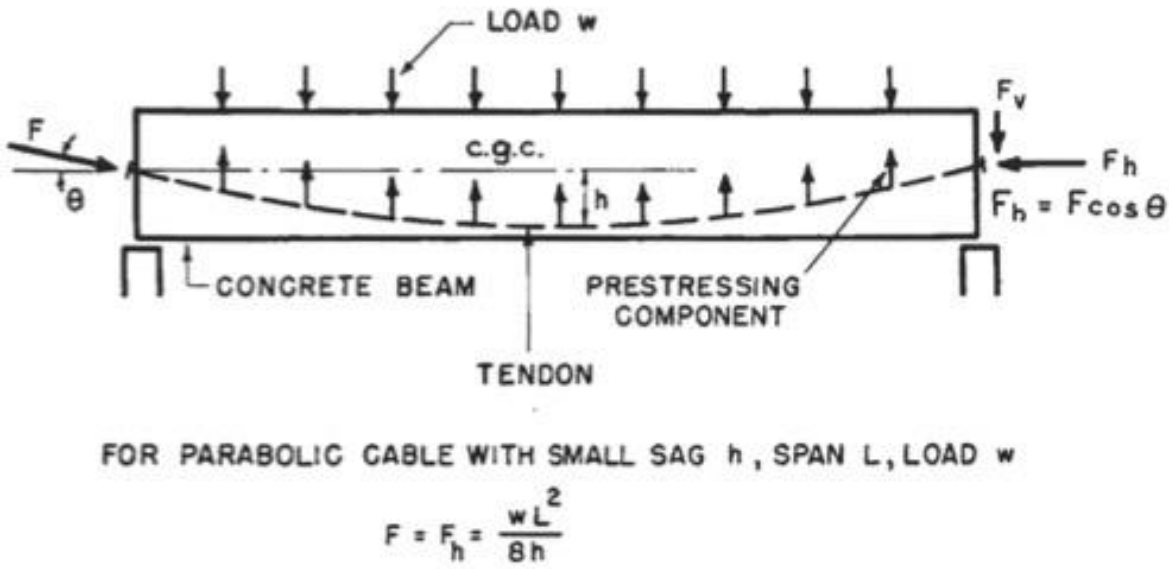

Figure 2.8 Load balancing design of prestressed concrete [12]

2.4.2.1 Equivalent loads along the prestressing steel

When using the load balancing method, the concept of equivalent loads is used. Non-linear prestressed steel in post-tensioned concrete will lead to a distributed load on the concrete, called equivalent loads. This is shown in Figure 2.9 [10].

By using equivalent loads, one considers the forces from the prestressing tendons to be externally applied loads [11]. Calculation of the equivalent load q is shown below, where y describes the prestressing profile.

$$y = f(x) \tag{2.1}$$

$$\theta(x) = tan\theta(x) = \frac{dy}{dx} \tag{2.1}$$

$$q = q(x) \tag{2.2}$$

$$q(x)dx \approx Fd\theta \tag{2.3}$$

$$q(x) = F\frac{d\theta}{dx} = F\frac{d^2y}{dx^2} \tag{2.4}$$

For Figure 2.9, the total force will be

$$q * L = F * \theta \tag{2.5}$$

where

$$\theta = \frac{2e}{L/2} * 2 = \frac{8e}{L} \tag{2.6}$$

This gives the formula for the equivalent force, q:

$$q = \frac{8Fe}{L^2} \tag{2.8}$$

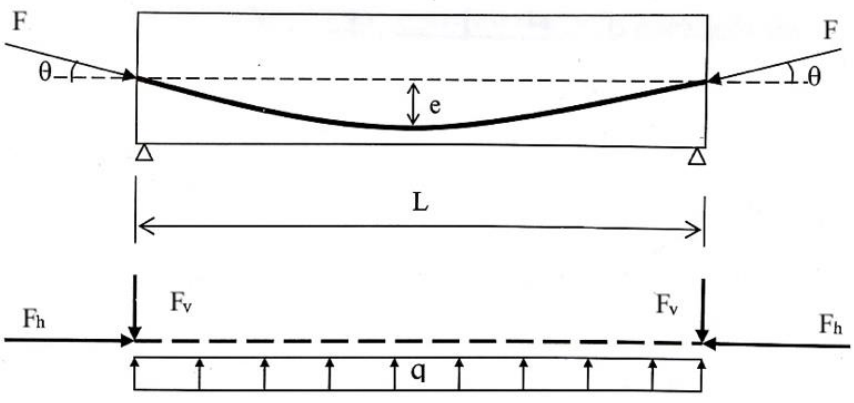

Figure 2.9 Equivalent loads from pre-stressing [10]

2.4.2.2 Equivalent loads due to end forces

In addition to the equivalent forces acting along the prestressed steel, there are concentrated loads at the anchoring. These forces are called end forces [10]. As shown in Figure 2.10, one can imagine the prestressing force *F* being decomposed to a horizontal and vertical component, viz. F_h and F_v, which is acting at the c.o.g. with an eccentricity moment M_F. As the span of the reinforcement often is large compared with the height of the structural element, the angle θ is considered to be very small. Hence,

$sin\theta \approx \theta$

$cos\theta \approx 1$

where θ is in radians [10]. Further, the equivalent forces can be simplified:

$$F_h = Fcos\theta = F \quad (2.7)$$

$$F_v = Fsin\theta = F * \theta \quad (2.8)$$

$$M_F = Fcos\theta * e = F * e \quad (2.9)$$

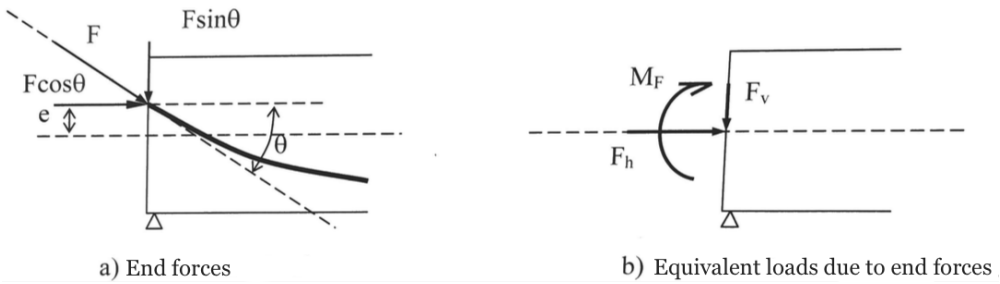

Figure 2.10 Anchoring of prestressing steel [10]

2.4.2.3 Statically indeterminate system

Moments due to prestressing are, as explained in the former chapters, by multiplying the prestressing force by the eccentricity for each section for structures that are statically determinate. For statically indeterminate systems, a secondary moment is to be calculated. Figure 2.11a) shows a beam with straight prestressing at an eccentricity *e*. To calculate the moments due to prestressing, the method for statically indeterminate systems is to imagine removing a support to such that the beam becomes a statically determinate system.

The moment due to the eccentricity is then found as the sum of the primary moment M_0 and the secondary moment M_1.Moments and deflections are calculated after premeditated rules given in “Stålkonstruksjoner” [11].

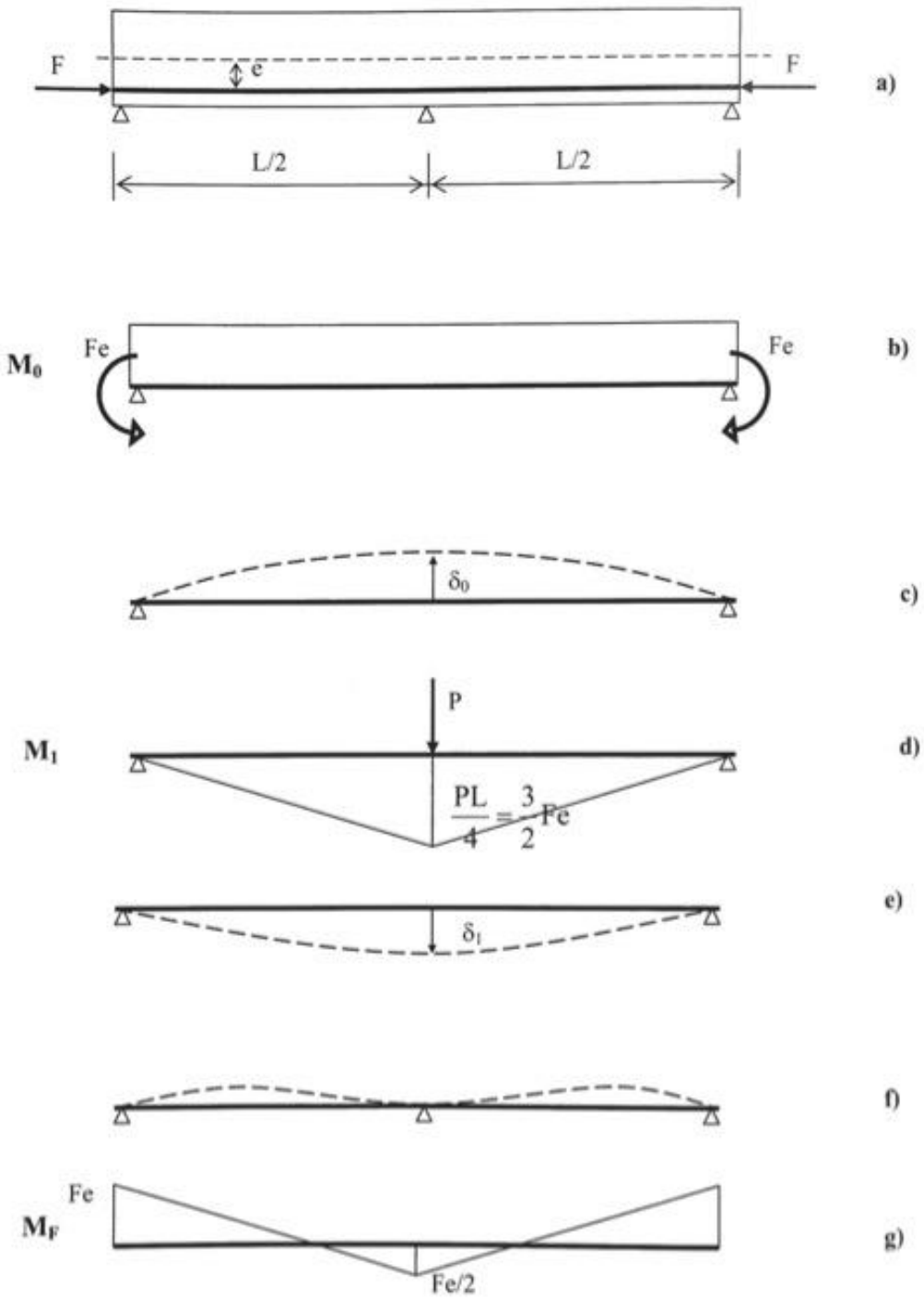

Figure 2.11 Determination of secondary moment

2.4.3 TENDON PROFILE

By using post-tensioning, it is possible to adjust the tendon profile to the load curve applied. A curved profile is used for continuous beams through the construction to fit the pre-tensioning with the moments from external loads [10]. For continuous beams, the moment diagram will sag in the spans and hog over the supports], so will the ducts.

For ILM, two tendon profiles are used. To withstand moments during the launching, each segment is post-tensioned with centric prestressing cables. The centric prestressing consists of the total number of straight aligned prestressing tendons necessary for the launching stages. This prestressing, along with extra reinforcement, must be sufficient during launching.

After the bridge is launched to the final position, it is post-tensioned with parabolic tendons. These tendons are placed to fit the moment diagram, as explained above. Typical tendon profile for ILM is shown in Figure 2.12, with straight tendons in top and bottom flange, and parabolic tendons in webs.

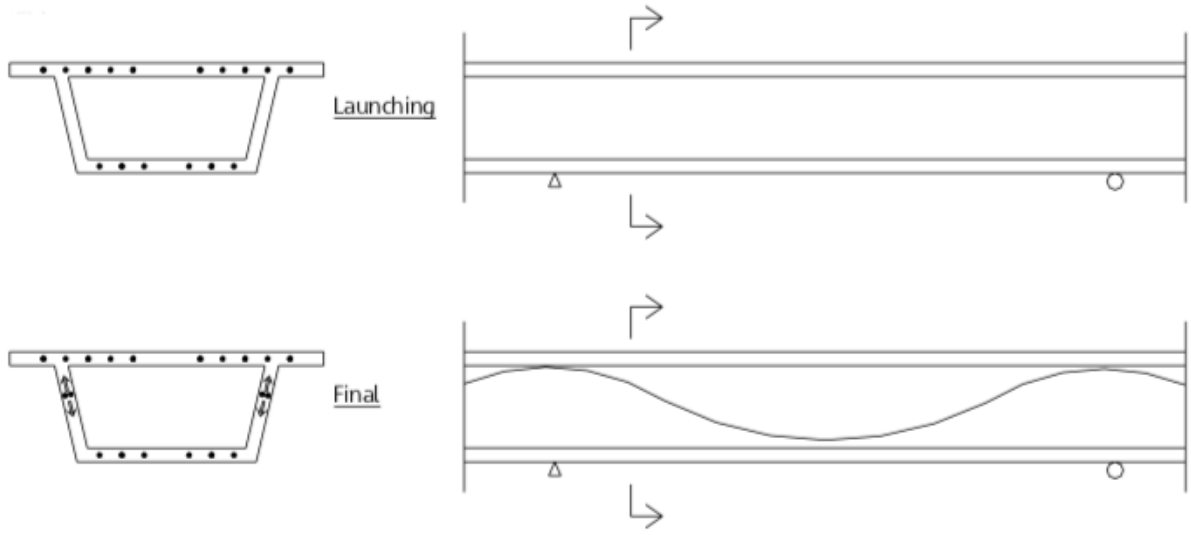

Figure 2.12 Tendon profile for both launching and final state

2.5 LOSS OF PRESTRESSING FORCE

According to EC2, the force which is applied to the steel tendon should not exceed the following:

$$P_{max} = A_p \sigma_{p,max} \tag{2.12}$$

where

A_p is the cross-sectional area of the tendon

$\sigma_{p,max}$ is the maximum stress applied to the tendon = min $\{k_1 f_{pk}\,;\, k_2 f_{p0,1k}\}$

k_1 is a constant with value 0,8

k_2 is a constant with value 0,9

f_{pk} is the characteristic tensile strength of prestressing steel

$f_{p0,1k}$ is the 0,1% proof-stress of prestressing steel

Due to different reasons such as friction, anchoring and elastic deformation, the prestressing force will be reduced. When considering these losses of prestress in tendons one differs between immediate losses and time-dependent losses, as illustrated in Figure 2.13.

2.5.1 INTERMEDIATE LOSS OF PRESTRESS

The intermediate loss of prestress is defined as the difference between the imposed force on the tendon by the hydraulic prestressing jack, P_{max}, and the force in the tendon which appears immediately after transfer at x distance for the tendon, $P_{m0}(x)$ as shown in equation 2.13 [11].

$$Immediate\ loss = P_{max} - P_{m0}(x) \tag{2.13}$$

where $P_{m0}(x)$ is the initial prestressing force, given as following

$$P_{m0}(x) = A_p \sigma_{pmo}(x) \tag{2.14}$$

and $\sigma_{pm0}(x)$ is the stress in the tendon immediately after tensioning

$$\sigma_{pmo}(x) = min\{k_7 f_{pk}\,;\, k_8 f_{p0,1k}\} \tag{2.15}$$

Values for k_7 and k_8 is given in EC2, and recommended values are 0,75 and 0,85 respectively.

Immediate losses appear due to different phenomena, and the total immediate loss is the sum of the losses resulting from these phenomena.

2.5.1.1 Elastic deformation losses

The elastic deformation of concrete for post-tensioned members occurs before the tendons are anchored, during the stressing operation. This can be members with one tendon, or members with multiple tendons that are stressed simultaneously. At this point, the losses are equal to zero. The elastic shortening losses are caused by the stressing of members containing more than one tendon, where the tendons are stressed sequentially. This way, the stressing of tendons will cause elastic shortenings in all of the previously stressed and anchored tendons. As a result, the first tendon that is stressed will suffer the largest elastic shortening loss and the last tendon will not suffer any elastic shortening loss. This type of loss may be reduced by re-stressing the tendons [11].

The loss, ΔP_{el}, is determined after EC2 as following [13]

$$\Delta P_{el} = A_p E_p \sum \left[\frac{j \Delta \sigma_c(t)}{E_{cm}(t)}\right] \qquad 2.16$$

where

$\Delta\sigma_{el}$ is the variation of stress at the center of gravity of the tendons applied at a time *t*

j is a coefficient equal to

- (n-1)/2n where n is the number of identical tendons successively prestressed. As an approximation j may be taken as ½
- 1 for the variations due to permanent actions applied after prestressing

E_p is the design value of modulus of elasticity of prestressing steel

$E_{cm}(t)$ is the elastic modulus of concrete

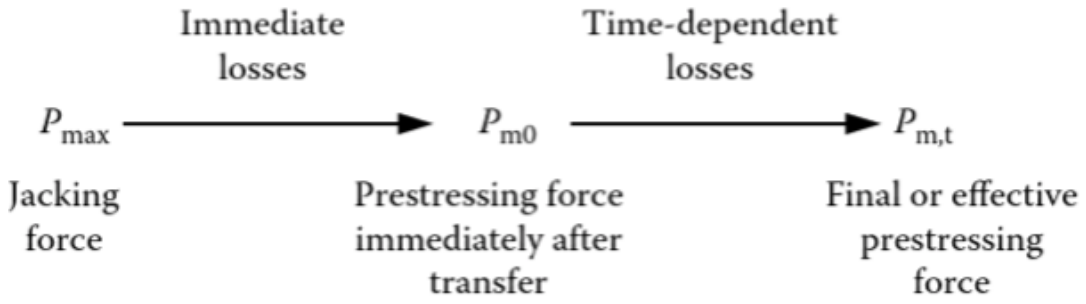

Figure 2.13 Losses of prestress in the tendons [11]

2.5.1.2 Losses due to friction

Friction losses in post-tensioned members occurs during the stressing operation along the tendon. It is caused by friction between the duct and the tendon, which causes a gradual reduction in prestress with the distance x along the tendon [11]. Losses due to friction is determined in EC2 as following [13]:

$$\Delta P_{\mu}(x) = P_{max}(1 - e^{-\mu(\vartheta + kx)}) \quad 2.17$$

where

θ is the sum of angular displacements over a distance x

μ is the coefficient of friction between the tendon and its duct

k is an unintentional angular displacement for internal tendons

x is the distance along the tendon from the point where the prestressing force is equal to P_{max}

For Bagn bridge, the friction factor μ is set to 0,2

2.5.1.3 Losses at anchorage

There may occur an additional loss of prestress caused by a slip or draw-in as the prestressing force is transferred to the anchorage from the jack. Losses due to anchorage loss, ΔP_s, is determined by equation 2.18 and equation 2.19.

$$\Delta P_s = 2\beta L_d \quad 2.18$$

$$L_d = \sqrt{\frac{\Delta s E_p A_p}{\beta}} \quad 2.19$$

where

L_d is the draw-in length

β is the slope of the friction loss line

Δs is the anchorage slip

2.5.2 TIME-DEPENDENT LOSSES

By considering creep and shrinkage in the concrete or the relaxation in the steel, one can calculate the time dependent losses. The time dependent losses may be determined by a simplified method, given by equation 2.20 [13].

$$\Delta P_{c+s+r}(x) = A_p \frac{\varepsilon_{cs} * E_p + 0{,}8 * \Delta\sigma_{pr} + \frac{E_p}{E_{cm}} * \varphi(t,t_0) * \sigma_{c,QP}}{1 + \frac{E_p}{E_{cm}} * \frac{A_p}{A_c} * \left(1 + \frac{A_c}{I_c} * z_{cp}^2\right)[1 + 0{,}8 * \varphi(t,t_0)]} \quad 2.20$$

where

$\Delta\sigma_{p,c+s+r}$ is the absolute value of the variation of stress in the tendons due to creep, shrinkage and relaxation at location x, at time t

ε_{cs} is the estimated shrinkage strain

E_p is the modulus of elasticity for the prestressing steel

E_{cm} is the modulus of elasticity for the concrete

$\Delta\sigma_{pr}$ is the absolute value of the variation of stress in the tendons at location x, at time t, due to the relaxation of the prestressing stress.

$\varphi(t,t_0)$ is the creep coefficient at a time t and load application at time t_0

$\sigma_{c,QP}$ is the stress in the concrete adjacent to the tendons, due to self-weight and initial prestress and other quasi-permanent actions where relevant

A_p is the area of all the prestressing tendons at location x

A_c is the area of the concrete section

I_c is the second moment of area of the concrete section

z_{cp} is the distance between the centre of gravity of the concrete section and the tendons [13]

2.6 LOAD COMBINATIONS

According to EC0 one shall differ between two limit states: ultimate limit state and serviceability limit state. Design for the limit states shall be based on the use of load models and models for KONSTRUKSJONSBEREGNING for the relevant limit states [14].

2.6.1 ULTIMATE LIMIT STATE

The ultimate limit state (ULS) are the limit states that is of importance for the safety of people and/or the safety of the construction. ULS has sets a requirement that structures are able to resist the maximum loads that are likely to act with a safety margin. This limit state is generally used for design of reinforced concrete structures, but these structures should also behave satisfactorily at serviceability limit state [15].

Equation 6.10a and 6.10b in EC0 gives formulas for load combinations, whereas the least favourable is to be used [14].

$$\sum_{j\geq 1} \gamma_{G,j} G_{k,j} + \gamma_P P + \gamma_{Q,1}\psi_{0,1} Q_{k,1} + \sum_{i>1} \gamma_{Q,i}\psi_{0,i} Q_{k,i} \qquad 2.21$$

$$\sum_{j\geq 1} \xi_j \gamma_{G,j} G_{k,j} + \gamma_P P + \gamma_{Q,1} Q_{k,1} + \sum_{i>1} \gamma_{Q,i}\psi_{0,i} Q_{k,i} \qquad 2.22$$

where

$\gamma_{G,j}$ is the partial factor of a permanent action j

$G_{k,j}$ is the characteristic value of permanent action j

γ_P is the partial factor of the prestressing forces

P is the representative value of a prestressing action

$\psi_{0,i}$ is a factor for combination value of a variable action i

$Q_{k,i}$ is the characteristic value of a variable action i

$\gamma_{Q,i}$ is the partial factor of a variable action i

ξ_j is a reduction factor of a variable action j

EC0 states that the following ULS shall be detected where applicable:

EQU Loss of static equilibrium for a construction or structural parts,

STR Fracture or too large deformations in the structure or structural parts, including foundations, piles, walls etc., where the strength of the structural materials are of importance.

GEO Fracture of too large deformations in the ground, where the strength in the soil or rock are of importance to ensure capacity.

FAT Fracture due to fatigue in the structure or the structural parts.

UPL Loss of equilibrium in the structure or in the ground caused by uplift due to water pressure or other vertical loadings.

HYD Hydraulic fracture in the ground, inner erosion and duct formation in the ground caused by hydraulic gradients [14].

The part relevant for this thesis will only be STR. For further reference, the following abbreviations are used:

G Self-weight

PS Prestressing

CSR Creep/shrinkage/relaxation

TR Traffic load

TE Temperature load

W/W-TR Wind load on the bridge without traffic load / with traffic load

Load combinations for Bagn bridge are found by using table NA.A2.4(B) in EC0, and are represented in Table 2.1.

Table 2.1 Load combinations at ULS (STR)

ULS – Characteristic								
Load combination		**G**	**PS**	**CSR**	**TR**	**TE**	**W**	**W-TR**
1	(2.21), with TR	1,35	0,9/1,1	0,0/1,0	0,945	0,84	-	1,12
2	(2.21), without TR	1,35	0,9/1,1	0,0/1,0	-	0,84	1,12	-
3	(2.22), TR dom.	1,20	0,9/1,1	0,0/1,0	1,35	0,84	-	1,12
4	(2.22) TE dom.	1,20	0,9/1,1	0,0/1,0	0,945	1,20	-	1,12
5	(2.22) W-TR dom.	1,20	0,9/1,1	0,0/1,0	0,945	0,84	-	1,6
6	(2.22) W dom.	1,20	0,9/1,1	0,0/1,0	-	0,84	1,6	-

2.6.2 SERVICEABILITY LIMIT STATE

The serviceability limit state (SLS) has significant meaning for the functionality of the structure, human comfort and the appearance of the structure. SLS requires that structures with working loading shall be able to withstand loads without excessive deflection, unpleasant vibrations, unacceptable crack widths, etc. Pre-stressed concrete members are usually designed to satisfy the requirements for SLS and are then controlled for adequate safety at the ULS. The reason for this is that the SLS conditions are more critical for prestressed concrete structures than the ULS conditions [15].

When checking for SLS, EC0 states that the following limit is to be proven

$$E_d \leq C_d \tag{2.23}$$

where C_d is the design limit value for the current serviceability criteria and E_d is the design value for the load effect for the current serviceability criteria [14].

Load combinations for SLS are defined and categorized in EC0 by three different categories; characteristic combination, frequent combination and quasi-permanent combination as described in equation 2.24, 2.25 and 2.26 [14].

Characteristic combination:

$$\sum_{j\geq 1} G_{k,j} "+" P "+" Q_{k,1} "+" \sum_{i>1} \Psi_{0,i} Q_{k,i} \tag{2.24}$$

Frequent combination

$$\sum_{j\geq 1} G_{k,j} "+" P "+" \Psi_{1,1} Q_{k,1} "+" \sum_{i>1} \Psi_{2,i} Q_{k,i} \tag{2.25}$$

Quasi-permanent combination

$$\sum_{j\geq 1} G_{k,j} "+" P "+" \sum_{i\geq 1} \Psi_{2,i} Q_{k,i} \tag{2.26}$$

Load combinations for Bagn bridge is given in Table 2.2, according to EC0 NA.A2.4.1(1).

Table 2.2 Load combinations in SLS

SLS – Characteristic combination								
Load combination		**G**	**PS**	**CSR**	**TR**	**TE**	**W**	**W-TR**
1	2.24, TR dom.	1,0	1,0	1,0	1,0	0,7	-	0,7
2	2.24, TE dom.	1,0	1,0	1,0	0,7	1,0	-	0,7
3	2.24, W dom.	1,0	1,0	1,0	-	0,7	1,0	-
4	2.24, W-TR dom.	1,0	1,0	1,0	0,7	0,7	-	1,0
SLS – Frequent combination								
Load combination		**G**	**PS**	**CSR**	**TR**	**TE**	**W**	**W-TR**
1	2.25, TR dom.	1,0	1,0	1,0	0,7	-	-	-
2	2.25, TE dom.	1,0	1,0	1,0	0,2	0,7	-	-
3	2.25, W dom.	1,0	1,0	1,0	-	-	0,7	-
4	2.25, W-TR dom.	1,0	1,0	1,0	0,7	0,2	-	0,7
SLS – Quasi-permanent combination								
Load combination		**G**	**PS**	**CSR**	**TR**	**TE**	**W**	**W-TR**
1	2.26, TR dom.	1,0	1,0	1,0	0,5	-	-	-
2	2.26, TE dom.	1,0	1,0	1,0	0,2	0,5	-	-
3	2.26, W dom.	1,0	1,0	1,0	-	-	0,5	-
4	2.26, W-TR dom.	1,0	1,0	1,0	0,7	-	-	0,5

3 MATERIAL PROPERTIES

3.1 CONCRETE

When casting prestressed structures, it is normal to use concrete with higher strength than what is used in regular reinforced structures. A reason for this is that the relatively large forces acting on the prestressed concrete section demands large dimensions to withstand the pressure. A high strength makes it possible to minimize the dimensions, and thereof minimize the self-weight. The high strength also keeps the structure from having large deformations. Concrete classes B35 – B55 are mostly used, but in some cases higher strength is needed [11] [10].

To achieve a concrete which provides as little creep and losses as possible, special mix design and composition are chosen. By avoiding large creep and losses, it is possible to reduce the loss of effective prestressing.

By using a firm concrete with low water-to-cement-relation, corrosion in the prestressing tendons is avoided.

3.1.1 COMPRESSIVE STRENGTH

To describe the compressive strength of concrete, the characteristic cylinder strength f_{ck} at 28 days is used. EC2 states that this compressive strength is taken as the strength where there is a 95% or more of which test results do not fail. Corresponding mechanical properties are given in EC2 [13] [15].

If it is necessary, the compressive strength at a specific time *t* different from 28 can be found as following [13]:

$$f_{ck}(t) = f_{cm}(t) - 8(MPa) \quad for\ 3 < t < 28\ days \tag{3.1}$$

$$f_{ck}(t) = f_{ck} \quad for\ t \geq 28\ days \tag{3.2}$$

According to EC2 one can determine the mean compressive strength of concrete $f_{cm}(t)$ at age *t* from the mean strength f_{cm} at age 28 days as shown in equation 3.3. This value depends on type of cement, temperature and curing conditions [13].

$$f_{cm}(t) = \beta_{cc}(t) f_{cm} \tag{3.3}$$

where

$$\beta_{cc}(t) = exp\left\{s\left[1 - \left(\frac{28}{t}\right)^{0,5}\right]\right\} \tag{3.4}$$

The factor *s* depends on the cement strength class, and *t* is given in days.

To determine the value for the design compressive strength f_{cd}, the characteristic cylinder strength is divided with a safety factor, as following

$$f_{cd} = \frac{\alpha_{cc} f_{ck}}{\gamma_c} \tag{3.5}$$

where γ_c is the partial safety factor for concrete set to 1,5, and α_{cc} is a coefficient which takes the long-term effects on the compressive strength into account. α_{cc} is normally set to 0,85 [13]. For concrete class B45 the design compressive strength is equal to $f_{cd} = \frac{0,85*45MPa}{1,5} = 25,5MPa$. From this, stress-strain relation can be used to design the cross-section.

$$\sigma_c = f_{cd}\left[1 - \left(1 - \frac{\varepsilon_c}{\varepsilon_{c2}}\right)^n\right] \quad for\ 0 \le \varepsilon_c \le \varepsilon_{c2} \tag{3.6}$$

$$\sigma_c = f_{cd} \quad for\ \varepsilon_{c2} \le \varepsilon_c \le \varepsilon_{cu2} \tag{3.7}$$

where

n is the exponent according to table 4.1 in EC2

ε_{c2} is the strain reaching the maximum strength, = $2.0*10^{-3}$ according to Figure 3.1

ε_{cu2} is the ultimate strain, = $3.5*10^{-3}$ according to Figure 3.1

3.1.2 TENSILE STRENGTH

EC2 states that the axial tensile strength f_{ct} is the highest stress the concrete can withstand when subjected to centric tensile loading [13]. As testing for uniaxial tensile strength are difficult to perform, a splitting tensile strength $f_{ct,sp}$ is found by testing to determine an approximate value [11]. This approximate value is found by equation 3.8.

$$f_{ct} = 0{,}9 f_{ct,sp} \tag{3.8}$$

The tensile strength $f_{ctm}(t)$ develops with time and depends on highly on the curing and drying conditions and the dimension of the structure, and is assumed equal to:

$$f_{ctm}(t) = (\beta_{cc}(t))^{\alpha} f_{ctm} \tag{3.9}$$

where

f_{ctm} is the mean tensile strength of the concrete, found in Figure 3.1

$\beta_{cc}(t)$ follows from equation 3.4

α = 1 for t < 28

= 2/3 for t ≥ 28

Strength class	C12/15	C16/20	C20/25	C25/30	C30/37	C35/45	C40/50	C45/55	C50/60	C55/67	C60/75	C70/85	C80/95	C90/105
f_{ck} (MPa)	12	16	20	25	30	35	40	45	50	55	60	70	80	90
$f_{ck,cube}$ (MPa)	15	20	25	30	37	45	50	55	60	67	75	85	95	105
f_{cm} (MPa)	20	24	28	33	38	43	48	53	58	63	68	78	88	98
f_{ctm} (MPa)	1.6	1.9	2.2	2.6	2.9	3.2	3.5	3.8	4.1	4.2	4.4	4.6	4.8	5.0
$f_{ctk,0.05}$ (MPa)	1.1	1.3	1.5	1.8	2.0	2.2	2.5	2.7	2.9	3.0	3.1	3.2	3.4	3.5
$f_{ctk,0.95}$ (MPa)	2	2.5	2.9	3.3	3.8	4.2	4.6	2.9	5.3	5.5	5.7	6.0	6.3	6.6
E_{cm} (GPa)	27	29	30	31	33	34	35	36	37	38	39	41	42	44
ε_{c1} ($\times 10^{-3}$)	1.8	1.9	2.0	2.1	2.2	2.25	2.3	2.4	2.45	2.5	2.6	2.7	2.8	2.8
ε_{cu1} ($\times 10^{-3}$)					3.5					3.2	3.0	2.8	2.8	2.8
ε_{c2} ($\times 10^{-3}$)					2.0					2.2	2.3	2.4	2.5	2.6
ε_{cu2} ($\times 10^{-3}$)					3.5					3.1	2.9	2.7	2.6	2.6
n					2.0					1.75	1.6	1.45	1.4	1.4
ε_{c3} ($\times 10^{-3}$)					1.75					1.8	1.9	2.0	2.2	2.3
ε_{cu3} ($\times 10^{-3}$)					3.5					3.1	2.9	2.7	2.6	2.6

Figure 3.1 Strength and deformation characteristics for concrete [11]

3.1.3 DEFORMATIONAL PROPERTIES

When looking at the deformational properties, the once of most interest are the elastic moduli, creep and shrinkage deformation.

3.1.3.1 Elastic moduli

The elastic modulus is a value which tells us something about the stiffness of the concrete. With higher elastic modulus, the stiffness increases. Deformations due to elasticity are highly dependent on the composition of the concrete, especially the aggregates.

The secant modulus, also called modulus of elasticity or Young´s modulus, are shown in Figure 3.2 as E_{cm} and is defined as the ratio between the applied stress and the corresponding strain which occurs within the elastic limit. Values for E_{cm} between $\sigma_c=0$ and $\sigma_c=0{,}4f_{cm}$ are given in Figure 3.1 for concrete with quartzite aggregates. For concrete with aggregates such as limestone and sandstone, the value of E_{cm} are to be reduced by 10% and 30% respectively. The value is to be reduced by 20% when using basalt aggregates [13] [16].

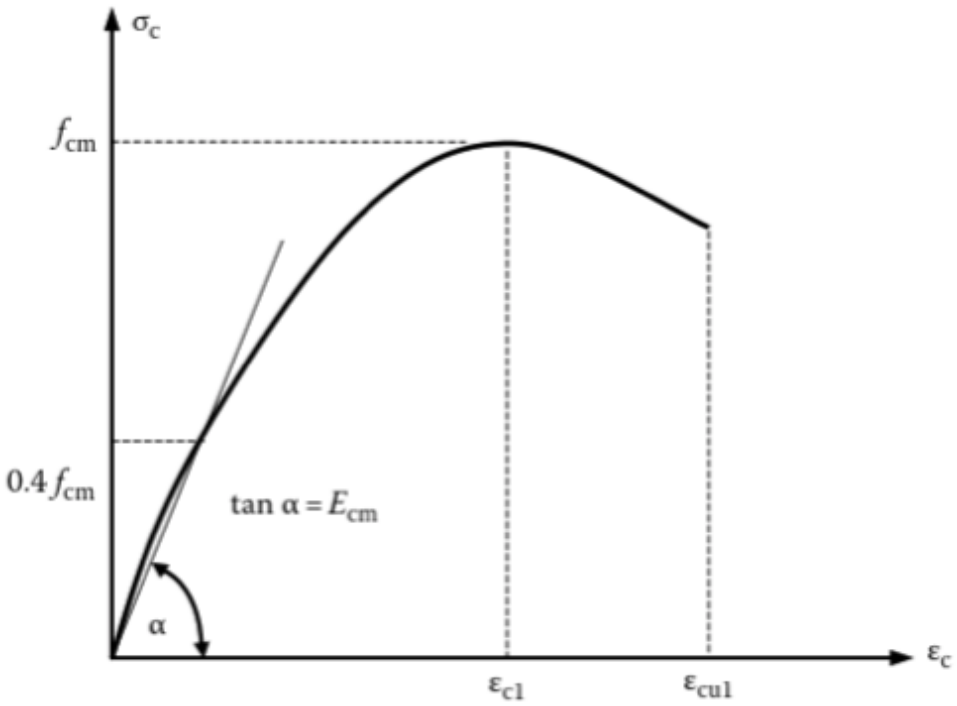

Figure 3.2 Idealised stress-strain relationship for concrete in uniaxial compression [11]

3.1.3.2 Creep coefficient

Deformation due to creep occurs after a load is applied to the structure. With time the deformation of the concrete gradually increases, an may reach a value as high as three to four times the immediate elastic deformation. P. Bhatt states that “creep is defined as the increase of strain with time when the stress is held constant” [15].

The total creep deformation of concrete $\varepsilon_{cc}(\infty,t_0)$ due to constant compressive stress σ_c applied at time t_0 is calculated as in equation 3.10 [13].

$$\varepsilon_{cc}(\infty, t_0) = \varphi(\infty, t_0)\frac{\sigma_c}{E_c} \qquad 3.10$$

Where

$\varphi(\infty,t_0)$ is the creep coefficient. This value is related to the tangent modulus E_c that can be taken as 1.05 $E_{cm.}$ If the compressive stresses which are subjected to the concrete are less than $0{,}45f_{ck}(t_0)$ at an age t_0, the tangent modulus can be taken from Figure 3.2 [13].

3.1.3.3 Shrinkage

The shrinkage of concrete is affected by the same parameters as the creep coefficient, such as the ambient humidity, compressive strength, element dimensions and composition of concrete. The total shrinkage strain ε_{cs} is made up by two components, the plastic shrinkage strain and the drying shrinkage strain. The plastic shrinkage appears during the hardening of the concrete, whereas the drying shrinkage develops slowly due to loss of water in the concrete [13] [15]. The total shrinkage strain is found as following:

$$\varepsilon_{cs} = \varepsilon_{cd} + \varepsilon_{ca} \qquad 3.11$$

where

ε_c is the drying shrinkage strain

ε_c is the autogenous shrinkage strain (plastic strain)

3.1.3.4 Thermal stress

Changes in temperature may have consequences for exposed structures, as large internal forces occur if the deformations are prevented. Heating or cooling of parts of a structure creates thermal gradients that induces stresses. For a structure of length L that rests on a frictionless surface, the raise in temperature ΔT gives an increase in length of $\Delta L=\alpha_T*\Delta T*L$. This gives the corresponding thermal strain ε_T:

$$\varepsilon_T = \alpha_T * \Delta T \qquad 3.12$$

where α_T is the coefficient of thermal expansion which from EC2 is set to $10*10^{-6}/^oC$. If the deformations are prevented, a compressional stress of $\sigma = E * \varepsilon_T$ occurs [2][11] [13].

3.1.4 MATERIAL PARAMETERS

Material properties for Bagn bridge are given in Table 3.1.

Table 3.1 Material properties for concrete

Concrete B45		
Characteristic compressive strength	f_{ck}	45 MPa
Mean axial tensile strength	f_{ctm}	3.8 MPa
Mean elastic modulus	E_{cm}	36 GPa
Characteristic cylinder strength after 28 days	f_{cck}	36 MPa
Coefficient	α_{cc}	0.85
Partial factor of safety	γ_c	1.5
Weight of unreinforced concrete	W_c	2400 kg/m^3

3.2 PRESTRESSING STEEL

Prestressing steel are used as a way to increase the tensile strength in concrete. The most commonly used prestressing steel are cold-drawn high tensile steel wires or alloy steel bars. A common cross-section of a standard and drawn strand is shown in Figure 3.3 and consists of 7 wire strands, whereas six of them are spun around the central wire. The overall nominal diameter may vary from 12.5 mm to 18 mm. The overall diameter for drawn cables is slightly smaller as they are compressed into trapezoidal shapes [15].

To achieve full prestressing of a structure, it is necessary to use steel with high strength. As concrete gets shortened by creep and shrinkage, so does the prestressing steel that are attached to the concrete by bonding. This results in a loss in stress in the steel. By using steel tendons with high strength, it is capable to carry higher initial stress. This way the loss of prestresses will be significantly smaller than the initial prestressing force. The typical tensile strength in prestressing steel is normally between 1000 and 1900 MPa [10], [11].

For Bagn bridge, the prestressing steel of type CONA CMI 1506-140-1860 is used with an outer radius of 80mm. The prestressing system consists of 15 strands with a nominal diameter of 15,3 mm.

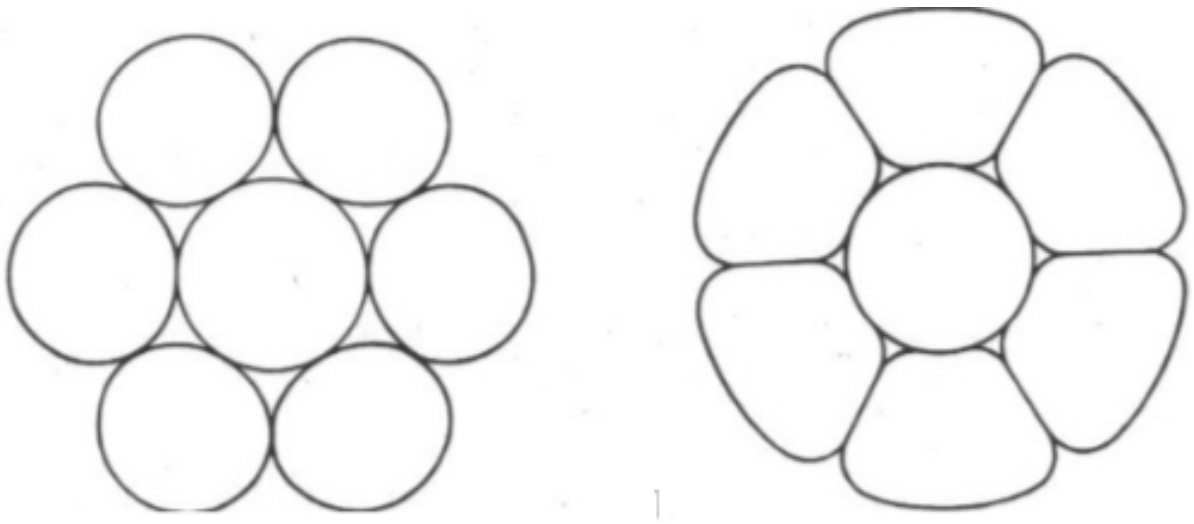

Figure 3.3 Cross-section of a standard and drawn strand [15]

3.2.1 STRENGTH AND DUCTILITY

Figure 3.4 shows a typical stress-strain curve for the characteristic tensile strength f_{pk} and the yield stress $f_{p0,1k}$ is taken as the 0,1% proof stress. The stress is calculated as normal, where the characteristic maximum load in axial tension and the characteristic value of the 0,1% proof load is divided by the nominal cross-sectional area. The elongation at maximum load ε_{uk} is the corresponding strain to f_{pk} [13], [15].

To ensure adequate ductility of prestressing steel in tension, the expression in equation 3.13 is used.

$$\frac{f_{pk}}{f_{p0,1k}} \geq k \qquad 3.13$$

where k is a value normally set to 1,1. The design value for the prestressing steel strength f_{pd} is taken as $f_{p0,1k}/\gamma_s$ according to EC2.

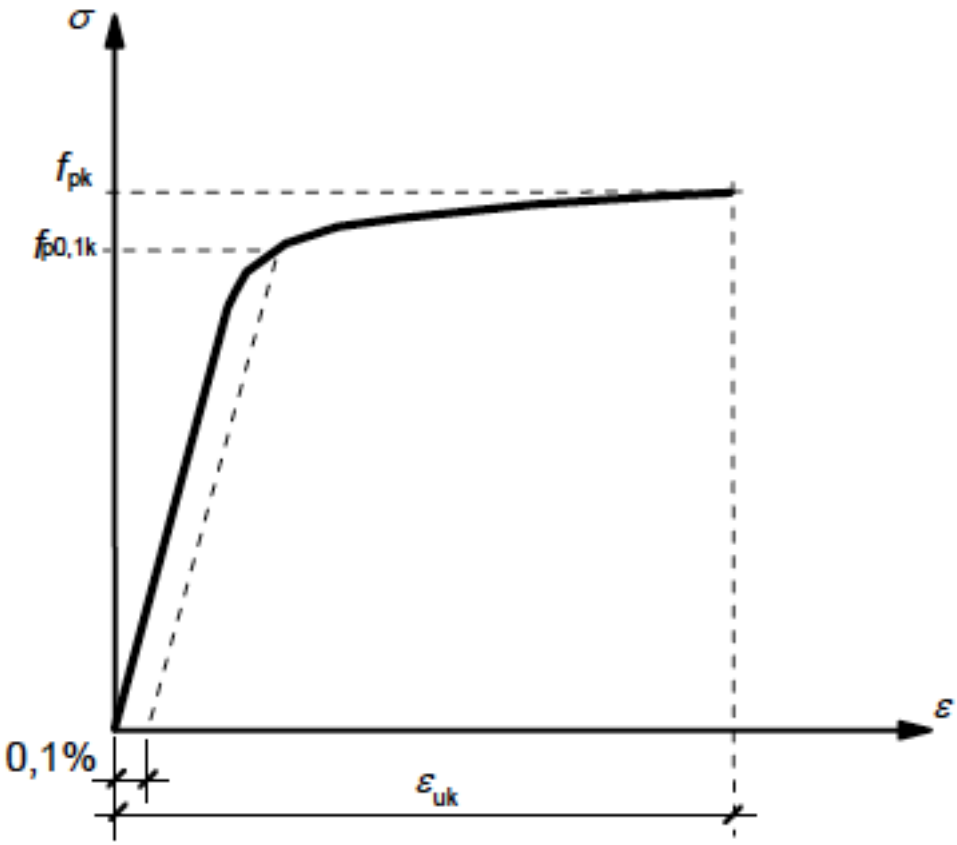

Figure 3.4 Stress-strain curve for prestressing steel [13]

3.2.2 ELASTIC MODULUS

As for the concrete, stiffness is described by the modulus of elasticity. To find the modulus of elasticity E_p, a direct tension test is done where the elongation of the test tendons is measured. Otherwise, values may be found in tables in Eurocodes. Normal value for steel strands is given as [13], [15]:

$$E_p = 195\ GPa \tag{3.14}$$

3.2.3 STEEL RELAXATION

The relaxation of steel is defined as the ratio between the variation of the prestressing stress and the initial prestressing stress in percent and is determined in as in equation. The steel relaxation of steel is divided into three classes according to EC2. Class 1 and 2 is for wires and strands with ordinary and low relaxation for class 1 and 2 respectively. Class 3 is for hot-rolled and prestressed bars [13].

$$Class\ 1 \qquad \frac{\Delta\sigma_{pr}}{\sigma_{pi}} = 5{,}39\ \rho_{1000} e^{6{,}7\mu} \left(\frac{t}{1000}\right)^{0{,}75(1-\mu)} 10^{-5} \tag{3.13}$$

$$Class\ 2 \qquad \frac{\Delta\sigma_{pr}}{\sigma_{pi}} = 0{,}66\ \rho_{1000} e^{9{,}1\mu} \left(\frac{t}{1000}\right)^{0{,}75(1-\mu)} 10^{-5} \tag{3.14}$$

$$Class\ 3 \qquad \frac{\Delta\sigma_{pr}}{\sigma_{pi}} = 1{,}98\ \rho_{1000} e^{8\mu} \left(\frac{t}{1000}\right)^{0{,}75(1-\mu)} 10^{-5} \tag{3.15}$$

where

$\Delta\sigma_{pr}$ is the absolute value of the relaxation losses of the prestress

σ_{pi} is the absolute value of the initial prestress $\sigma_{pi} = \sigma_{pm0}$

t is the time after tensioning in hours

ρ_{1000} is the value of relaxation loss in percent, at 1000 hours after tensioning and at mean temperature of 20°C

3.2.4 MATERIAL PROPERTIES

The material properties for the prestressing steel is shown in Table 3.2.

Table 3.2 Material properties for prestressing steel

Prestressing steel – 15 strand tendon (140mm^2)	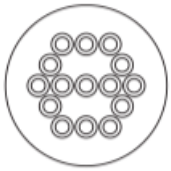	
Area of single tendon	A_p	2100 mm^2
Diameter of duct	d_{p2}	80 mm
Nominal strength	f_{pk}	1860 MPa
Nominal yield strength	$f_{p0,1k}$	1640 MPa
Mean elastic modulus	E_p	195 GPa
Flytekraft	$F_{p0,1k}$	4672 kN
Kabelkraft etter forankring	F_{pm0}	3973 kN

3.3 STEEL REINFORCEMENT

Steel reinforcement are used in concrete for several reasons. In prestressed structures, reinforcement is added to give the structure more tensile strength and ductility where the prestressing steel is not sufficient. Steel reinforcement is also added to prestressed concrete to provide crack control, reduce long-term deflection/shortening due to shrinkage and creep and to provide more resistance to transverse tension in anchorage zones [11].

3.3.1 STRENGTH AND DUCTILITY

For Bagn bridge, reinforcement of quality B500NC is used. This describes both the strength and the ductility of the steel. The characteristic yield strength of the steel f_{yk} is described as the characteristic value of the yield load divided by the nominal cross-sectional area of the steel bar, and for B500NC it is given as 500 MPa. The characteristic tensile strength f_{tk} is described by the maximum direct axial load divided by the nominal cross-sectional area [8].

EC2 states that the reinforcement steel is to have adequate ductility defined by the ratio $k = f_{tk}/f_{yk}$ and the elongation at maximum force ε_{uk}. Values for k and ε_{uk} are given in EC2 and are based on the ductility classes. According to EC2-2, the reinforcement used in bridges shall have high ductility corresponding to class C [13] [15].

3.3.2 ELASTIC MODULUS

For steel reinforcement, the elastic modulus is set to be 200 GPa [11].

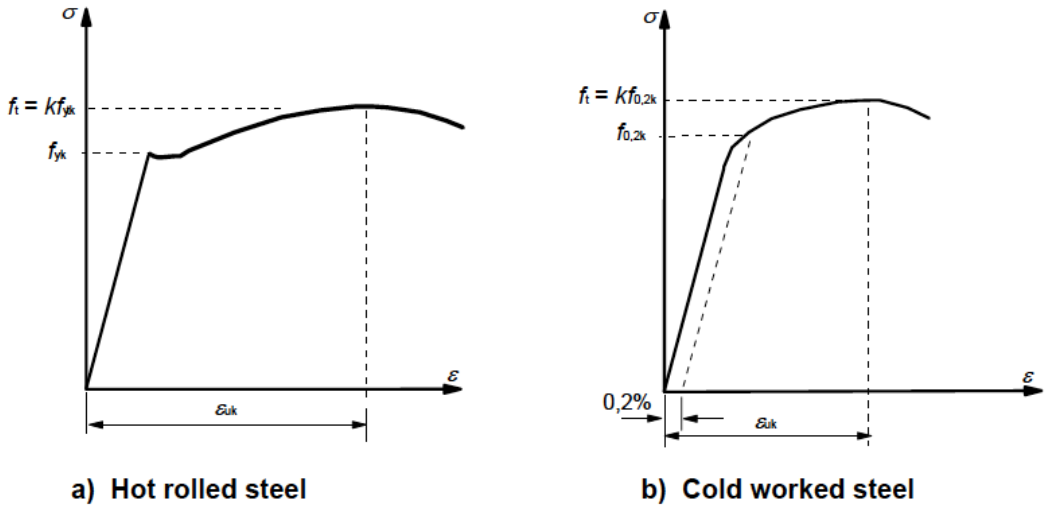

Figure 3.5 Stress-strain diagrams for typical reinforcing steel [11]

3.3.3 MATERIAL PROPERTIES

Material properties for the steel reinforcement is given in Table 3.3.

Table 3.3 Material properties for reinforcement

Reinforcement B500NC		
Characteristic strength	f_{yk}	500 MPa
Mean elastic modulus	E_s	200 GPa
Partial safety factor	γ_s	1.15
Diameter of longitudinal reinforcement	$Ø_L$	Ø25
Diameter of transverse reinforcement	$Ø_S$	Ø12

SVV states that for the construction measurement of steel reinforcement, the diameters given in Table 3.4 are to be used [3]:

Table 3.4 Construction measurements for steel reinforcement

Diameter	Ø12	Ø25
Construction measurement	15 mm	30 mm

3.4 DURABILITY AND COVER TO REINFORCEMENT

Bridges are designed for 100 year working life, sometimes even longer. For a structure to be durable, it should meet the requirements of strength, serviceability and stability for its entire design working life. This should happen without need for excessive maintenance or loss of utility to keep repair costs as small as possible [3] [11].

The environment affects structures in form of chemical and physical conditions. To classify the environmental conditions, one uses exposure classes defined in EC2. The exposure classes are shown in Table 3.5 [13].

Table 3.5 Exposure classes [13]

Exposure class	Description of the environment
X0	No risk of corrosion or attack
XC1, XC2, XC3, XC4	Corrosion induced by carbonisation
XD1, XD2, XD3	Corrosion induced by chlorides
XS1, XS2, XS3	Corrosion induced by chlorides from sea water
XF1, XF2, XF3, XF4	Freeze/thaw attack
XA1, XA2, XA3	Chemical attack

A minimum distance between concrete surface and reinforcement is to be provided to make sure that there is a safe transmission of bond forces, there is an adequate fire resistance and to protect the steel against corrosion. The latter is especially important when considering the durability of the structure [13].

$$c_{min} = max\{c_{min,b};\ c_{min,dur} + \Delta c_{dur,\gamma} - \Delta c_{dur,st} - \Delta c_{dur,add}; 10mm\} \qquad 3.16$$

where

$c_{min,b}$ is the minimum cover due to bond requirement

$c_{min,dur}$ is the minimum cover due to environmental conditions

$\Delta c_{dur,\gamma}$ is the additive safety element

$\Delta c_{dur,st}$ is the reduction of minimum cover for use of stainless steel

$\Delta c_{dur,add}$ is the reduction of minimum cover for use of additional protection

Gohler and Pearson states that when using ILM a minimum cover to reinforcement of 150 mm to ensure capacity in the flanges [6]. Appendix B shows calculations of cover to reinforcement according to EC2. As the results from this calculation is smaller than the limit given in [6], a cover to reinforcement of 150mm is chosen. Exposure classes and covers are given in Table 3.6. In this thesis, the top and bottom deck is the relevant parts.

Table 3.6 Chosen exposure classes and corresponding cover values

Surface	Durability class	Exposure class	Cover [mm]
Top deck	MF40	XD3, XF3, XF4	150
Bottom box girder		XD3, XC4	150

Minimum spacing between ducts are calculated after EC2-2, here represented in Figure 3.6. From Appendix B, the horizontal and vertical spacing is found to be the following:

$$a_h = \max(d_g\,; \emptyset_{duct}\,; 40mm) = \emptyset_{duct} = 80mm \qquad 3.17$$

$$a_v = \max(d_g + 5mm\,; \emptyset_{duct}\,; 50mm) = \emptyset_{duct} = 80mm \qquad 3.20$$

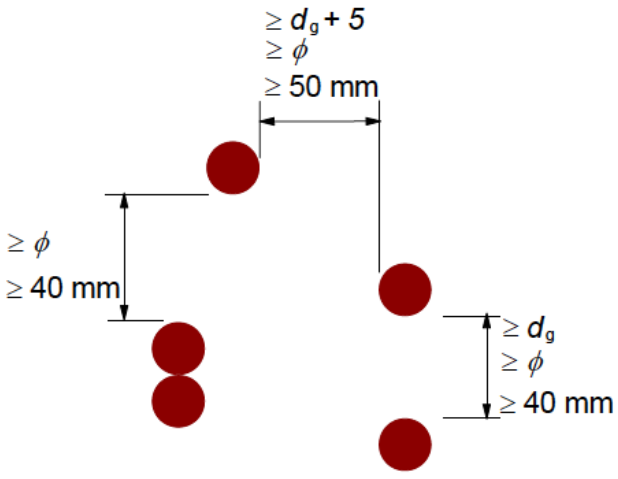

Figure 3.6 Minimum clear spacing between ducts

4 MODELLING IN NOVAFRAME

In this thesis, NovaFrame is used to analyse the bridge. Novaframe is a frame analysis software based on beam element theory. This software is a part of NovaProg, a program developed by Aas-Jakobsen and is used for static and dynamic analyses. Besides NovaFrame, NovaProg also consists of NovaDesign.

The input in NovaFrame can either be done directly in the program, or by using ASCII input files. The input file may be edited in a normal text editor program. The ability to edit and copy makes this very efficient. Also, the fact that models are made in text editor programs makes it possible to work on models on any computer, even those without Novaprog installed. For this thesis, most of the input has been done through ASCII files [16].

This chapter will show and explain different factors which are relevant when modelling in NovaFrame.

4.1 COORDINATE SYSTEM

There are two sets of coordinate systems that are used in NovaFrame, local and global. The global coordinate system is the XYZ-system, and the local is the LMN-system as shown in Figure 4.1. The global system is used for nodes and boundary conditions, and the local system is used for geometric sections [16].

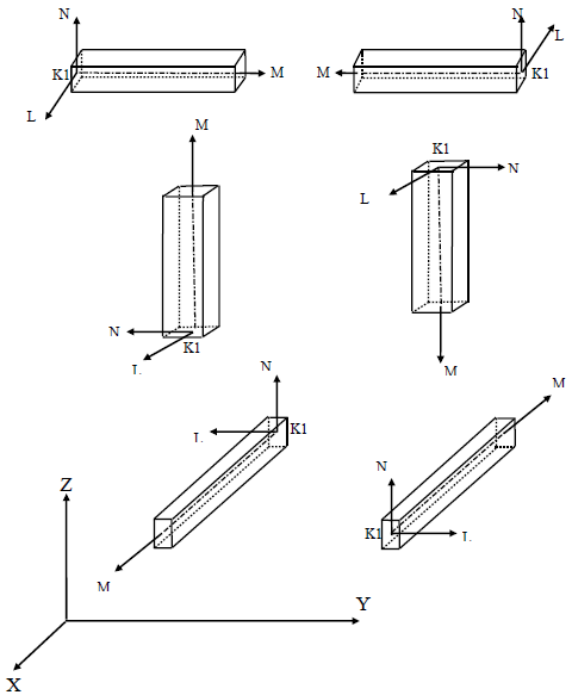

Figure 4.1 Local and global coordinate system in NovaFrame

4.2 REFERENCE LINES AND CROSS-SECTION

Reference lines are used in NovaFrame to keep control of cross-sections. In the model for Bagn bridge, only reference line no 0 is used. This reference line is not really a line, but a collection of cross-sections by their numbers [16].

The cross-section is defined in the cross-section input dialog. For Bagn Bridge, a massive cross-section is used. The dimensions of the cross-section are defined in an ACSII file by coordinates. The cross-section used in the NovaFrame model is shown in Figure 4.2. Cross-sections for the launching nose are also defined. As a simplification, the information input for the launching nose are provided by SVV from a different project.

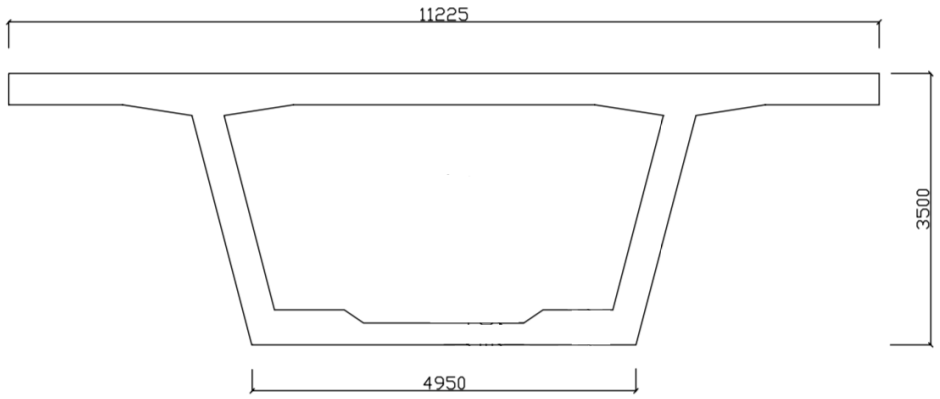

Figure 4.2 Cross-section in NovaFrame (dimensions are given in mm)

4.3 NODES AND ELEMENTS AND BOUNDARY CONDITIONS

When modelling a frame, nodes and elements has to be introduced. For Bagn bridge nodes are defined for each meter and the elements are defined as a straight line between the nodes. The boundary conditions are defined in the Boundaries input dialog. Initial boundary conditions are defined as following:

Node 1: fixed in X, Y and Z direction and fixed for rotation about Y axis.

Remaining nodes: fixed in X and Z direction and fixed for rotation about Y axis [16].

The boundary conditions will then change for the different models, as explained in CH4.4.

Figure 4.3 shows nodes and boundary conditions for the bridge after the final launch, where nodes are shown on the top side and boundary conditions are shown on the bottom side.

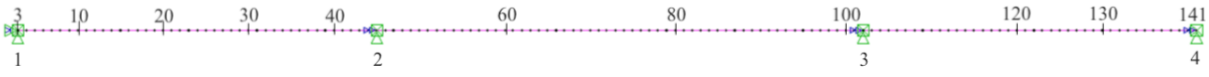

Figure 4.3 Nodes and boundary conditions for the final bridge model in NovaFrame

4.4 MODELS

When modelling for ILM it is necessary to create models and run multiple analyses. Different analytical models are defined in the Models input dialog [16]. For Bagn bridge, 137 models are created. Model 1 illustrates when the launching has reached 39 meters from support 1. This is shown in Figure 4.4. The following models represent the launching of the bridge of one meter from the previous models, i.e. each model is the launch of one meter.

As shown in Figure 4.4, a bridge superstructure of 140 meters is modelled with temporary supports prior to support 1. The nodes from number 141 to the end represents the launching nose. For every model, the boundary conditions are moved one element backwards. When the launching nose reaches a new support, a new boundary condition is introduced. The bridge deck is connected to the final support when support 1 reaches node no 3. Node 1 and 2 are then deleted.

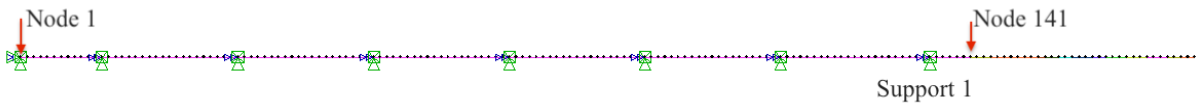

Figure 4.4 Bridge model 1

4.5 LOADS

4.5.1 PERMANENT LOADS

Loads are added manually in NovaFrame. The self-weight is modelled by using the input for self-weight, where the density of the concrete is given for the relevant elements. When using ILM, the self-weight input is used for both the box girder and the launching nose.

Four walls are placed in the box-girder and are places such that each will land on top of columns in the final construction. These are to ensure stiffness over the columns and are modelled as point-loads in the load input. All the permanent loads are used for both the launching stages and for the final bridge analysis and are given below. The point loads are defined below. Calculations of the self-weights are found in Appendix C-1.

$$P_{wall.1} = 480\ kN \tag{4.1}$$

$$P_{wall.2} = P_{wall.3} = 450\ kN \tag{4.2}$$

$$P_{wall.4} = 600\ kN \tag{4.3}$$

4.5.2 VARIABLE LOADS

The same variable loads are not used for both launching and for the final stage. For launching, the only variable load that are considered are the thermal impact. This will be explained in chapter 5. For the final construction, the following variable loads are included: thermal impact, wind- and traffic loads.

4.5.2.1 Traffic

Traffic loads has to be defined in NovaFrame. Parameters and loads due to traffic are defined in the *Traffic load input* card, where minimum and maximum eccentricities, distributed load or point load and distances between point loads are defined. Calculations are done after EC1-2 and are shown in Appendix C-2. As a simplification, horizontal loads due to traffic are neglected in this thesis. Results from Appendix C-2 are given in Table 4.1.

Table 4.1 Traffic loads in NovaFrame

LM1		LM2
	Q_{ik} [kN]	Q_{ak} [kN]
Lane 1	300	400
Lane 2	200	
Lane 3	100	

4.5.2.2 Wind load

Wind loads are defined in the *Load* input card as distributed loads given in kN/m. From N400, the following wind classes are found:

Wind class I: Bridges with insignificant dynamic effect from wind

Wind class II: Bridges with dynamic effect from wind which is non-neglectable

Wind class III: Bridges with severe dynamic effect from wind

Full calculations are found in Appendix C-3. Results from the calculations are given in Table 4.2.

Table 4.2 Wind loads

Wind load	F_{wx} [kN/m]	F_{wy} [kN/m]	F_{wz} [kN/m]
WITHOUT traffic	4,01997	1,00499	5,89602
WITH traffic	2,8889	0,72223	2,32953

4.5.2.3 Thermal load

Thermal loads are defined in the *Loads* input card. The thermal load is given differently for the launching model and the final construction model. This is because of simplicity when analysing all of the launching stages. The thermal load for launching is given by a temperature gradient *N*, which is calculated in Appendix C-4. In the input, the thermal coefficient $\alpha=10^{-5}$ m/ºC is used for both launching and final stage.

This thermal load for the final construction gives an increase in temperature in degrees and temperature gradient for local axes L and N. For the whole bridge, from element 3 to element 140, a temperature increase and temperature coefficient of 1,0 is added. The different temperature loads are added under *Load combinations*, where load combinations after EC1-1-5 are determined. The different load combinations are given in Table 4.3, and full calculations are found in Appendix C-4. From the command *Sortcomb*, the worst temperature load is found.

Table 4.3 Temperature loads in NovaFrame

Launching stages					
ΔT_{Mheat} [ºC]	ΔT_{Mcool} [ºC]	Temp. gradient over positive		Temp. gradient over negative	
10	5	2.85 [ºC/m]		1.43 [ºC/m]	
Final construction					
Load-combination	ΔT_{Mheat} [ºC]	ΔT_{Mcool} [ºC]	$\Delta T_{N.exo}$ [ºC]	$\Delta T_{N.con}$ [ºC]	Result [ºC]
1	10	-	0.35*21.525	-	17.534
2	10	-	-	0.35*(-42.681)	-4.938
3	-	5	0.35*21.525	-	12.534
4	-	5	-	0.35*(-42.681)	-9.938
5	0.75*10	-	21.525	-	29.025
6	0.75*110	-	-	-42.681	-35.181
7	-	0.75*5	21.525	-	25.275
8	-	0.75*5	-	-42.681	-38.931

4.5.3 CREEP

Loads due to creep are defined under the *Creep Load* input card. Before the creep loads are defined, the creep combination must be established. For Bagn bridge, there are only defined creep loads and combinations for the final bridge. As the effect of creep will be minimal and because of the large number of models during launching, a simplification is done to neglect the effect of creep during launching.

Two creep combinations are defined, one for 28 days after the final construction is done and one for 100 years. Both creep combinations are used for the same loadings: total self-weight and full prestressing. Factors used in creep combinations are set to 1,0.

Two creep load cases are defined – one for 28 days after final launch and one for when the bridge is 100 years old. Both load cases are set to act on the whole bridge, from element 3 to element 140. The creep factor is calculated by hand after Annex B in EC2, and full calculations are found in Appendix C-5. Results from calculations are given below.

$$\phi(t = 28, t_0) = 0{,}4732 \tag{4.4}$$

$$\phi(t = 36500, t_0) = 1{,}5679 \tag{4.5}$$

A simplification is made, where the fact that each segment has different age is neglected.

4.5.4 SHRINKAGE

Load due to shrinkage are defined under the *Loads* input card. Load type number 12 defines shrinkage, with a shrinkage strain in ‰. As for the creep loads, the shrinkage is defined for the whole bridge from element 3 to element 140.

The shrinkage strain is calculated after Annex B in EC2, and the calculations are done for 100 years. Full calculations are shown in Appendix C-6, which gave the following result:

$$\Delta\varepsilon_{p.shrinkage} = -0.2172‰ \tag{4.6}$$

4.6 PRESTRESSING

There are some parameters that need to be determined before the model in NovaFrame can be made. Among these are the area of prestressing tendons, tendon profile and loss of prestressing. In this chapter, parameters that need to be defined in NovaFrame are determined.

4.6.1 PRESTRESSING DURING LAUNCHING

For the launching stages, straight prestressing tendons are used. As a simplification in the model, the tendons are modelled as centric prestressing cables located a small eccentricity from the centre of gravity. For ILM, it is important that the centric prestressing tendons are placed as close to the CoG as possible to avoid undesirable deformations during launching. 26 tendons are used, with a duct diameter of 80 mm. The tendons consist of 12 strands, each with an area of 140mm^2.

The centric prestressing the resultant of the prestressing tendons placed at top and bottom flange of the box-girder. The realistic prestressing tendons are shown in Figure 4.5, where the eccentricities are found as following:

$$e_1 = H - cog - c_{nom} - \frac{Ø_{duct}}{2} = 1.06m \tag{4.7}$$

$$e_2 = cog - c_{nom} - \frac{Ø_{duct}}{2} = 2.06m \tag{4.8}$$

where

H is the height of the cross-section = 3500mm

CoG is the distance from the bottom to CoG = 2250,8mm

C_{min} is the cover to the duct, found in Chapter 3.4 to be 150 mm for top and bottom

$Ø_{duct}$ is the outer diameter of the duct, found in Chapter 3.2.4 to be 80mm

VSL Systems [17] states that for ILM, e_2 should be two times e_1. This is because the negative bending stresses for the most parts are twice the size of the positive bending stresses. Therefore, a cross-section with twice as big bottom modulus than top modulus is recommended. As seen from the equations above, this requirement is almost met. The centre of gravity should be moved up a little bit for better accuracy, but for simplicity this cross-section is used and assumed sufficient. The eccentricities are illustrated in Figure 4.5.

The placement of the centric prestressing is found by finding the resultant from the 14 pre-stressing tendons at top at distance e_1 and the 12 pre-stressing tendons at the bottom at distance e_2. By taking the moment about the CoG, the distance is found as following:

$$-14A_p\sigma_{p.max}e_1 + 8\sigma_{p.max}e_2 = 1.64A_p\sigma_{p.max} \quad 4.9$$

$$1.64A_p\sigma_{p.max} = 22 * x * A_p\sigma_{p.max} \rightarrow x = 0.0745m \quad 4.10$$

Figure 4.5 shows the arrangement of pre-stressing tendons during launching. The centric pre-stressing is illustrated at eccentricity *x*.

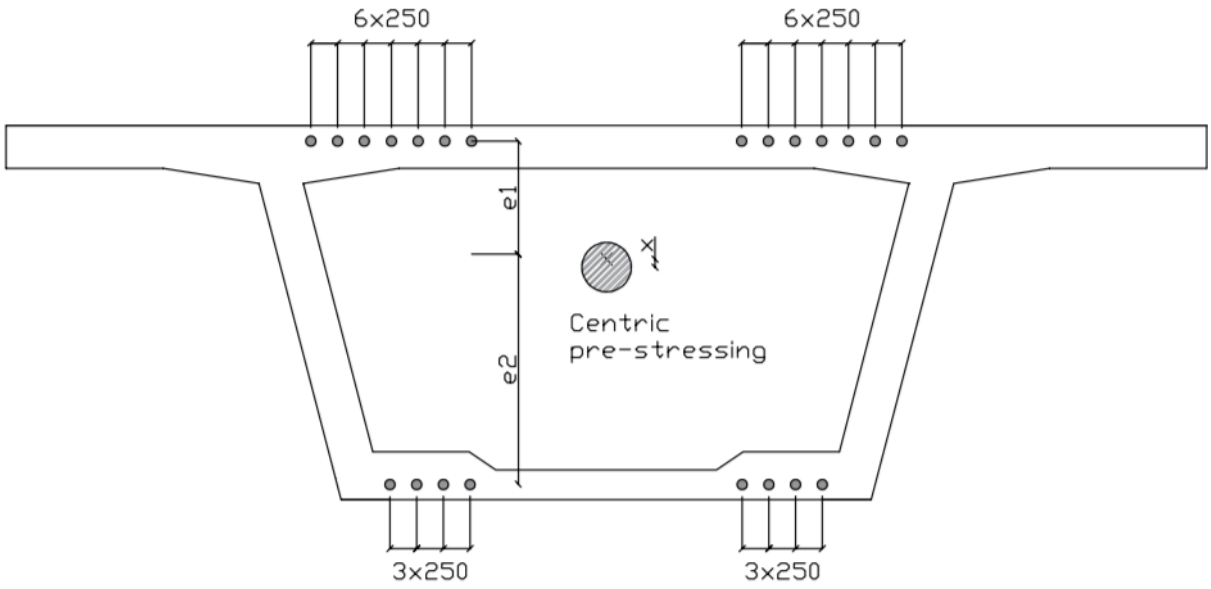

Figure 4.5 Arrangement of pre-stressing tendons during launching (Dimensions given in mm)

4.6.1.1 Prestressing force

The maximum prestressing force P_{max} and the initial prestressing force P_{m0} are calculated as explained in Chapter 2.5 and Chapter 2.5.1, and is found to be

$$P_{max} = A_p\sigma_{p,max} = 68\,191.2\ kN \quad 4.11$$

$$P_{m0} = A_p\sigma_{pmm0} = 64\,402.8\ kN \quad 4.12$$

4.6.2 PRESTRESSING FOR FINAL CONSTRUCTION

As explained in Chapter 2.4.3 additional prestressing tendons are needed for the final construction. An idealized prestressing profile is used to determine the tendon sag in each span. This profile is usually not used for post-tensioning, as the sharp cups over the supports do not appear in the tendons. These are adjusted to avoid the kinking, and the profile is fitted to a continuous curve with gradient continuity throughout.

Load balancing, as explained in Chapter 2.4.2 are used to define the prestressing forces. The eccentricities e_1 and e_2 are necessary to compute the equivalent loads. By using an idealized tendon profile, as shown in Figure 4.7, the eccentricities are found. The same values are used here as in equation 4.7 and 4.8. The arrangement of tendons is shown in Figure 4.6

$$e_1 = 1.06\ m \tag{4.13}$$

$$e_2 = 2.06\ m \tag{4.14}$$

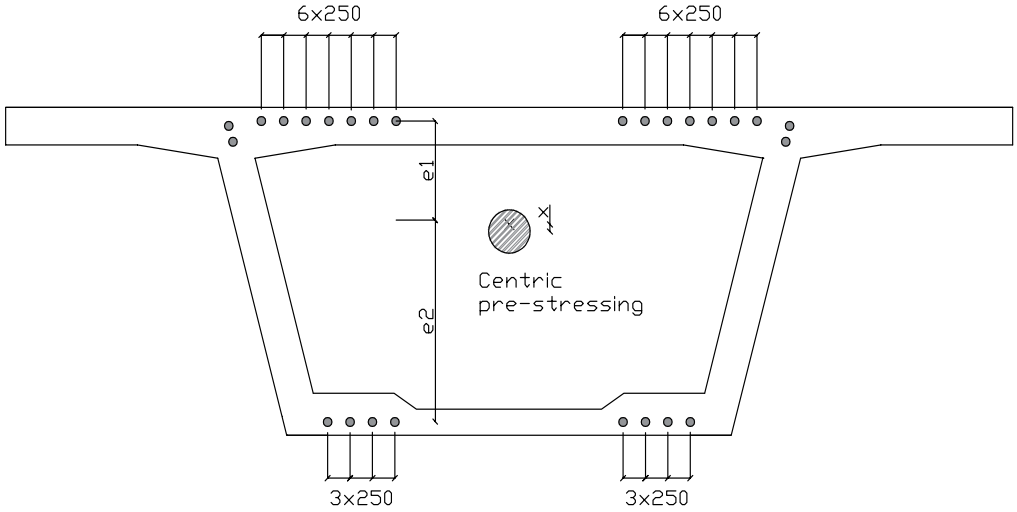

Figure 4.6 Arrangement of tendons for the final construction (Dimensions given in mm)

To make the idealized tendon profile as shown in Figure 4.6 such that it is a parabolic curve with gradient continuity, the sharp cups over the supports has to be made as continuous parabolas. NovaFrame requires distances in X and Y-direction for the tendon profile. These are found by looking at each span separately.

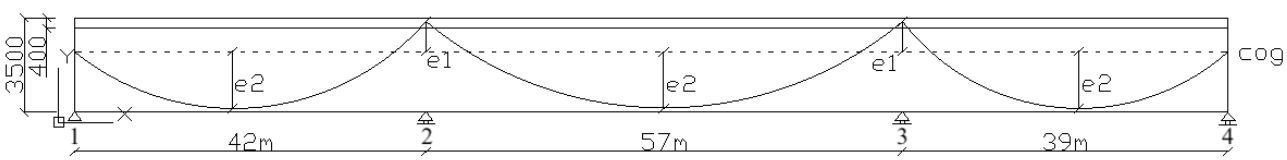

Figure 4.7 Idealized tendon profile for Bagn bridge

4.6.2.1 Prestressing profile for span 1-2

The actual cable profile is given in Figure 4.7 for span 1-2. Properties of parabolic tendon profile has been calculated. To find the distance *a*, one has to look at each curve separately. Curve ABC is formed by the following equation.

$$y_{ABC} = -e_2 + A_1(a - x)^2 \tag{4.11}$$

By examining the given heights in Figure 4.7, one may see that when *x=0*, *y* is also equal to zero. By adding this to the curve equation, A_1 is found as following:

$$A_1 = \frac{e_2}{a^2} \tag{4.12}$$

It is also found that for x=a, y=-e_2. The second curve, CD, is given by the formula.

$$y_{CD} = e_1 + A_2(L - x)^2 \tag{4.13}$$

As they shall form a curve with gradient continuity, equation 4.11 should be equal to equation 4.13 for x=L_1-b. From Sørensen [8] it is known that b=0,1L_1=4,2m. The gradient should also be ensured at the connecting point, which is done by setting the derivative with respect to x=L_1-b of equation 4.11 and equation 4.13. When these two requirements are ensured, the constants A_1 and A_2 are found to be the following:

$$A_1 = -\frac{e_1 + e_2}{(a - L + b)(L - a)} \tag{4.14}$$

$$A_2 = -\frac{e_1 + e_2}{(L - a)b} \tag{4.15}$$

Further, the distance *a* is determined by setting equation 4.12 equal to equation 4.14. This gives:

$$a = 17{,}842m \tag{4.16}$$

and the height of the curve at x=L-b is found to be:

$$y_{x=L-b} = 0{,}5176m \tag{4.17}$$

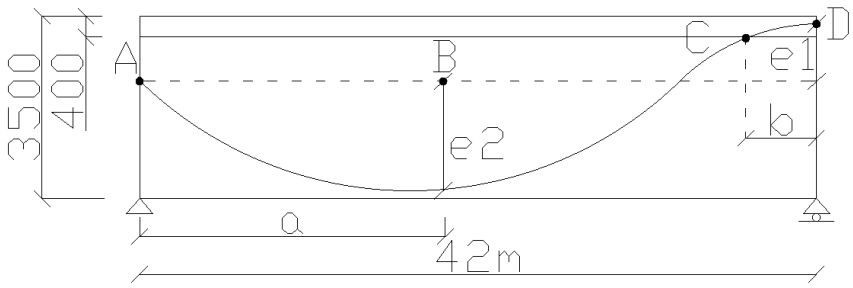

Figure 4.8 Realistic tendon profile for span 1-2

4.6.2.2 Tendon profile for span 2-3

Because of symmetry, *a*, *b* and *c* are found by looking at Figure 4.8. Distance *a* and *c* are calculated the same way as for span 1-2, whereas they are considered to be 0,1*the length of the span. The distance *b* is found to be half of the span length.

$$a = c = 0{,}1L = 5{,}7m \tag{4.18}$$

$$b = \frac{L}{2} = 28{,}5m \tag{4.19}$$

The heights at point B and D are found by looking at the curve formulas.

Curve AB: 0<x<a

$$y_{AB} = e_1 + A_1 x^2 \tag{4.20}$$

Curve BCD: a<x<L-c

$$y_{BCD} = -e_2 + A_1 (b - x)^2 \tag{4.21}$$

Curve DE: L-c<x<L

$$y_{DE} = e_1 + A_3 (L - x)^2 \tag{4.22}$$

As all three curves shall form one curve with gradient continuity, equation 4.20 should be equal to equation 4.21 for x=a and the derivative with respect to x=a of the same equations should also be equal.

$$e_1 + A_1 a^2 = -e_2 + A_2 (b - a)^2 \tag{4.23}$$

$$\frac{dy_{AB}}{d(a)} = \frac{dy_{BCD}}{d(a)} \rightarrow 2A_1 a = -2A_2 (b - a) \tag{4.24}$$

By solving these two, one will get the following formulas for A_1 and A_2:

$$A_2 = \frac{e_1 + e_2}{b(b - a)} \tag{4.25}$$

$$A_1 = -\frac{e_1 + e_2}{ab} \tag{4.26}$$

The gradient continuity shall also be ensured at the connecting point D. This is done by setting equation 4.21 equal to equation 4.22 for x=L-c and the derivative with respect to x=L-should also be equal for the same equations.

$$-e_2 + A_2(b-(L-c))^2 = e_1 + A_3(L-(L-c))^2 \quad 4.27$$

$$\frac{dy_{BCD}}{d(L-c)} = \frac{dy_{DE}}{d(L-c)} \rightarrow -2A_2(b-L+c)^2 = -2A_3c \quad 4.28$$

From Equation 4.27. and 4.28, A_2 and A_3 may be calculated, and are found to be

$$A_2 = \frac{e_1 + e_2}{(b-L)(b-L+c)} \quad 4.29$$

$$A_3 = \frac{e_1 + e_2}{c(b-L)} \quad 4.30$$

From this, the heights at point B and D may be found as following:

$$y_{AB,x=a} = e_1 + A_1a^2 = 0{,}436m \quad 4.31$$

$$y_{DE,x=L-c} = e_1 + A_3(L-(L-c))^2 = 0.436m \quad 4.32$$

Equation 4.31 and 4.32 both give the same height, which proves that the curved profile shown in Figure 4.9 is symmetric.

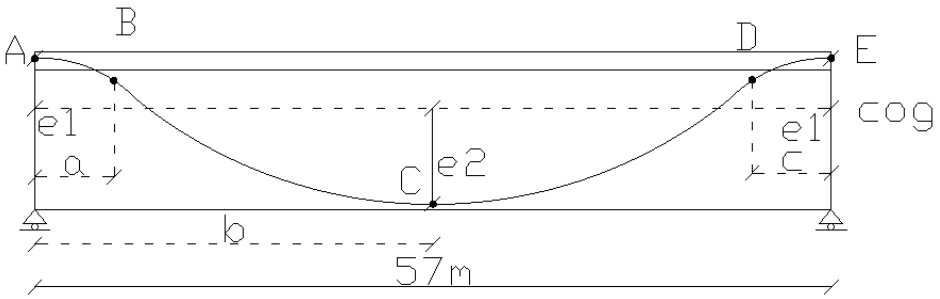

Figure 4.9 Realistic tendon profile for span 2-3

4.6.2.3 Tendon profile for span 3-4

Calculations for span 3-4 are identical to the calculations for 1-2, except the span length is 39 meters. This gives the following:

$$y_{DCB} = -e_2 + A_1(a - x)^2 \quad 4.33$$

$$y_{BA} = e_1 + A_2(L - x)^2 \quad 4.34$$

$$A_1 = -\frac{e_1 + e_2}{(a - L + b)(L - a)} = \frac{e_2}{a^2} \quad 4.35$$

$$A_2 = -\frac{e_2 + e_3}{(L - a)b} \quad 4.36$$

Further, the distance *a* is determined by setting equation 4.33 equal to equation 4.34. This gives

$$a = 16{,}5677m \quad 4.37$$

and the height of the curve at x=b is found to be:

$$y_{x=b} = 0{,}5175m \quad 4.38$$

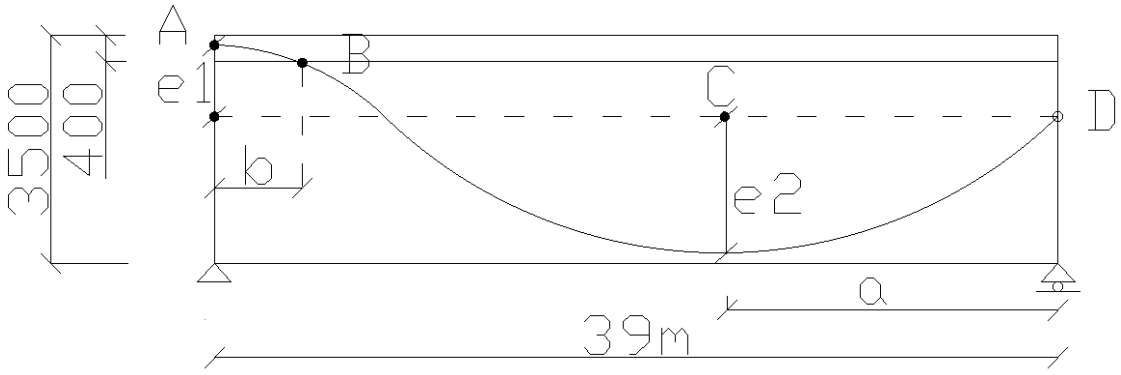

Figure 4.10 Realistic tendon profile for span 3-4

4.6.2.4 Summary – tendon profile

The placement of the tendons in L-direction is not of any importance when it comes to the analysis. Therefore, as a simplification, all prestressing tendons are placed in CoG in L-direction. The placements in N-direction is given in Table 4.4.

Table 4.4 Tendon geometry in N-direction

Tendon	Element start	Element end	Curve type	Offset A	Offset B
2-5	3	20	1	0.00	-2.06
2-5	20	40	2	-2.06	0.5176
2-5	40	45	2	0.5176	1.06
2-5	45	49	1	1.06	0.436
2-5	49	72	3	0.436	-2.06
2-5	72	95	2	-2.06	0.436
2-5	95	102	2	0.436	1.06
2-5	102	106	1	1.06	0.5175
2-5	106	127	3	0.5175	-2.06
2-5	127	140	1	-2.06	0.00

Explanations for the different curve types are given in Figure 4.10.

Type	Curve segments	Properties
Type 1 Typically left end of tendon	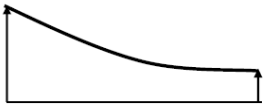	Length = L Y'' (0) = 0 Y'(L) = 0
Type 2 S-curve	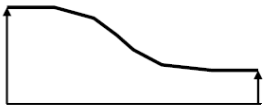	Length = L Y' (0) = 0 Y'(L) = 0 Y''(L/2) = 0
Type 3 Typically right end of tendon	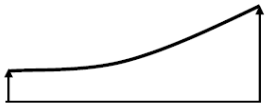	Length = L Y' (0) = 0 Y''(L) = 0

Figure 4.11 Explanation of tendon curve types in NovaFrame [16]

4.6.2.5 Prestressing force

The maximum prestressing force P_{max} and the initial prestressing force P_{m0} are calculated as explained in Chapter 2.5 and Chapter 2.5.1, and is found to be

$$P_{max} = A_p \sigma_{p,max} = 12\,398.4\ kN \quad (4.39)$$

$$P_{m0} = A_p \sigma_{pmm0} = 11\,709.6\ kN \quad (4.40)$$

4.6.3 LOSS OF PRESTRESSES

There will be a loss of the measured jacking force in the prestressing steel. This loss occurs due to different reasons, such as loss of strain-difference, creep and shrinkage in the concrete and relaxation in the prestressing steel [8].

4.6.3.1 Loss of pre-stress due to friction

Friction forces will occur in the ducts in the superstructure as the prestressing steel is post-tensioned. These friction forces will counteract the sliding between the steel and the duct.

For the straight centric prestressing tendons, the duct is fixed at certain points in the box-girder. Therefore, the duct will never be perfectly straight. This will lead to friction during post-tensioning.

NovaFrame requires input of the factors for friction and wobble effect to calculate the losses. The coefficient of friction μ are given in [16] for 12 strand wires as 0,18 rad^{-1}. The wobble factor is given as 0,005 rad/m.

4.6.3.2 Creep

Loss of prestress due to creep is to be calculated before inserting values in NovaFrame.

Loss of prestressing force is calculated for both the launching stages and for the final construction. For the launching stages creep is calculated at time t=28 days and for the final construction, creep is calculated for time t=100years.

Full calculations are found in Appendix D-1 and D-2 for launching stages and the final bridge construction. The results are represented in Table 4.5 and 4.6.

Table 4.5 Loss of prestress due to creep – FINAL CONSTRUCTION

	$M_{t.span}$ [kNm]	σ_c [MPa]	$\Delta\varepsilon_p$	$\Delta\sigma_p=\Delta\varepsilon_p*E_p$ [MPa]
Long-term	- 117 977	-5,522	$-3{,}939*10^{-4}$	-76,803
Short-term	- 125 745	-8,455	$-2{,}349*10^{-4}$	-45,799

Table 4.6 Loss of prestress due to creep – LAUNCHING STAGES

	$M_{t.span}$ [kNm]	σ_c [MPa]	$\Delta\varepsilon_p$	$\Delta\sigma_p=\Delta\varepsilon_p*E_p$ [MPa]
Short-term	- 78 268	-3,386	$-9{,}405*10^{-5}$	-18,339

4.6.3.3 Shrinkage

Loss of prestress due to shrinkage is determined to be included in the model. As in Chapter 4.5.4, shrinkage is determined with a simplified method according to EC2. The loss of prestressing due to shrinkage is calculated after formulas given in [8]. Total calculations are found in Appendix D-1 and D-2 for the final construction and the launching stages, which gave the following result:

$$Final: loss_{long-term} = 2{,}192\% \quad 4.41$$

$$Final: loss_{short-term} = 0{,}933\% \quad 4.42$$

$$Launch: loss_{short-term} = 0{,}906\% \quad 4.42$$

4.6.3.4 Relaxation

NovaFrame requires input when it comes to the relaxation of the prestressing steel. The following values are to be defined:

S1 Relaxation, stress with no losses [%]

S2 Relaxation, stress with losses [%]

T2 Relaxation, loss at stress S2 [%]

These three values are given as a percentage of $f_{p0,1k}$. For Class 2: wire or strand with low relaxation, the value for T2 is given as 2,5%. This value is determined by tests which are conducted for 1000 hours, with an initial stress of 70% of the tensile strength f_{pk} [13]. It is also normal to use calculations with 4,5% relaxation at $0{,}8f_{pk}$. From extrapolation, S1 is found to be at $0.575f_{pk}$. This gives the following:

$$S1 = \frac{0{,}575 f_{pk}}{f_{p0,1k}} * 100\% = 65\% \quad 4.43$$

$$S1 = \frac{0{,}70 f_{pk}}{f_{p0,1k}} * 100\% = 79\% \quad 4.44$$

$$T2 = 2{,}5\% \quad 4.45$$

4.7 VERIFICATION OF MODEL IN NOVAFRAME

Manual calculation is performed to ensure that the output from NovaFrame are within reasonable values. There are a lot of input to the NovaFrame model, and errors may occur. Verifications are done for the final construction stage.

4.7.1 CONTROL OF CROSS-SECTIONAL PARAMETERS

A control is performed to check that the cross-sectional parameters in NovaFrame are correct. To do this, a simplified cross-section is used. The simplified cross-section has the same flange width as the model in NovaFrame but is rectangular. The simplified cross-section is illustrated in Figure 4.11.

Complete calculations are found in Appendix E-1 and are represented in Table 4.6. From the table one can see that there is little deviation between the two cross-sections.

Table 4.7 Verification of cross-sectional parameters in NovaFrame

	NovaFrame	Simplified cross-section	Deviation[%]
Area	8,82 m^2	9,03 m^2	2.3
I_x	14,92 m^4	16,72 m^4	10
I_y	70,72 m^4	70,83 m^4	0

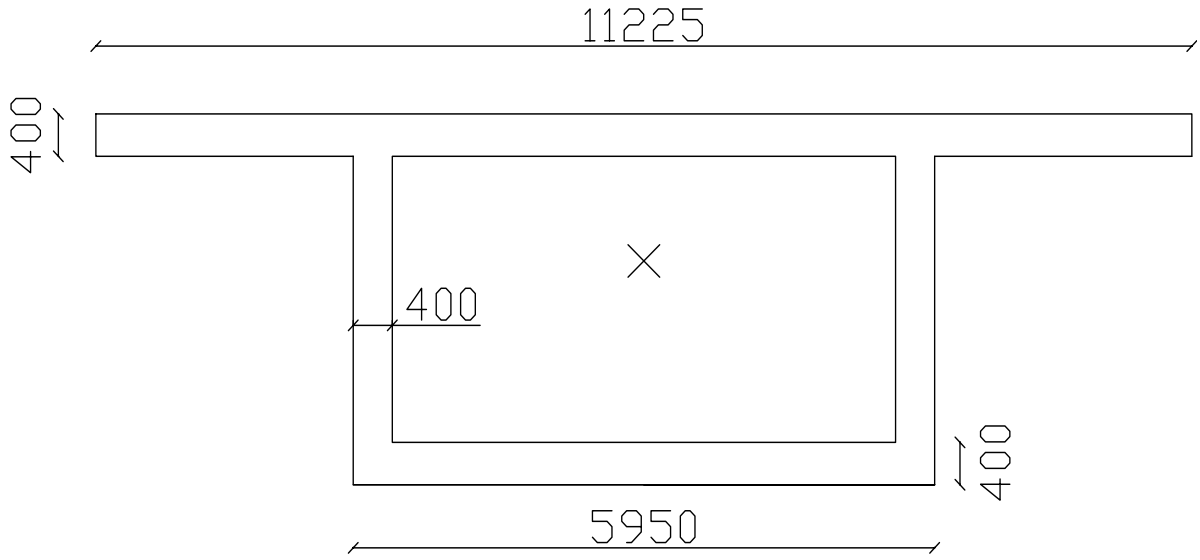

Figure 4.12 Simplified cross-section (Dimensions given in mm)

4.7.2 *CONTROL OF SELF-WEIGHT*

For Bagn bridge, the prestressed concrete has a self-weight of 26kN/m^3. From Table 4.6, the area of the cross-section is found to be 8,82m^2. This gives the evenly distributed load q_{SW}, as shown in equation 4.46.

$$q_{SW} = 26\ \frac{kN}{m^3} * 8{,}82\ m^2 = 229.32\ kN/m \tag{4.46}$$

This load is used to calculate the moments due to self-weight. Full calculations are shown in Appendix E-2. The load is applied as illustrated in Figure 4.12. The model in NovaFrame is simplified, as explained in Chapter 1.3, and does not include the columns of the bridge. These will not be included in further calculations either.

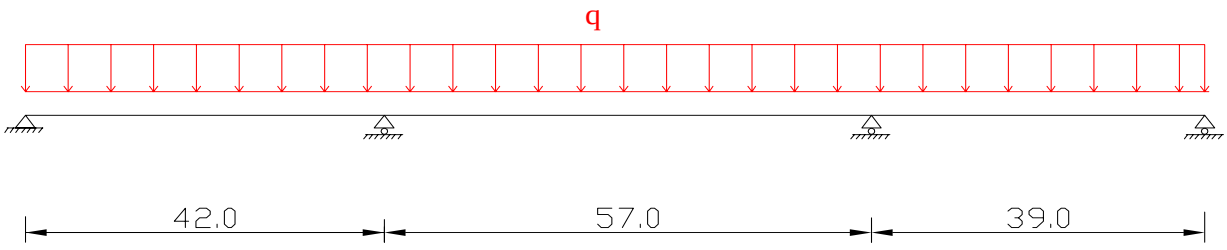

Figure 4.13 Static model of Bagn bridge (Dimensions given in m)

As Figure 4.12 illustrates, the bridge consists of four supports: one which is pinned and three which are roller supports. This gives the total of five reaction forces, NF. The number of equations, NE, used to solve the system is three. The degree of indeterminacy, or the reduntants, is given by the following equation:

$$R = NF - NV = 5 - 3 = 2 \tag{4.47}$$

As the degree of indeterminacy is higher than one, the moment distribution method is used. The results are represented in Table 4.7.

Table 4.8 Verification of moments in NovaFrame

	Span 1-2	Support 2	Span 2-3	Support 3	Span 3-4
Calculations by hand [kNm]	25 330	-59 099	35 854	-55 465	20 267
NovaFrame [kNm]	25 328	-59 108	35 852	-55 463	20 268
Deviation [%]	0	0	0	0	0

4.7.3 SUMMARY

The results from the verification calculations shows that there are small deviations from the model in NovaFrame in regard to moments due to self-weight and the cross-sectional parameters, and it is considered safe to assume that result from NovaFrame are correct.

5 ANALYSIS OF STAGE CONSTRUCTION

When analysing the bridge, there are different stages which are crucial for the design. In this analysis, 136 stages of the bridge are modelled, and some stages are shown in Figure 5.1. As the bridge acts as a cantilever during the launching, the bending moments will be high. Centric prestressing is used to withstand these moments.

Only permanent loads and loads due to temperature is included in the analysis. Traffic loads will not act on the bridge before after the final launch and is therefore irrelevant for this analysis. Also, effects due to creep are not considered. This is simply because it would be very time consuming to add creep to all 136 models compared to how little effect it would give. Wind load is also neglected in the analysis for the launching of the bridge. Calculations are done by hand in Appendix C-3 shows that the loads due to wind are very small. It is the piers that would be affected the most due to wind. As these are neglected (ref. chapter 1.3), a simplification is therefore made to exclude the effect due to wind in the launching stages.

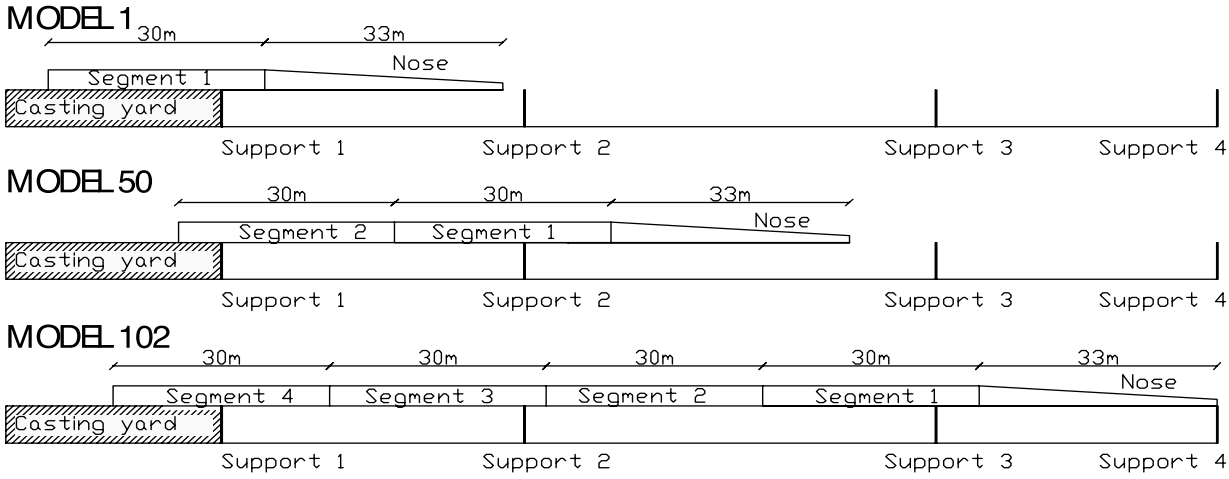

Figure 5.1 Illustration of selected models

Figure 5.2 shows the variation of bending moments at span 1-2 and 2-3 and at support 2 and 3. The x-axis is given as the position in meters of the launching nose at distance *x* from support 1. From analysis of the models in NovaFrame, it is found that the worst-case loadings which gave the highest moments at support and span were found in model 62 and model 92 respectively. Design at ULS for these two models are performed.

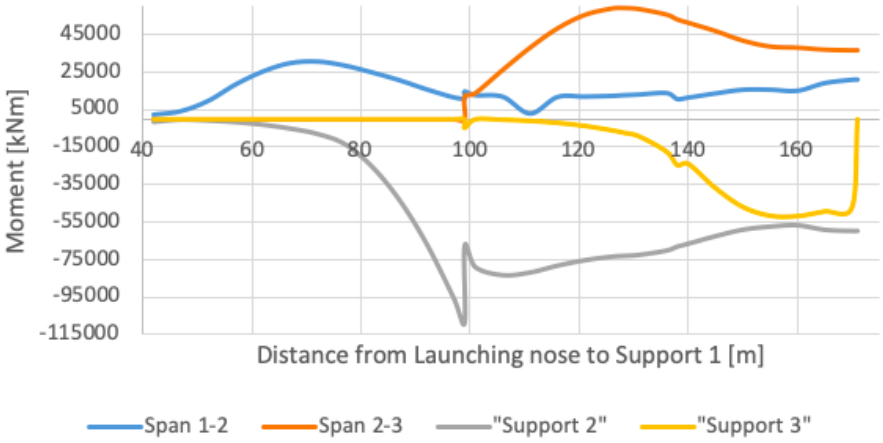

Figure 5.2 Variation of moments for all 136 models at distance x [m] from support 1

5.1 ULS

Even though bridges are usually performed in SLS, it is important to control that the structure has sufficient capacity at ULS. During launching, most of the variable loads are neglected. The load cases used in the design at ULS are self-weight, prestressing and thermal load. At ULS, it is controlled that the design values for shear and moment are within the limits of the capacity. Simplified load combinations after Table 2.1 is created for the analysis of launching. Load combinations during launching at ULS is shown in Table 5.1.

Table 5.1 ULS load combinations - during launching

ULS – Characteristic				
Load combination		**G**	**PS**	**TE**
1	(2.21)	1,35	0,9/1,1	0,84
2	(2.22)	1,20	0,9/1,1	1,20
3	(2.22)	1,20	0,9/1,1	0,84

5.1.1 ULTIMATE MOMENT CAPACITY

Complete calculations are found in Appendix F-1.

Figure 5.2 shows a rectangular cross-section with prestressed steel, A_p, in the tensile zone. From this figure, the ultimate moment capacity, M_{Rd}, can be found as following:

$$M_{Rd} = T_c z \tag{5.1}$$

Where T_c is the resultant force of the compressive zone of the concrete and z is the inner leaver arm.

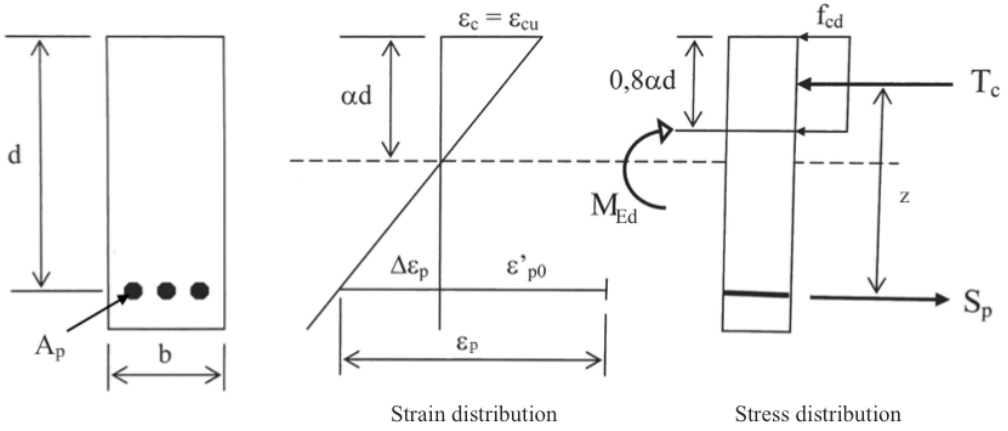

Figure 5.3 Cross-section with prestressing steel in tensile zone [10]

The height of the tensile zone, αd, is determined by axial equilibrium, as shown in equation 5.2.

$$T_C = S_P \tag{5.2}$$

Where T_c is calculated as following:

$$T_c = 0.8 f_{cd} \alpha b d \tag{5.3}$$

The force in the prestressed steel, S_p, depends on whether the total strain for the prestressed steel $\varepsilon_p \geq \frac{f_{02}}{E_{sk}}$ (yield) or $\varepsilon_p < \frac{f_{02}}{E_{sk}}$ (elastic). This is determined by defining a "balanced" cross-section for prestressed steel, when the steel reaches yield at the same time as the concrete reaches compressional fracture strain [10]. This is shown in Figure 5.3 where α_b is found as following:

$$\alpha_b = \frac{\varepsilon_{cu}}{\Delta\varepsilon_p + \varepsilon_{cu}} = \frac{\varepsilon_{cu}}{\frac{f_{pd}}{E_p} - \varepsilon'_{p0} + \varepsilon_{cu}} \tag{5.4}$$

where

ε_{cu} is the compressive strain in the concrete

$\varepsilon`_{p0}$ is the effective strain difference

ε_{p0} is the initial strain difference

σ_{pm0} is the stress in the tendon immediately after tensioning

When inserting values in equation 5.4, the compression-zone height factor is found to be

$$\alpha_b = 0{,}739 \tag{5.5}$$

Equation 5.2 and 5.3 gives the following expression, where S_p is taken as $f_{pd}A_{pb}$

$$0{,}8 f_{cd} \alpha_b b d = f_{pd} A_{pb} \tag{5.6}$$

With the current effective difference in strain, the balanced prestressing steel area, A_{pb}:

$$A_{pb} = 0{,}8 \frac{f_{cd}}{f_{pd}} \alpha_b b d \tag{5.7}$$

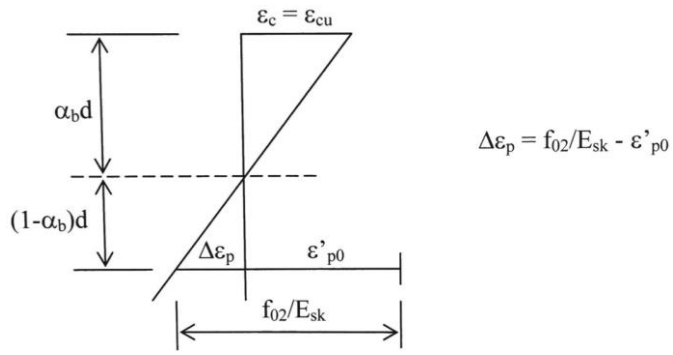

Figure 5.4 Strains at fracture for balanced prestressed cross-section [10]

5.1.1.1 Design for maximum moment at support

When finding the prestressing in the top of the superstructure, the minimum moment from the envelope is used. From analysing the model, it is found that this moment corresponds to the moments in model 62, at support 2. This model is the model right before the launching nose reaches the third support. Moment diagram is shown in Figure 5.4.

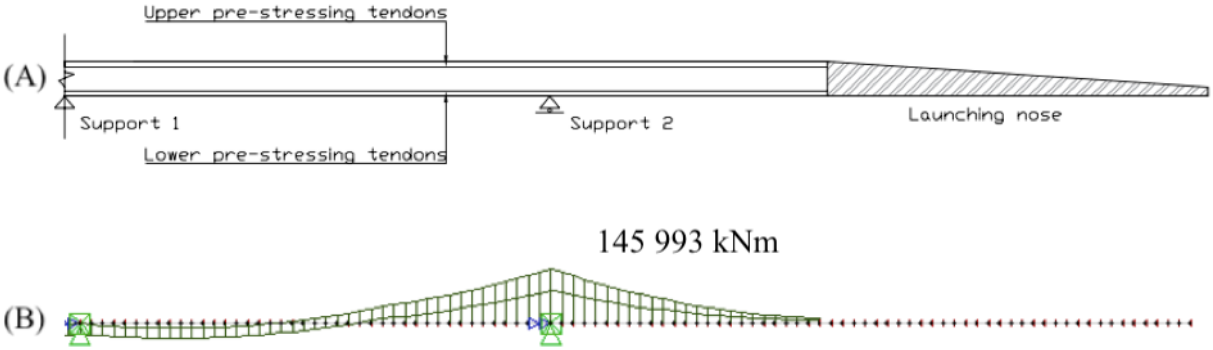

Figure 5.5 (A) Tendon layout and (B) moment diagram for model 62

$$M_{Ed} = 145\ 993\ kNm \tag{5.8}$$

When using the moment at supports, EC2 states that the design moment shall be set equal to the moment at the edge of the support. However, the reduced design moment may also be taken as a 10% reduction of the design moment [13] [18]. For Bagn bridge, the reduces design moment is found as following:

$$M_{Ed.red} = 0.90 * M_{Ed} = 131\ 394\ kNm \tag{5.9}$$

When considering the moment at support, the top flange of the box-girder will be in tension. Therefore, the effective width at supports are found as the bottom width of the cross-section: $b_{bottom} = 4.95\ m$. The effective depth at the support is found to be $d_{support} = 3.31\ m$.

From equation 5,7, the balanced prestressed steel area is found to be the following.

$$A_{pb} = 0{,}17\ m^2 > A_p = 0{,}017\ m^2 \quad 5.10$$

For prestressed steel with $A_p \leq A_{pb}$ the section has to little reinforcement, and the force in the prestressed steel S_p may be found as $f_{pd}A_p$. From equation 5.6, α can now be determined.

$$\alpha = \frac{f_{pd}A_p}{0{,}8f_{cd}bd} = 0.13 \quad 5.11$$

The internal leaver arm, z, is found as in equation 5.12, but shall not be smaller than 0,9d

$$z = (1 - 0{,}4\alpha)d = 3{,}14\ m > 0{,}9d = 2{,}979 \quad OK! \quad 5.12$$

Further, the ultimate moment capacity is calculated

$$M_{Rd} = T_c z = 131\ 394\ kNm \quad 5.13$$

A control of the ultimate moment to check if it is more than or equal to the design moment is then performed.

$$M_{Rd} > M_{Ed.red} \quad 5.14$$

Moment capacity is sufficient to withstand the design moment.

5.1.1.2 Control of moments in span

When finding prestressing in the bottom of the superstructure, the maximum moment in the moment envelope is used. This moment is found in model 92, in span 2-3. Moment diagram is shown in Figure 5.5.

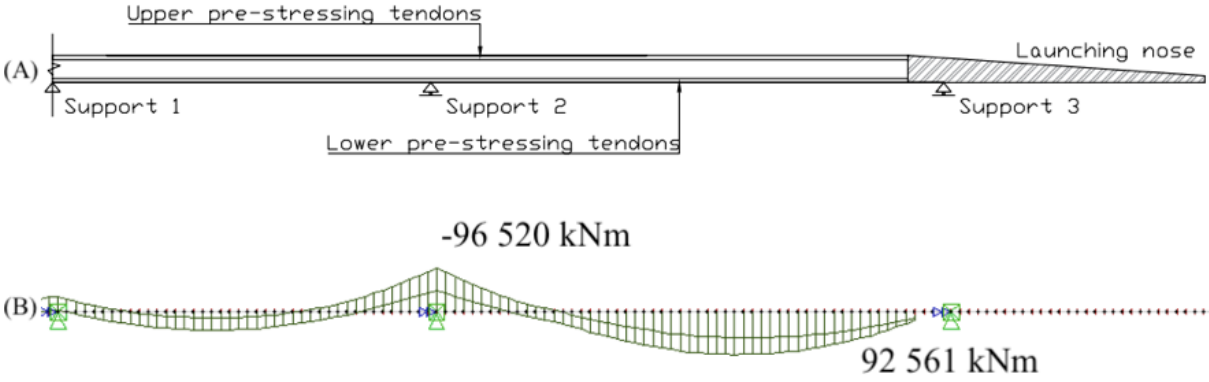

Figure 5.6 (A) Tendon layout and (B) Moment diagram for model 92

$$M_{Ed} = 92\,561\ kNm \tag{5.15}$$

When considering the moment in span, the bottom flange of the box-girder will be in tension. Therefore, the effective width at supports are found as the width of the top flange of the cross-section: $b_{top} = 11\,225\ m$. The effective depth over the support is found to be $d_{support} = 3.31\ m$.

When inserting values into equation 5,7, the balanced prestressing steel area is found to be

$$A_{pb} = 0{,}393\ m^2 > A_p = 0{,}0202\ m^2 \tag{5.16}$$

From equation 2.16, α can now be determined. As $A_p \leq A_{pb}$ the section has to little reinforcement, and one can use S_p as $f_{pd}A_p$. This gives

$$\alpha = \frac{f_{pd}A_p}{0{,}8 f_{cd} b d} = 0.03 \tag{5.17}$$

The internal leaver arm, z, is calculated and found in equation 5.18.

$$z = (1 - 0{,}4\alpha)d = 3{,}27\ m > 2{,}979 \quad OK! \tag{5.18}$$

Further, the ultimate moment capacity is calculated

$$M_{Rd} = T_c z = 78\,299\ kNm \tag{5.19}$$

A control of the ultimate moment to check if it is more than or equal to the design moment is then performed.

$$M_{Rd} < M_{Ed.red} \tag{5.20}$$

Moment capacity is NOT sufficient to withstand the design moment. Additional reinforcement of 15Ø25c330 is required.

5.1.2 *SHEAR RESISTANCE*

Full calculations are found in Appendix F-2.

When structures are subjected to shear forces, cracks may occur. Determination of the shear resistance and the required shear reinforcement is necessary to minimize these cracks. Shear calculations are done after EC2 Clause 6.2.2. The maximum shear force is found in the analysis of the model in NovaFrame and are shown in Figure 5.6. This maximum shear force corresponds to model 93, at support 2. This is the shear force that are controlled.

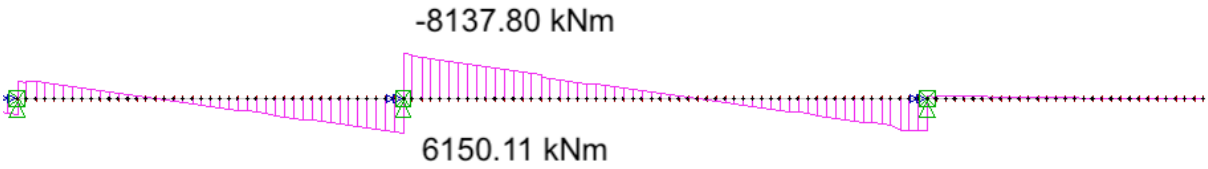

Figure 5.7 Shear force for model 93

$$V_{Ed} = 8138\ kN \tag{5.21}$$

Equal to the reduced moment at support, the shear force is reduced by 10%:

$$V_{Ed.red} = 0.9 * V_{Ed} = 7324\ kNm \tag{5.22}$$

EC2 states different verification procedures which are to be used when checking for shear resistance. These are shear capacity without shear reinforcement, shear capacity with shear reinforcement and the design value of the maximum shear force.

The cross-section is assumed to be uncracked and a control is performed to check if there is, on the basis of design calculations, a need for shear reinforcement. To check for this, the following requirement has to be met:

$$V_{Ed} \leq V_{Rd,c} \tag{5.23}$$

$V_{Rd,c}$ is found by the following formula

$$V_{Rd,c} = max\{[C_{Rd,c}k(100\rho_1 f_{ck})^{1/3} + k_1\sigma_{cp}]b_w d\ ;(v_{min} + k_1\sigma_{cp})b_w d\ \} \tag{5.24}$$

where

k is a factor found by the formula $1 + \sqrt{\frac{200}{d}} = 1{,}25 \leq 2{,}0$ for d=3310mm

ρ_1 is found by the formula $\frac{A_p}{b_w * d} = 0{,}01$

b_w is the width of the web. For box-girders this corresponds to 2*web width = 900mm

k_1 is a factor of value 0,15 when in compression

$C_{Rd,c}$ is given as following: $\frac{k_2}{\gamma_c} = 0{,}12$

k_2 is a factor of value 0,18

σ_{cp} is given as: $\sigma_{cp} = \frac{N_{Ed}}{A_c} = \frac{P_s}{A_c} = 5{,}06\ kN \leq 0{,}2 f_{cd} = 5{,}1 MPa\ OK!$

P_s is the axial force from the prestressing tendons, equal to 44 634 kN

A_c is the concrete cross-sectional area = 8,82m^2

v_{min} is found by the formula $0{,}035 k^{3/2} f_{ck}^{1/2} = 0{,}324$

A_p is the total area of the prestressing tendons, and is equal to 33 600mm^2

This gives the following design shear capacity:

$$V_{Rd,c} = 3998{,}3\ kN \tag{5.25}$$

As V_{Ed} > capacity $V_{Rd.c}$, it is required to calculate the design shear reinforcement.

5.1.2.1 Shear capacity with shear reinforcement

EC2 states that structures with vertical shear reinforcement, the shear capacity is found as following:

$$V_{Rd.max} = \frac{\alpha_{cw} b_w z v_1 f_{cd}}{cot\theta + tan\theta} \tag{5.26}$$

where

α_{cw} is a coefficient taking the state of the stress in the compression chord into account

$= 1 + \frac{\sigma_{cp}}{f_{cd}} = 1{,}2$

b_w is the width of the web. For box-girders this corresponds to 2*web width = 900mm

z is the inner leaver arm $= 0{,}9d = 2{,}979m$

v_1 is a strength reduction factor for the concrete cracked in shear $= 0{,}6$

θ is an angle determined by the national annex in EC2

$\theta_{max} = 45\ degrees$

$\theta_{max} = 38{,}66\ degrees$

This gives

$$V_{Rd.max} = 21\ 831\ \text{kN} \tag{5.27}$$

As $V_{Rd.max}$ is larger than V_{Ed}, the shear reinforcement may be calculated. By assuming 8 bars of diameter Ø12, the spacing is calculated by equation 5.28. $V_{Ed.red}$ is used in this formula, as this will provide the exact required reinforcement.

$$s = \frac{A_{sw} z f_{ywd} cot\theta}{V_{Ed.red}} = 250\ mm \tag{5.28}$$

Thus, 8Ø12s250 is the required shear reinforcement.

5.2 SLS

Prestressed structures are usually designed at SLS. For the launching stages, only crack limitations are performed. The decompressions are only considered a requirement for the durability to protect the reinforcement from the loads when traffic is considered. As there are no traffic load during launching, the decompression is neglected. The stress limitations are performed to limit cracks and large deformations due to creep. The allowable crack width is 0.6mm during launching [3]. The stress limitations will apply for smaller cracks than what is allowable during the launching process and are therefore not relevant.

Load combinations at SLS is defined in Table 2.2. As many of the loads are neglected during launching, simplified load combinations are created for the launching stages at SLS. These are given in Table 5.2.

Table 5.2 Load combination at SLS - Launching stages

SLS – Characteristic combination				
Load combination		**G**	**PS**	**TE**
1.1	2.24	1,0	1,0	1,0
1.2	2.24	1,0	1,0	0,7
SLS – Frequent combination				
Load combination		**G**	**PS**	**TE**
2.1	2.25	1,0	1,0	0,7
2.2	2.25	1,0	1,0	0,2
SLS – Quasi-permanent combination				
Load combination		**G**	**PS**	**TE**
3.1	2.26	1,0	1,0	0,5

5.2.1 CRACK CONTROL

According to EC2, cracks are to be limited so that the function or durability of the structure are not damaged or gives it an unacceptable appearance. Cracks occurs when the structure is subjected to bending, shear, torsion, tension or plastic shrinkage, but as long as the cracks don´t affect the structures, they are acceptable [13]. EC2 gives recommended values for crack width, as shown in Figure 5.7. The value k_c takes the effect of a cover which are greater than the required $c_{min,dur}$ into account, and are given by the following formula:

$$k_c = \frac{c_{nom}}{c_{minmdur}} \leq 1{,}3 \qquad 5.22$$

Exposure Class	Reinforced members and prestressed members with unbonded tendons		Prestressed members with bonded tendons [3]	
	Load combination	Limiting value	Load combination	Limiting value
X0	Quasi-permanent	0,40 [1]	Frequent	0,30 k_c
XC1, XC2, XC3, XC4	Quasi-permanent	0,30 k_c	Frequent	0,20 k_c
XD1, XD2, XS1, XS2	Quasi-permanent	0,30 k_c	Frequent	0,20 k_c
			Quasi-permanent	Decompression [2]
XD3, XS3	Frequent	0,30 k_c	Frequent	Decompression [2]
XSA	Given special consideration [4]		Given special consideration [4]	

[1] For the X0 exposure class, crack width has no influence on durability, and this limit is set to guarantee acceptable appearance. In the absence of appearance conditions, this limit may be relaxed.

[2] Where verification that decompression does not occur is required, the whole section of pre-stressing steel and where relevant the duct for post-tensioned tendons, should lie at least Δc_{dev} within the compression zone.

[3] Where the pre-stressing steel lies within a layer of ordinary reinforcement, the calculated crack width must meet the requirements for both ordinary reinforcement and pre-stressing steel. For verification against the requirement for prestressing steel the frequent load combinations are used, the calculated crack width may be adjusted with the formula $w_{2k} = w_k (\varepsilon_{s2} / \varepsilon_{s1})$, where ε_{s1} is the tensile strain in the reinforcement on the side with greatest strain, ε_{s2} is the tensile strain at the level of the prestressing steel and w_{2k} is an adjusted calculated crack width that is compared with the limiting values in the table.

[4] A total assessment is necessary in these cases in order to arrive at an appropriate combination of structural detailing, material composition, cover, limitation of crack width and other protective measures.

Figure 5.8 Limiting values of w_{max}(mm) [13]

5.2.1.1 Analysis of cracked section

Full calculations are found in Appendix F-3. A control is performed to establish if the cross-section is to be considered as cracked or uncracked. A section is considered as cracked if the tensile stress exceeds the allowable tensile stress f_{ctm} [13]. For negative values of stresses, the section is considered in compression. For this case, the stresses should not exceed the following:

$$\sigma_{allow} \leq -0.6 f_{ck} = -27MPa \qquad 5.23$$

A transformed cross-section is necessary to determine the stresses. The transformed cross-section is found by the following formula

$$A_t = A_c + (\eta_p - 1)A_p \tag{5.24}$$

where $\eta_p = \frac{E_p}{E_{cm}}$ .Figure 5.8 shows a concrete cross-section with centre of gravity *CoG*. The centre of gravity for the transformed cross-section is found by looking at the moment of the areas around the *CoG*. This way, the distance y_t between the CoG and the transformed CoG is determined as following:

$$y_t = \frac{(\eta_p - 1)A_p * e}{A_t} \tag{5.25}$$

Further, the second moment of area for the transformed section is determined

$$I_t = I_c + (\eta_p - 1)A_p * (e - y_t)^2 \tag{5.26}$$

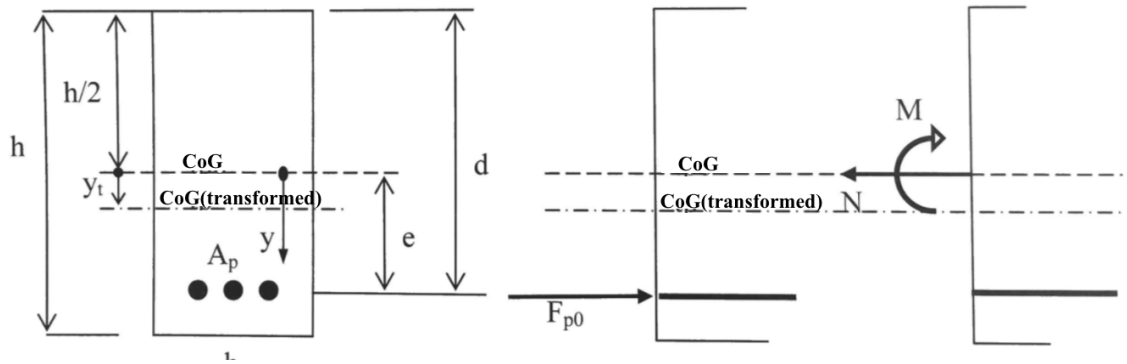

Figure 5.9 Cross-section with moment and axial force [8]

The stresses in top and bottom of the box-girder for both span and support are calculated to check if the cross-section should be considered as cracked or uncracked. Two cases are considered when calculating the stresses; maximum moment at support and maximum moment in span. For calculations of stresses at support, model 62 is used as this gave the highest moments. This model is considered as statically determinate, and equation 5.27 and 5.28 are used for stresses in top and bottom respectively.

$$\sigma_{c.tenson} = -\frac{P}{A_t} + \frac{P(e-y)y_t}{I_t} + \frac{M}{W_t} \leq f_{ctm} = 3.8\ MPa \tag{5.27}$$

$$\sigma_{c.comp} = -\frac{P}{A_t} - \frac{P(e-y)y_t}{I_t} - \frac{M}{W_t} \leq 0{,}6f_{ck} = -27\ MPa \tag{5.28}$$

Results for stresses at support are calculated in Appendix F-3 and are given in Table 5.3.

When checking the stresses in the span, model 92 is used as the highest moment for span were found in this model. The system is statically indeterminate for model 92, and it is necessary to determine the secondary moment as explained in Chapter 2.4.2.3. Figure 5.10 shows an illustration of the total moment $M_p=M_0+M_1$, where M_0 is the primary moment and M_1 is the secondary moment.

The deflection due to the primary moment $M_0=Pe$ is determined by equation 5.29.

$$\delta_0 = \frac{Pe}{EI}\frac{L^2}{8} \tag{5.29}$$

The secondary moment M_1 is determined by equation 5.30. This formula is taken from the book "Stålkonstruksjoner". The corresponding deflection is also found from "Stålkonstruksjoner" and is given in equation 5.31 [19].

$$M_1 = \frac{FL_1L_2}{L} = \frac{266}{11}m * F \tag{5.30}$$

$$\delta_1 = \frac{1}{48}\frac{PL}{EI}\left(3\frac{L_1}{L} - 4\left(\frac{L_1}{L}\right)^2\right) = 19553{,}625m^3\frac{F}{EI} \tag{5.31}$$

where $L=L_1+L_2$, and EI is constant for the whole section.

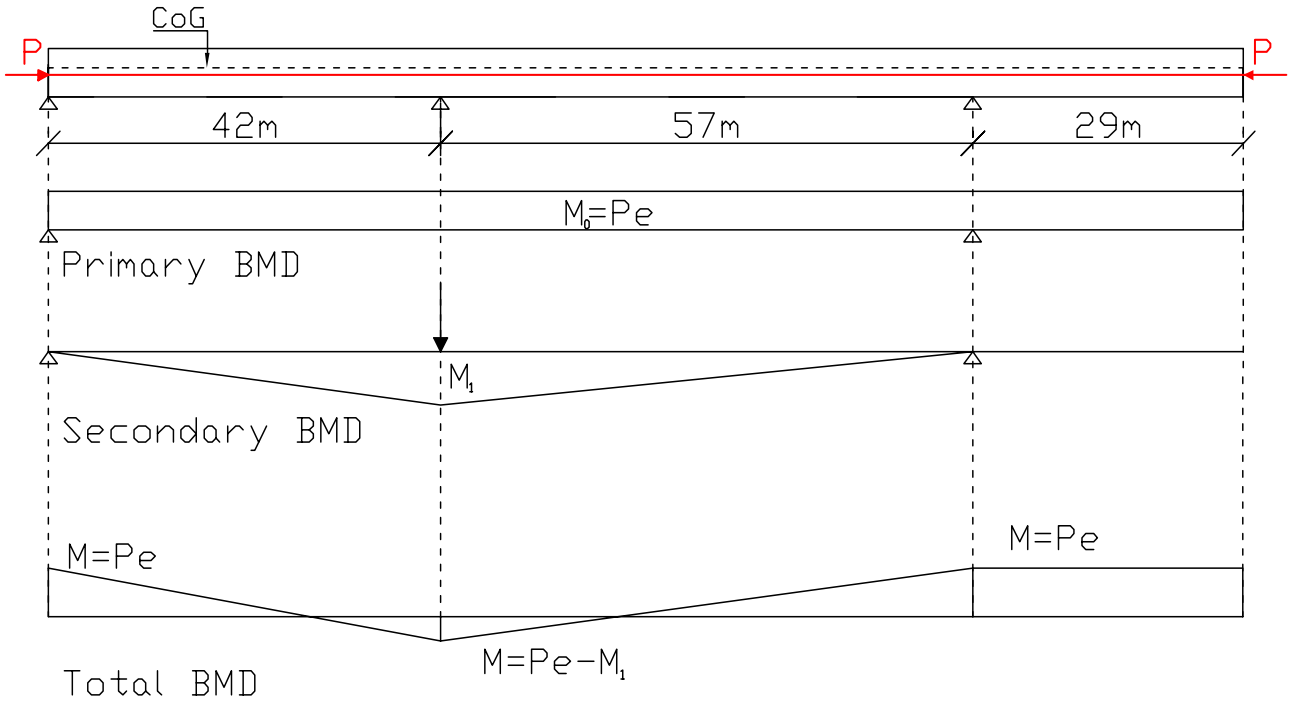

Figure 5.10 Total moment due to prestress for model 92

The deflection from the primary moment over length $L=L_1+L_2$ should be equal to the deflection due to the secondary moment to ensure no deflection at the point where the support is removed. From this, the force F is determined.

$$\delta_0 = \delta_1 \rightarrow F = \frac{Pe}{8}\frac{(L_1+L_2)^2}{19553{,}625\ m^3} \tag{5.32}$$

Further, the secondary moment is found to be the following:

$$M_1 = 1{,}515Pe \tag{5.33}$$

Thus, the stresses are determined as in equation 5.34 and 5.35.

$$\sigma_{c.tenson} = -\frac{P}{A_t} + \frac{P(e-y)y_t}{I_t} - \frac{1.515P(e-y)y_t}{I_t} - \frac{M_{span}}{W_{span}} \tag{5.34}$$

$$\sigma_{c.comp} = -\frac{P}{A_t} - \frac{P(e-y)y_t}{I_t} + \frac{1.515P(e-y)y_t}{I_t} + \frac{M_{span}}{W_{span}} \tag{5.35}$$

Table 5.3 shows that all $\sigma \leq \sigma_{allow}$, the section is therefore to be considered as uncracked.

Table 5.3 Stresses - control of cracked section

		σ [MPa]	σ_{allow} [MPa]	
Model 62	Support – top	-4,451	-27	OK
	Support – bottom	-13,323	-27	OK
Model 92	Span – top	-18,219	-27	OK
	Span – bottom	-1,404	-27	OK

6 ANALYSIS OF FINAL CONSTRUCTION

The final construction will have to carry more load than previous stages, because it has to carry traffic as well as the other loads. Therefore, there is a need for extra prestressing at the final stage.

Load combinations for the final construction at ULS and SLS are found in Table 2.1 and 2.2.

6.1 ULS

6.1.1 DESIGN FORCES IN ULS

The following diagrams were found for Bagn bridge under ULS for moment and shear force. Each model represents the envelop curve for the ULS and may be given by different load combinations. This is illustrated in Table 6.1, where the maximum and minimum moments for ULS is found for each span and support.

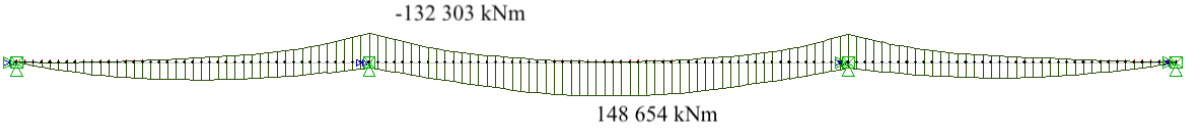

Figure 6.1 Moment diagram for ULS

Figure 6.2 Shear force diagram for ULS

Table 6.1 Moments in ULS

Span	Element	Moment [kNm]	Support	Moment [kNm]
1-2	23	76510	1	-
2-3	74	148 654	2	132 303
3-4	121	67 739	3	127 829

6.1.2 ULTIMATE MOMENT CAPACITY

6.1.2.1 Moment capacity at support

Complete calculations are found in Appendix G-1.

The maximum support moment is found in Table 6.1 at support 2, with a value of 132 303 kNm. Similar to the design for moment at support for the launching stages, the moment is to be reduced by 10%. For Bagn bridge, the reduced design moment is found as following:

$$M_{Ed.red} = 0.90 * M_{Ed} = 119\,073 kNm \quad 6.1$$

When considering the moment over support, the top flange of the box-girder will be in tension. Therefore, the effective width at supports are found as the bottom width of the cross-section: $b_{bottom} = 4.95\ m$. The effective depth over the support is found to be $d_{support} = 3.31\ m$.

When inserting values into equation 5,7, the balanced prestressing steel area is found to be

$$A_{pb} = 0{,}173\ m^2 > A_p = 0{,}038\ m^2 \quad 6.2$$

From equation 5.6, α can now be determined. As $A_p \leq A_{pb}$ the section has to little reinforcement, and one can use S_p as $f_{pd}A_p$. This gives

$$\alpha = \frac{f_{pd}A_p}{0{,}8 f_{cd} b d} = 0{,}1613 \quad 6.3$$

The internal leaver arm, z, is found in equations 6.4, but shall not be smaller than 0,9d=2,979m

$$z = (1 - 0{,}4\alpha)d = 3{,}096\ m > 0{,}9d \quad OK! \quad 6.4$$

Further, the ultimate moment capacity is calculated

$$M_{Rd} = T_c z = 166\,918\ kNm \quad 6.5$$

A control of the ultimate moment to check if it is more than or equal to the design moment is then performed.

$$M_{Rd} > M_{Ed.red} \quad 6.6$$

From equation 6.6 it is found that the moment capacity is sufficient to withstand the design moment.

6.1.2.2 Moment capacity at span

Complete calculations are found in Appendix G-1. The maximum moment in span occurs at span 2-3 at a distance of 71 meters from support 1, and is found in Table 6.1 to be

$$M_{Ed} = 148\,654\ kNm \tag{6.7}$$

When considering the moment at span, the bottom of the box-girder will be in tension. Therefore, the effective width at supports are found as the width of the top flange of the cross-section: $b_{top} = 11.225\ m$. The effective depth over the support is found to be $d_{span} = 3.31\ m$.

When inserting values into equation 5,7, the balanced prestressing steel area is found to be

$$A_{pb} = 0{,}393\ m^2 > A_p = 0{,}025\ m^2 \tag{6.8}$$

From equation 5.6, α can now be determined. As $A_p \leq A_{pb}$ the section has to little reinforcement, and one can use S_p as $f_{pd}A_p$. This gives

$$\alpha = \frac{f_{pd}A_p}{0{,}8 f_{cd} b d} = 0.047 \tag{6.9}$$

The internal leaver arm, z, is found in equations 6.10.

$$z = (1 - 0{,}4\alpha)d = 3.25\ m > 0.9d = 2.979 \quad OK! \tag{6.10}$$

Further, the ultimate moment capacity is calculated

$$M_{Rd} = T_c z = 116\,697\ kNm \tag{6.11}$$

A control of the ultimate moment to check if it is more than or equal to the design moment is then performed.

$$M_{Rd} < M_{Ed.red} \tag{6.12}$$

From equation 6.12 it is found that the moment capacity is not sufficient to withstand the design moment, and it is therefore necessary to use more reinforcement at span.

Additional reinforcement of 33Ø25c150 is required to ensure adequate capacity at span.

6.1.3 SHEAR RESISTANCE

Full calculations are found in Appendix G-2. From Figure 6.2, the design shear force is found over support 2 to be:

$$V_{Ed} = 14\,053\ kN \tag{6.13}$$

Equal to the reduced moment at support, the shear force is reduced by 10%:

$$V_{Ed.red} = 0.9 * V_{Ed} = 12\,648\ kNm \tag{6.14}$$

EC2 states different verification procedures which are to be used when checking for shear resistance. These are shear capacity without shear reinforcement, shear capacity with shear reinforcement and the design value of the maximum shear force.

The cross-section is assumed to be uncracked and a control is performed to check if there is, on the basis of design calculations, a need for shear reinforcement. To check for this, the following requirement has to be met:

$$V_{Ed} \leq V_{Rd,c} \tag{6.15}$$

$V_{Rd,c}$ is found by the following formula

$$V_{Rd,c} = max\{[C_{Rd,c}k(100\rho_1 f_{ck})^{1/3} + k_1\sigma_{cp}]b_w d\ ; (v_{min} + k_1\sigma_{cp})b_w d\ \} \tag{6.16}$$

where

k is a factor found by the formula $1 + \sqrt{\frac{200}{d}} = 1{,}246 \leq 2{,}0$ for d=3,31m

ρ_1 is found by the formula $\frac{A_p}{b_w * d} = 7{,}931 * 10^{-4}$

b_w is the width of the web. For box-girders this corresponds to 2*web width = 800mm

k_1 is a factor of value 0,15 when in compression

$C_{Rd,c}$ is given as following: $\frac{k_2}{\gamma_c} = 0{,}12$

k_2 is a factor of value 0,18

σ_{cp} is given by the following formula: $\sigma_{cp} = \frac{N_{Ed}}{A_c} = \frac{P_s}{A_c} = 6{,}853\ kN$

P_s is the axial force from the prestressing tendons, equal to 60 442 kN

A_c is the concrete cross-sectional area = 8,82m^2

v_{min} is found by the formula $0{,}035k^{3/2}f_{ck}^{1/2} = 0{,}324$

A_p is the total area of the prestressing tendons, and is equal to 47 040 mm^2

This gives the following design shear capacity:

$$V_{Rd,c} = 3586{,}5\ kN \tag{6.17}$$

As V_{Ed} > capacity $V_{Rd.c}$, it is required to calculate the design shear reinforcement.

6.1.3.1 Shear capacity with shear reinforcement

EC2 states that structures with vertical shear reinforcement, the shear capacity is found as following:

$$V_{Rd.max} = \frac{\alpha_{cw} b_w z v_1 f_{cd}}{cot\theta + tan\theta} \tag{6.18}$$

where

α_{cw} is a coefficient taking the state of the stress in the compression chord into account

$= 1 + \frac{\sigma_{cp}}{f_{cd}} = 1{,}269$

b_w is the width of the web. For box-girders this corresponds to 2*web width = 800mm

z is the inner leaver arm $= 0{,}9d = 2{,}979m$

v_1 is a strength reduction factor for the concrete cracked in shear $= 0{,}6$

θ is an angle determined by the national annex in EC2

$\theta_{max} = 45\ degrees$

$\theta_{max} = 38{,}66\ degrees$

This gives

$$V_{Rd.max} = 22\ 567 \text{ kN} \tag{6.19}$$

As $V_{Rd.max}$ is larger than V_{Ed}, the shear reinforcement may be calculated. By assuming 8 bars of diameter Ø12, the spacing is calculated by equation 6.20. $V_{Ed.red}$ is used in this formula, as this will provide the exact required reinforcement.

$$s = \frac{A_{sw} z f_{ywd} cot\theta}{V_{Ed.red}} = 217\ mm \tag{6.20}$$

Thus, 12Ø12s220 is the required shear reinforcement.

6.2 SLS

6.2.1 DESIGN MOMENTS IN SLS

The design moments in SLS are shown in Figure 6.3. The corresponding load combination is the characteristic combination. The design moments occur in span 2-3 at a distance of 71 meters from support 1 and at support 2 with values as shown in Figure 6.3.

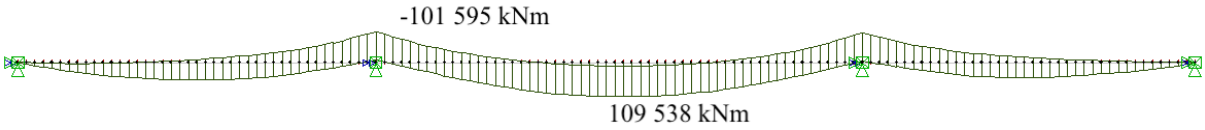

Figure 6.3 Moment diagram for SLS

Results from all load combinations are shown in Table 6.2

Table 6.2 Maximum moments for load combinations at SLS

Moments for characteristic load combination [kNm]		
Span	1-2	55 096
	2-3	109 538
	3-4	47 546
Support	2	101 595
	3	98 384
Max moments for frequent load combination		
Span	1-2	36 272
	2-3	87 790
	3-4	30 561
Support	2	83 119
	3	80 002
Max moments for quasi permanent load combination		
Span	1-2	47 816
	2-3	80 376
	3-4	40 844
Support	2	92 453
	3	87 783

The stresses used in controls at SLS for the final construction are taken from NovaFrame. By using the command *SECTFACE*, the upper and lower face of the cross-section is found. By defining these, NovaFrame can calculate the stresses at the top and bottom of the box-girder. Appendix G-3 to G-5 shows the stresses which are relevant for the different controls at SLS.

6.2.2 CRACK CONTROL

6.2.2.1 Analysis of cracked section

Analysis of cracked section is performed as for the launching stages, except that the stresses are taken directly from NovaFrame. For control of cracked section, stresses due to prestressing and self-weight are used. Appendix G-3 shows values for stresses in top and bottom for the whole bridge. Worst-case stresses for all three spans and for support 1 and 2 are given in Table 6.3. Table 6.3 shows that all stresses are smaller than the allowable stresses, and the section may therefore be considered as uncracked.

Table 6.3 Stresses - control of cracked section

		σ [MPa]		σ_{allow} [MPa]		
		Top	Bottom	Top	Bottom	
Span	1-2	-7.338	-10.148	-27	-27	OK
	2-3	-6.695	-1.26			
	3-4	-6.032	-10.344			
Support	2	-1.979	-14.263	-27	-27	OK
	3	-2.417	-13.999			

6.2.2.2 Decompressions

Note 2 in Figure 5.7 states that for sections where it is required to verify that decompression does not occur, the prestressing steel and post-tensioned duct shall lie at least ΔC_{dev} within the compression zone [11]. For Bagn bridge, ΔC_{dev} is found as 15mm.

The control of decompressions simply means that a control is performed to check if there are compressional strains. For most bridges, Bagn bridge included, the superstructure has the largest support-moment in the column-axes, with tension in the top of the cross-section. Practically, this means that there should be compressional strains in the whole cross-section in the superstructure at supports for the quasi permanent load combination. SVV states that, by experience, this in most cases is considered as the design values for the required prestressing [16].

New section parameters are determined from this new cross-section, such as area, second moment of area and the centre of gravity. Just as for the control of cracks, a transformed cross-section is found to be used when determining the stresses. The following formula for the stresses is used:

$$\sigma = \frac{N}{A} + \frac{M}{I}y \qquad 6.28$$

where N is the axial force provided by the prestressing force, and M is the moment due to prestressing and due to external loading.

SVV states that for decompressions, the moments due to the quasi permanent load case is to be used [16]. From analysis of the model in NovaFrame, the stresses in top and bottom for support 2 and support 3 are found. The results are represented in Table 6.4, found from Appendix G-5. As the stresses at support 2 and 3, both in top and in bottom, gives compressional strain, it is safe to assume that the calculated amount of prestressing is sufficient.

Table 6.4 Results from decompression

	σ [MPa]		σ_{allow} [MPa]		Control
	Top	Bottom	Top	Bottom	
Support 2	-4.556	-20.499	-27	-27	OK
Support 3	-5.035	-19.895			

6.2.3 *STRESS LIMITATIONS*

The compressive stresses in the concrete should be limited to avoid longitudinal cracks, micro cracks or large creep deformations if it can cause unacceptable effects of the structures function.

Longitudinal cracks can occur if the stress level for the characteristic load combination exceeds a critical value. As these cracks effects the durability of the structures, measures have to be done. One option to increase the cover to reinforcement. If this for some reason is not done, the compressive stresses should be limited to a value of $k_1 f_{ck}$ in the exposed areas. According to EC2, the recommended value for k_1 is 0,6 [13]. This gives limitations under characteristic load combination as shown in equation 6.23, where f_{ck} is 45MPa as given in Table 3.1.

$$\sigma_{c,char} \leq 0.6 f_{ck} = 27MPa \tag{6.23}$$

To ensure linear creep, stress in the concrete under quasi-permanent loads should be less than $k_2 f_{ck}$. If the stress exceeds this limitation, non-linear creep should be considered. Recommended value for k_2 is set to 0,45 in EC2 [13], which gives the following limit:

$$\sigma_{c,quasi} \leq 0.45 f_{ck} = 20{,}25MPa \tag{6.24}$$

To avoid inelastic strain, unacceptable cracking or deformation a limit is set to the tensile stresses in the reinforcement. The tensile stresses are set to be less than $k_3 f_{yk}$, where the value for k_3 is 0,8. This gives the following limit, where f_{yk} is given in Table 3.3 as 500MPa.

$$\sigma_{s,reinf} \leq 0.8 f_{yk} = 400MPa \tag{6.25}$$

The tensile stresses shall not exceed a limit of $k_4 f_{yk}$ where the tensile stresses are caused by imposed deformation. As for the prestressing tendons, the mean value of the stress should not exceed $k_5 f_{pk}$. Values for k_4 and k_5 are 1 and 0,75 respectively. These forms the limits

$$\sigma_{s,imposed} \leq f_{yk} = 500MPa \tag{6.26}$$

$$\sigma_{s,prestr} \leq 0.75 f_{pk} = 1395\ MPa \tag{6.27}$$

6.2.3.1 Stress limitations at transfer

For the stress limitation at transfer, stresses due to self-weight and prestressing are used. These are the same stresses as found in Table 6.4 for crack control of the bridge. In this table, all stresses were found to be compressive and smaller than the limit given in equation 6.28.

$$\sigma_{c.allow} \leq -0{,}6 f_{ck} = -27\ MPa\ for\ compression \qquad 6.28$$

$$\sigma_{t.allow} \leq f_{ctm} = 3{,}8\ MPa\ for\ tension \qquad 6.29$$

Table 6.4 shows that the stresses satisfy the limits from equation 6.28 and 6.29. No extra reinforcement is needed, as there is compressional strain over the whole bridge length.

6.27.1.1 Stress limitations at service

At service, there are two load cases that are to be controlled: characteristic load combination and quasi permanent load combination. Moment diagrams for the two load combinations are given in Figure 6.4 and Figure 6.5 respectively.

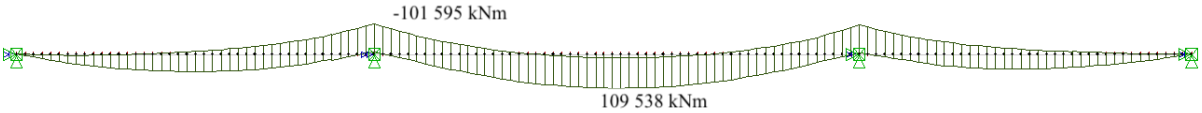

Figure 6.4 Moment diagram for characteristic load combination

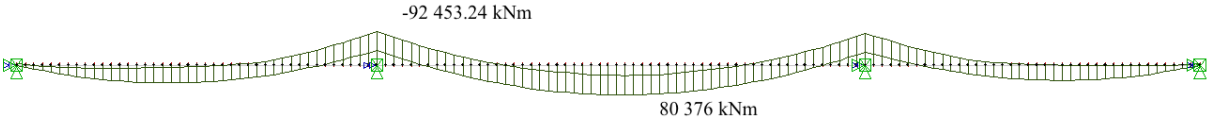

Figure 6.5 Moment diagram for quasi-permanent load combination

Appendix G-4 and G-5 shows the resulting stresses from NovaFrame for both the characteristic load combination and for the quasi-permanent load case respectively. At service, the stresses shall not exceed the following:

$$\sigma_{c.allow.quasi} \leq -0{,}45 f_{ck} = -20.25\ MPa\ for\ compression \qquad 6.30$$

$$\sigma_{t.allow.quasi} \leq f_{ctm} = 3{,}8\ MPa\ for\ tension \qquad 6.31$$

For characteristic load combination, equation 6.28 and equation 6.29 are controlled. Results from NovaFrame for selected sections are given in Table 6.5 and Table 6.6.

Table 6.5 Stresses in the cross-section - Characteristic

	σ_{top} [MPa]	σ_{bottom} [MPa]	Control
Span 1-2	-12.776	-15.543	OK
Span 2-3	-12.617	-6.548	OK
Span 3-4	-11.563	-16.201	OK
Support 2	-7.368	-19.756	OK
Support 3	-7.728	-19.644	OK

Table 6.6 Stresses in the cross-section - Quasi permanent

	σ_{top} [MPa]	σ_{bottom} [MPa]	Control
Span 1-2	-11.854	-10.166	OK
Span 2-3	-11.798	-5.186	OK
Span 3-4	-11.333	-11.182	OK
Support 2	-4.556	-20.499	NOT OK
Support 3	-5.035	-19.895	OK

Table 6.5 shows that the stresses at characteristic load combination satisfy the limits from equations 6.28 and 6.29. As there are compressional strains at all points → no extra reinforcement needed. For the quasi-permanent load combination, the stresses at support 2 exceeds the limit given in equation 6.30. Therefore, extra reinforcement is required.

6.27.2 DEFLECTION CONTROL

According to EC2, a member or structure should not be subjected to deformation that affects it function or appearance. EC2 states that deflections should not exceed the limit given in equation 6.32. This check will in most cases be adequate to avoid deflection problems [13]. N400 has a different requirement for deflections, which is given in equation 6.33.

$$\delta \leq \frac{L}{250} \qquad 6.12$$

$$\delta \leq \frac{L}{350} \qquad 6.33$$

Where L is the span length.

There are two ways to check the limit state of deformations; either by limiting the span/depth ratio as shown in Clause 7.4.2 in EC2, or by comparing a calculated deflection with a limit value according to Clause 7.4.3 in EC2 [13]. Clause 7.4.2 is usually not used for pre-stressed members.

N400 states that for calculation of deflection of bridges due to permanent loads including long-term effects are to be compensated with pre-camber. This pre-camber is calculated in SLS with quasi permanent load combination. The combination factor ψ_2 is set to zero for variable loads [3]. Deflections due to self-weight, quasi-permanent load combination and full prestressing are given in Table 6.7, where positive direction is set as positive z-direction. Deflection due to traffic load is also calculated, as it is not possible to find in NovaFrame. Calculations done by hand are found in Appendix G-6.

Table 6.7 Deflections

	δ_{EC2} [mm]	δ_{N400} [mm]	δ_{SW} [mm]	δ_{PS} [mm]	δ_{TR+SW} [mm]
Span 1-2	168	120	-6.845	3.908	Smaller than span 2-3
Span 2-3	228	163	-18.784	0.767	-67.096<δ<-13.621
Span 3-4	156	111	-4.239	3.477	Smaller than span 2-3

All deflections are below the limit given in EC2 and N400 and are therefore considered safe.

7 DISCUSSION AND CONCLUSION

Bagn bridge is a bridge of 138 meters that is built over Begna in Valdres. The bridge consists of four axes and three spans of 42m, 57m and 39m. Some limitations were made in this thesis, as it is the construction method that is in focus and not the geometry of the planned bridge. The bridge, which has a horizontal curvature with a radius of 750m, was considered straight. This is possible as the curvature was less than 12 degrees. The cross-section was originally designed with a 7.8-degree slope in the top flange. As the main focus of this thesis is analysis of the construction method ILM, this slope is not considered to have large impact on results. Therefore, the bridge is designed as a box girder with straight top flange.

As explained in Chapter 2.3, ILM requires expensive equipment and is not considered as a good construction method for bridges with total length smaller than 200m when looking at the economical aspect. Therefore, it is not recommended to use this construction method for bridges with length of 138 meters, such as for Bagn bridge. This thesis is simply to be used for comparison with other similar construction methods.

Concrete of class B45 is used for the entire superstructure, as this class has high strength and is recommended to use for prestressed concrete bridges.

The prestressing system BBR VT CONA CMI 1506-140-1860 is used. The cables have an outer diameter of 80mm and consists of 15 strands with diameter of 140mm^2. Thus, the total tendon area = 2100 mm^2.

Due to the launching, two types of cable profiles were used. For the launching of the bridge, a centric prestressing cable consisting of 22 cables was used. Four parabolic prestressing tendons were introduced after the final launch, so the bridge can withstand traffic loads. These are placed in 2x2 groups, one in each web. The tendon profile for this was decided by looking at the demands for prestressing bridges. For ILM, it is required to use a minimum cover of 150mm. This cover is used for tendons in both upper and lower flange.

The bridge was modelled in NovaFrame and consists of 136 different models defining the launch of one meter, starting from the launch of 39 meters from axis 1.

Two analyses were performed in this thesis, one for the construction stages and one for the final construction. For The launching stages, control calculations for both ULS and SLS were performed. For the final construction, control calculations were performed for ULS and controls of output from NovaFrame were performed for SLS.

For the launching stages, results from calculations for ULS and SLS are given in Table 7.1 and 7.2 respectively. Only self-weight, prestressing and thermal loads are included in these calculations. This is because that the impact of other loads is considered to be very small compared to the. For ULS, control of ultimate moment capacity and shear resistance is completed. Worst case scenario of moment distributions is used for the top and bottom of the cross-sections, which were found in NovaFrame to be in model 62 and model 92, for max to identify maximum moment in support and span.

Calculations show that the amount of prestressing used in the launching stages, consisting of 22 tendons, was sufficient to carry the maximum moment over the support. The moment over support due to self-weight, prestressing and temperature load was higher than the capacity at the span, and additional longitudinal reinforcement was required. Calculations for model 92 show that 15Ø25c330 is sufficient at span 2-3. The moment in each element during launching will change depending on the launching stage. As a consequence, a conservative choice is made, and the reinforcement is placed over the whole bridge length to ensure a sufficient moment capacity to resist these moments.

Results shows that the calculated shear capacity is not sufficient to withstand the design shear force. According to EC2, shear resistance with shear reinforcement is calculated. Calculations show that the shear resistance with shear reinforcement is sufficient to withstand the design shear force. Required shear reinforcement is given in Table 7.1

Table 7.1 Results – ULS – Launching stages

ULS - LAUNCHING STAGES			
	Imposed force	Capacity	Control
Span moment	92 561 kNm	78 299 kNm	**NOT OK**
Support moment (reduced)	131 394 kNm	131 815 kNm	**OK**
Shear force (reduced)	7 324 kN	3 998 kN	**NOT OK**
Shear resistance w/reinforcement	21 831 kN		**OK**
Reinforcements and spacing			
Longitudinal reinforcement span	15Ø25c330		
Longitudinal reinforcement support	-		
Minimum shear reinforcement	8Ø12s250		

A simplified control of SLS is done for the construction stages. A control of cracked sections is applied to check if it is necessary to calculate crack widths. Results given in Table 7.2 show that all of the stresses in the crack control is within the limits, and the cross-section may therefore be considered as uncracked.

Table 7.2 Results – SLS – Constriction stages

SLS – CONSTRUCTION STAGES					
Control of cracks	Stress [MPa]		Capacity [MPa]		Control
	Top	Bottom	Top	Bottom	
Support 2	-4.451	-13.323	-27	-27	**OK**
Span 2-3	-18.219	-1.404	-27	-27	**OK**

For the final construction a more thorough control is performed for both ULS and SLS, as loads such as wind, creep, shrinkage and traffic are included. Load combinations are determined in Table 2.1. Results from the ULS calculations are given in Table 7.3. Calculations show that the moment capacity at both span and at support is insufficient, and additional reinforcement is required. The amount of longitudinal reinforcement at support is found to be the same as for launching stages. As a conclusion, the additional reinforcement placed for launching stages is sufficient for the final construction.

Longitudinal reinforcement at span is found to be 33Ø25s150. Additional shear reinforcement is also required, as the shear capacity is smaller than the imposed shear force. It is found that shear reinforcement of 12Ø12s200 is sufficient.

Table 7.3 Results – ULS – Final construction

ULS – FINAL CONSTRUCTION			
	Imposed force	Capacity	Control
Span moment	148 654 kNm	116 697 kNm	**NOT OK**
Support moment (reduced)	119 073 kNm	166 918 kNm	**OK**
Shear force (reduced)	12 648 kN	3 586 kN	**NOT OK**
Shear resistance w/reinforcement	22 567 kN		**OK**
Reinforcement and spacing			
Longitudinal reinforcement span	33Ø25s150		
Longitudinal reinforcement support	-		
Minimum shear reinforcement	12Ø12s220		

For SLS, load combinations are determined in Table 2.2. The results given in table 7.4 are based on the analysis of the model in NovaFrame. Results show that stresses from the crack control are smaller than the allowable limit, and the cross-section may therefore be considered as uncracked. From decompressions at support 2 and 3 it is found that there are compressive strains over the whole cross-section.

Stress limitations are done for two different cases: at transfer and at service. At transfer, only moments due to self-weight and full prestressing is used. At service, both moments due to the characteristic load combination and the quasi permanent load combination is controlled. From stress limitation calculations, it is found that the prestressing at support 2 for quasi permanent load combination is not sufficient, and extra reinforcement will be required. For all other values, the prestressing is sufficient.

The control of deflection at SLS gave satisfying values, as none of the deflections exceeded limitations given from EC2 and N400.

For further work, a more excessive analysis for launching stages, especially in regard to effects due to creep are recommended. It is also recommended to do calculations at SLS for the final construction by hand to prove that results from NovaFrame are correct. As results at SLS shows that the capacity is not sufficient and calculations of extra reinforcement is required.

Table 7.4 Results – SLS – Final construction

SLS – FINAL CONSTRUCTION						
Control of cracks		Stress [MPa]		Capacity [MPa]		Control
		Top	Bottom	Top	Bottom	
Span	1-2	-7.338	-10.148	-27	-27	**OK**
	2-3	-6.695	-1.26			
	3-4	-6.032	-10.344			
Support	2	-1.979	-14.263	-27	-27	**OK**
	3	-2.417	-13.999			
Decompression		Stress [MPa]		Capacity [MPa]		Control
		Top	Bottom			
Support 2		-4.556	-20.499	-27		**OK**
Support 3		-5.035	-19.895	-27		**OK**
Stress limitations		Stress at transfer [MPa]		Capacity [MPa]		Control
		Top	Bottom	Top	Bottom	
Transfer	Span 1-2	-7.338	-10.148	-27	-27	**OK**
	Span 2-3	-6.695	-1.26	-27	-27	
	Span 3-4	-6.032	-10.344	-27	-27	
	Support 2	-1.979	-14.263	-27	-27	
	Support 3	-2.417	-13.999	-27	-27	
Service Characteristic	Span 1-2	-12.776	-15.543	-27	-27	**OK**
	Span 2-3	-12.617	-6.548	-27	-27	
	Span 3-4	-11.563	-16.201	-27	-27	
	Support 2	-7.368	-19.756	-27	-27	
	Support 3	-7.728	-19.644	-27	-27	
Service Quasi	Span 1-2	-11.854	-10.166	-20.25	-20.25	**OK**
	Span 2-3	-11.798	-5.186	-20.25	-20.25	
	Span 3-4	-11.333	-11.182	-20.25	-20.25	
	Support 2	-4.556	-20.499	-20.25	-20.25	**NOT OK**
	Support 3	-5.035	-19.895	-20.25	-20.25	**OK**

8 REFERENCE LIST

[1] J. Corven, “Post-Tensioned Box Girder Design Manual,” U.S Department of Transportation, Washington DC, 2015.

[2] Statens Vegvesen, “E16 Bagn - Bjørgo_Planbeskrivelse Endelig,” 2013. [Online]. Available: https://www.vegvesen.no/_attachment/549890/binary/884671?fast_title=E16+Bagn+-+Bjørgo_Planbeskrivelse+Endelig+24.6.13.pdf. [Accessed 2019].

[3] P. K. Larsen, Konstruksjonsteknikk, Trondheim: Tapir Akademisk Forlag, 2004.

[4] Vegdirektoratet, *Bruprosjektering (håndbok N400)*, 2015.

[5] T. Y. Weiwei Lin, Bridge Engeneering, Oxford: Butterworth-Heinemann, 2017.

[6] Vegdirektoratet, *Bruregistrering (håndbok V440)*, 2014.

[7] B. P. Bernhard Göhler, Incrementally Launched Bridges - Design and Construction, Sydney: Ernst & Sohn, 2000.

[8] VSL, “Incremental launching method,” VSL, [Online]. Available: http://en.vsl.cz/incremental-launching-method/. [Accessed 16 01 2019].

[9] L. I. Loverud, “Nye bruløsninger?,” Multiconsult, 2017.

[10] S. I. Sørensen, Betongkonstruksjoner - Armert betong og spennbetong, Trondheim: Tapir Akademisk Forlag, 2005.

[11] R. I. Gilbert, N. C. Mickleborough and G. Ranzi, Design of Prestressed Concrete to Eurocode 2, Boca Raton: CRC Press, 2017.

[12] T. Y. Lin, “Load-Balancing Method for Design and Analysis of Prestressed Concrete Structures,” *Journal of the American Concrete Institute*, pp. 719-741, June 1963.

[13] NTNU, *Stålkonstruksjoner, Profiler og formler*, Trondheim: Tapir akademisk forlag, 2001.

[14] NS-EN 1992-1-1:2004+NA:2008, *Eurokode 2: Prosjektering av betongkonstruksjoner Del 1-1: Allmenne regler og regler for bygninger.*

[15] N.-E. 1990:2002+A1:2005+NA:2016, *Eurokode: Grunnlag for prosjektering av kontruksjoner.*

[16] P. Bhatt, Prestressed Concrete Design to Eurocodes, New York: Spon Press, 2011.

[17] Civil Engineering , "Modulus of Elasticity of Concrete," Civil Engineering, [Online]. Available: https://civiltoday.com/civil-engineering-materials/concrete/84-modulus-of-elasticity-of-concrete. [Accessed 2019].

[18] NS-EN 1992-2:2005/NA:2010, *Eurokode 2: Prosjektering av betongkonstruksjoner Del 2: Bruer.*

[19] Aas-Jacobsen AS, *User´s guide - NOVA FRAME.*

[20] VSL Systems, *Incremental Launching Method.*

[21] Statens Vegvesen, "Brukerveiledning for etteroppspente betongbruer," Vegdirektoratet, 2017.

[22] R. Benaim, The Design of Prestressed Concrete Bridges, New York: Taylor and Francis Group, 2008.

[23] Strukturas AS, "Overhead Movable Scaffolding System," Strukturas, [Online]. Available: http://strukturas.no/bridge-building-equipment/overhead-mss. [Accessed 16 01 2019].

[24] M. Däbritz, "Movable Scaffolding Systems," *Structural Engineering International,* pp. 413-418, 01 11 2011.

[25] Statens Vegvesen, "Tverrforbindelsen rv. 44 Skjæveland-E39 Bråstein," Statens Vegvesen, [Online]. Available: https://www.vegvesen.no/vegprosjekter/tverrforbindelsen44e39. [Accessed 25 01 2019].

[26] M. Rosignoli, Bridge Launching, Parma, Italy: ThomasTelford, 2002.

9 APPENDIX

Appendix A – Detail drawing of Bagn bridge

Appendix B – Concrete cover

Appendix C – Load calculations

Appendix D – Loss of prestressing force

Appendix E – Verification of results form NovaFrame

Appendix F – Design of launching stages

Appendix G – Design of final construction

Appendix A

Detail drawings

The detail drawings of Bagn bridge is provided by SVV and is used as a basis for the model in NovaFrame. As the detail drawings are for the bridge constructed with the movable scaffolding system, the cross-section is changed to fit for ILM.

A

PROFIL NR. ℄-VEG	600	650	700	750	800
PROFILHØYDER	+228.87	+229.87	+230.87	+231.87	+232.87
VERTIKALKURVE	2%				
HORISONTALKURVE		R=750			
TVERRFALL HS / VS	7.8%				

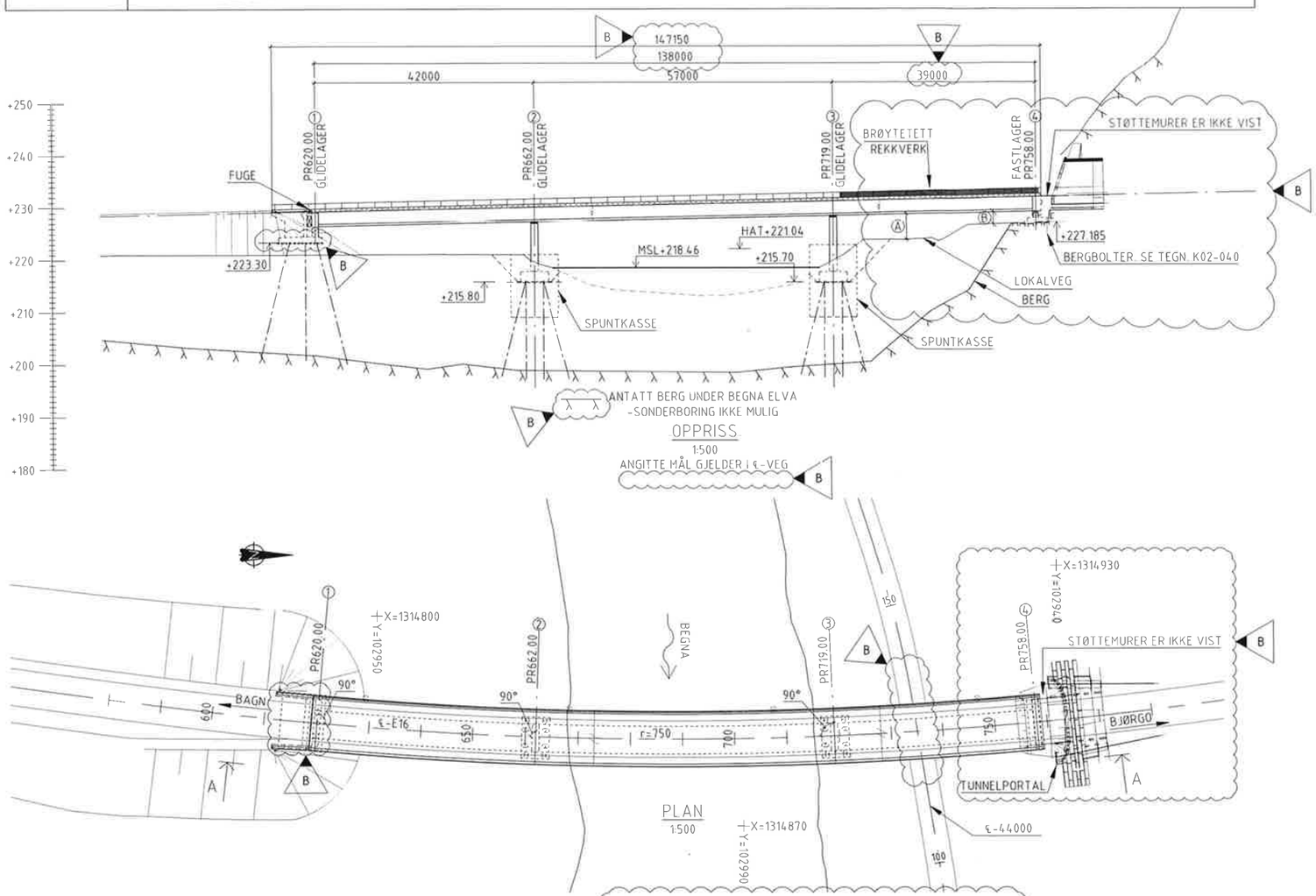

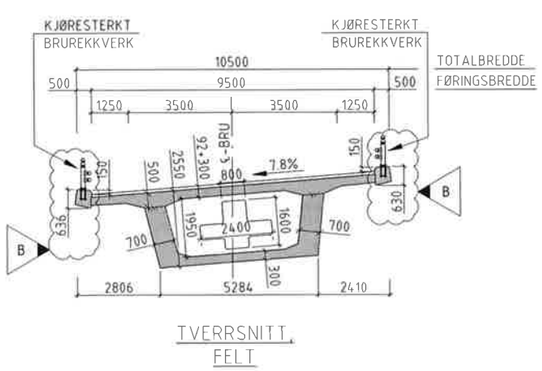

TVERRSNITT
FELT
1:100

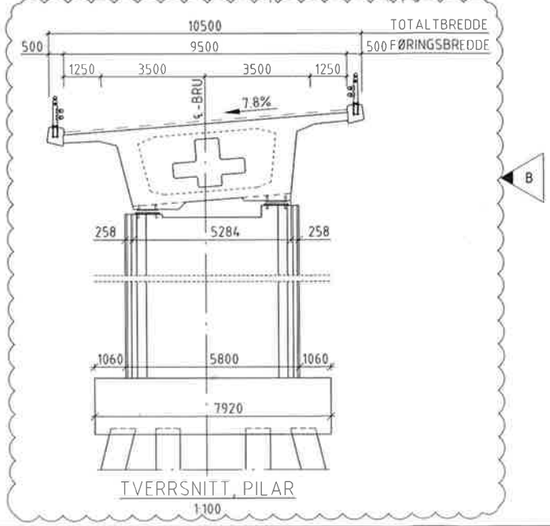

TVERRSNITT, PILAR
1:100

TEGNFORKLARINGER:
ANTATT/SPRENGT BERGKONTUR
ANTATT ELVEBUNN
Ⓐ $H_{min} \geq 4.9$m
Ⓑ $H_{min} \geq 1.2$m

MERKNADER:

1. GENERELT:
   - E16, VEGTYPE H2, ÅDT=3200(ÅR 2036), FARTGRENSE 80km/t
   - LOKALVEG, VEGTYPE A1, ÅDT=<1500, FARTSGRENSE 30km/t
   FERDIGSTILLELSE (OVERTAKELSE) 2018.

2. DIMENSJONERINGSGRUNNLAG:
   SV N400, PROSJEKTERINGSREGLER FOR BRUER, EUROKODEUTGAVE 2011
   SV V220, GEOTEKNIKK I VEGBYGGING, 2010

3. BRUKONSTRUKSJON: SPENNARMERT KASSETVERRSNITT

4. MATERIALKVALITET:
   BETONG: B45 SV-STANDARD
   ARMERING: B500NC
   SPENNARMERING:
   IHT HB R762 (2012) PROSESS 84.37. OVER AKSE 2:
   20 KABLER MED $F_{p0.1k}$=4674 kN, 4 KABLER MED $F_{p0.1k}$=2952 kN

5. BELEGNING OG MEMBRAN:
   BELEGNINGSKLASSE A3 IHT. HÅNDBOK R762 OG N400
   ASFALTSLITELAG OG FUKTISOLERING MED Pmb-BASERTE MATERIALER
   DIMENSJONERENDE BELEGNINGSVEKT: 2.5 kN/m², t=100mm
   SE TEGNING K02-083

6. UTFØRELSE:
   UTFØRELSE SKAL VÆRE I SAMSVAR MED STATENS VEGVESENS R762,
   PROSESSKODE 2- HOVEDPROSESS 8.
   UTFØRELSESKLASSE 3 IHT. NS-EN 13670
   NØYAKTIGHETSKLASSE A FOR KANTBJELKER, FOR ØVRIG KLASSE B.
   PÅLITELIGHETSKLASSE 3 IHT. NS-EN 1990, PKT. NA A.1.3.1.
   EKSPONERINGSKLASSE IHT. NS-EN 1992-1-1, TABELL 4.1 / N400
   BESTANDIGHETSKLASSE MF40 OG M40.

7. REKKVERK:
   REKKVERK STYRKEKLASSE H2. BRØYTETETT REKKVERK OVER VEG
   44000. GODKJENT OVERGANG TIL VEGREKKVERK IHT. HB N101, 3.4.1.
   KFR REKKVERKSTEGNING K02-081. REKKVERK SKAL VÆRE CE-MERKET.

8. LAGRE OG FUGER:
   AKSE 1: 1 stk ENSIDIG OG 1 stk ALLSIDIG BEVEGELIGE LAGER.
   AKSE 2 OG 3: 1 stk ENSIDIG OG 1 stk ALLSIDIG BEVEGELIGE LAGER.
   AKSE 4: 1 stk FAST OG 2 stk ALLSIDIG BEVEGELIGE LAGER.
   AKSE 1 UTFØRES MED FINGERFUGE. KFR TEGNING K2-050.
   AKSE 4 UTFØRES UTEN FUGE.
   VALGT FUGE OG LAGRE MED NØDVENDIG DOKUMENTASJON SKAL
   FORELEGGES BYGGHERREN MIN. 10 ARBEIDSDAGER FØR OVERSENDELSE
   AV ARBEIDSTEGNINGER OG BØYELISTER FOR FUGESENG OG ANDRE
   KONSTRUKSJONSDELER SOM AVHENGER AV FUGEUTFORMING.
   FOR ARMERINGSBØYLER MED TEMPERATURAVHENGIG FORM MÅ DET
   PÅREGNES HASTELEVERING.

9. EROSJONSSIKRING VED AKSE 2-3: IHT TEGNING J020.

10. JORDING: GJENGET CADWELD JORDINGSBOLT, SE TEGNING K02-050, -051, -052, -055 OG I214

11. FUNDAMENTERING:
    AKSE 1: KASSELANDKAR FUNDAMENTERT PÅ 8 STK BOREDE
    STÅLRØRSPELER SKAL BORES MIN. 1m NED I FRISKT BERG.
    AKSE 2: PILARFUNDAMENT FUNDAMENTERT PÅ 8 STK BOREDE
    STÅLRØRSPELER SKAL BORES MIN. 1m NED I FRISKT BERG.
    AKSE 3: PILARFUNDAMENT FUNDAMENTERT PÅ 8 STK BOREDE
    STÅLRØRSPELER SKAL BORES MIN. 1m NED I FRISKT BERG.
    AKSE 4: FUGEFRITT LANDKAR MED VINGER STØPT TIL OVERBYGNING.
    DIREKTEFUNDAMENTERT PÅ BERG. BERG SIKRES MED FJELLBOLTER.
    DIMENSJONERENDE GRUNNTRYKK MAKS 580 kN/m²
    UTFØRELSE OG KONTROLL AV PELEARBEIDER SKAL VÆRE IHT. PROSESS
    83.2 MED UNDERPROSESSER OG SPESIELL BESKRIVELSE.

12. VANNSTAND:

Q_{288}	HAT	MHWS	MSL	MLWS	LAT
480m³/s	+221,04	+220,59	+218,46	+218,35	+218,05

A3 GIR HALV MÅLESTOKK

B	Forlenget 8 meter mot tunnel. Landkar akse 1 og 4 endret. Snitt. Terreng	ØTM/IM	AK/EO	AIR	19.12.2017
A	Arbeidstegning	ØTM	AIR	EN	23.11.2016
Revisjon	Revisjonen gjelder	Utarb	Kontr	Godkjent	Rev. dato
Godkjent som arbeidstegning ifølge notat fra Vegdirektoratet		Saksnr. 15/204143-58			15.11.2016

Statens vegvesen	
Tegningsdato	30.09.2015
Bestiller	Statens Vegvesen
Produsert for	Region øst
Produsert av	ÅF Engineering AS

E16 Hp: 11
Bagn - Bjørgo

05-1928 BAGN BRU

K02, Oversiktstegning

ARBEIDSGRUNNLAG

ÅF ENGINEERING

PROF-nummer	104164
Arkivnummer	2013037198
Byggverksnummer	05-1928
Målestokk A1	1:100 1:500
Tegningsnummer / revisjonsbokstav	K02-001 B

Utarbeidet av	Kontrollert av	Godkjent av	Konsulentarkiv
MG/ØTM	MB	EN	2700025

A

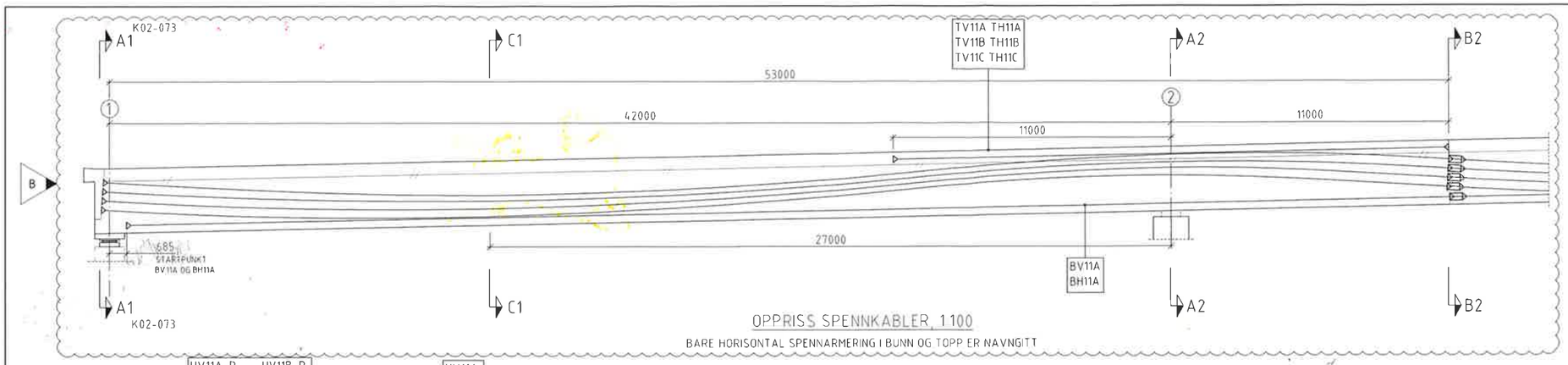

OPPRISS SPENNKABLER, 1:100

BARE HORISONTAL SPENNARMERING I BUNN OG TOPP ER NAVNGITT

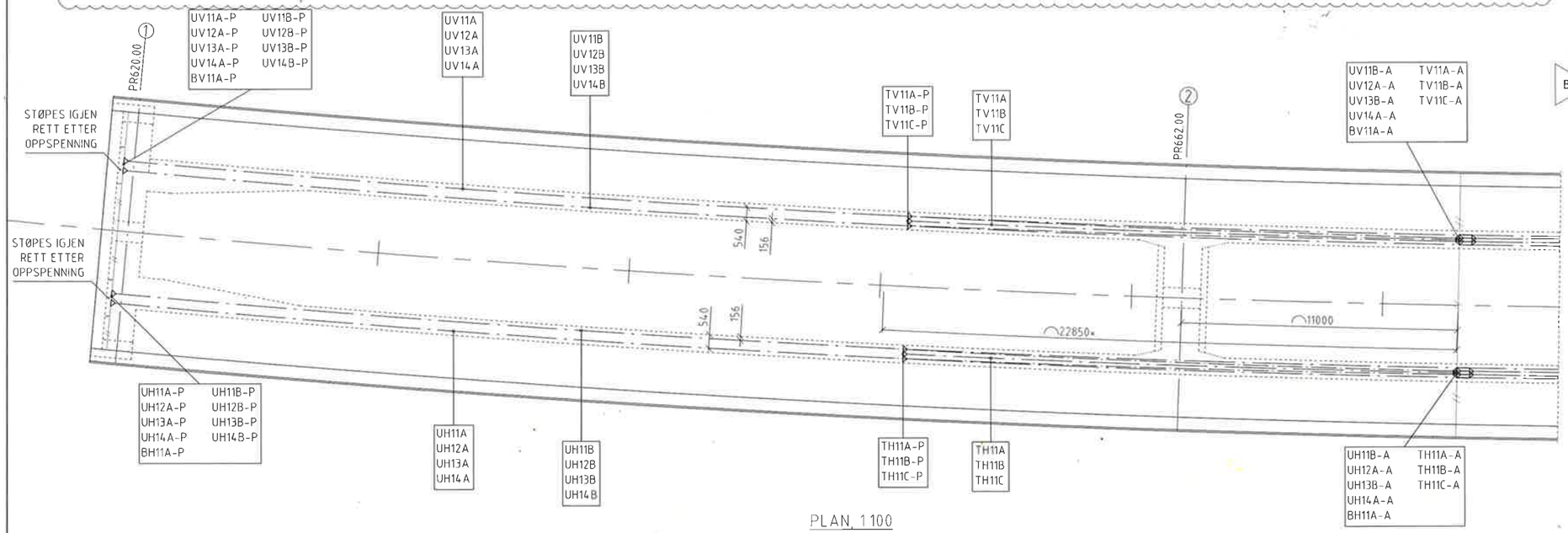

PLAN, 1:100

SPENNKABLENE BV11A OG BH11A ER IKKE VIST

×) SIDEVEGS PLASSERING AV KABLER VARIERER, SE TABELL TEGN K02-073

MERKNADER

1. OVER AKSE 2: TOTALT 24 KABLER IHT ETA GODKJENNING 09/0286, DERAV 20stk BBR CONA CMI BT 1906-150 1860 OG 4stk BBR CONA CMI BT 1206-150 1860 (TV11A, TV11C, TH11A OG TH11C)

   DATA: BBR CONA CMI BT 1906-150 1860
   KARAKTERISTISK FLYTELAST: $F_{p0\,1k}$=4674 kN
   OPPSPENNINGSKRAFT FØR LÅSING: F_{p}=4130 kN
   SPENNKRAFT ETTER LÅSING: F_{pm0}=3973 kN (ER IVARETATT MED 6mm KILEGLIPP)

   DATA: BBR CONA CMI BT 1206-150 1860
   KARAKTERISTISK FLYTELAST: $F_{p0\,1k}$=2952 kN
   OPPSPENNINGSKRAFT FØR LÅSING: F_{p}=2610 kN
   SPENNKRAFT ETTER LÅSING: F_{pm0}=2509 kN (ER IVARETATT MED 6mm KILEGLIPP)

2. KABELRØRENDE LEGGES GJENNOM DE ANGITTE PUNKTENE OG SLIK AT DE FERDIGE KANALER IKKE FÅR NOEN SKARP BØY.

3. TOLERANSER: VERTIKALT: ±10MM; HORISONTALT ±20MM

4. ANTATT STÅLKABELRØR MED INNVENDIG DIAMETER Ø100mm FOR BBR CONA CMI BT 1906-150 1860.
   ANTATT STÅLKABELRØR MED INNVENDIG DIAMETER Ø80mm FOR BBR CONA CMI BT 1206-150 1860.
   MINSTE BØYERADIUS PÅ KABELRØR ER 6.2m

5. MIN. BETONGFASTHET VED FULL OPPSPENNING f_{ck} > 43MPa (TERNINGFASTHET)

6. OPPSPENNING SKAL UTFØRES SYMMETRISK OM SENTERLINJE BRU. MAKS EN KABEL SKAL SPENNES EKSENTRISK

7. ALLE KABELKANALER SKAL INJISERES RETT ETTER OPPSPENNING.

8. PASSIVT OG AKTIVT ANKER: BBR VT CONA CMI BT 1906 ANKER. BBR VT CONA CMI BT 1206 ANKER.

9. FAST KOBLING: BBR VT CONA CMI BT COUPLER K 1906.

10. OPPSPENNINGSREKKEFØLGE:
    TRAU: 8 KABLER SPENNES VED STØPESKJØT,
    REKKEFØLGE: UV13B-UH13B-UV11B-UH11B-UV12A-UH12A -BV11A-BH11A
    SAMVIRKE: 8 KABLER SPENNES VED STØPESKJØT,
    REKKEFØLGE: UV14A-UH14A-TV11B-TH11B-TV11A -TH11A-TV11C-TH11C

FORKLARINGER:

KABELNAVNGIVING:
B=BUNNPLATE
U=STEG
T=TOPPLATE
V=VENSTRE SIDE, H=HØYRE SIDE
FØRSTE SIFFER GIR STØPEETAPPE KABELEN TREKKES FRA.
ANDRE SIFFER GIR PLASSERING I HØYDEN I KONSTRUKSJONSDEL
A=YTTERSTE KABEL I KONSTRUKSJONSDEL, B=NEST YTTERSTE osv

-A (STREK+A): AKTIV ENDE PÅ SPENNKABEL
-P (STREK+P): PASSIV ENDE PÅ SPENNKABEL

B

| | AKSE 1 | | |

Appendix B

Concrete cover

Calculations of concrete cover after EC2

Attachment
B

COVER TO REINFORCEMENT

Assuming Ø25 for longitudinal steel and Ø12 for strands. Structural dimensions are given below:

$\varnothing_L := 30\ mm$ $\varnothing_S := 15\ mm$

The ducts are assumed with outer diameter of 100mm

$\varnothing_o := 100\ mm$

Clear spacing between ducts are found as in Chapter 3.4 according to EC2

$d_g := 32\ mm$

$a_h := \max\left(d_g, \varnothing_o, 40\ mm\right) = 100.00\ mm$ Horizontal distance

$a_v := \max\left(d_g + 5\ mm, \varnothing_o, 50\ mm\right) = 100.00\ mm$ Vertical distance

Cover

The minimum cover is set to: $C_{min.b} := min\left(\varnothing_o, 80\ mm\right) = 0.08\ m$

Cover to upprt flange

$C_{min.durUF} := 60\ mm$

$C_{min.UF} := \max\left(C_{min.b}, C_{min.durUF}\right) = 80\ mm$

$\Delta C_{dev.UF} := 15\ mm$

$C_{nom.UF} := C_{min.UF} + \Delta C_{dev.UF} = 95\ mm$ Nomnal cover for upper flanger

Cover to lower flange

$C_{min.durLF} := 50\ mm$

$C_{min.LF} := \max\left(C_{min.b}, C_{min.durLF}\right) = 80\ mm$

$\Delta C_{dev.LF} := 15\ mm$

$C_{nom.LF} := C_{min.LF} + \Delta C_{dev.LF} = 95\ mm$ Nomnal cover for lower flanger

Created with PTC Mathcad Express. See www.mathcad.com for more information.

Appendix C

Load calculations

Calculations of loads used in NovaFrame

This appendix is divided into the following parts:

C-1: Self-weight

C-2: Traffic load

C-3: Wind load

C-4: Thermal load

C-5: Creep

C-6: Shrinkage

Attachment
C-1

Self-weight

Self-weight of 26 kN/m^3 is used for prestressed concrete.

$q_{sw} := 26 \frac{kN}{m^3}$

In the box-girder there are placed four walls that will fit over the supports after finl launching. These walls are added as point loads in NovaFrame, and are found as following:

$\rho_c := 22 \frac{kN}{m^3}$	Density of concrete of walls
$A_{inner} := 13.656262\ m^2$	Area of inner box-girder
$t_{wall.1} := 1.6\ m$	Thickness of wall 1
$t_{wall.2} := 1.5\ m$	Thickness of wall 2
$t_{wall.3} := t_{wall.2}$	Thickness of wall 3
$t_{wall.4} := 2.0\ m$	Thickness of wall 4

$P_{wall.1} := A_{inner} \cdot \rho_c \cdot t_{wall.1} = 480.7\ kN$	Point load - wall 1
$P_{wall.2} := A_{inner} \cdot \rho_c \cdot t_{wall.2} = 450.657\ kN$	Point load - wall 2
$P_{wall.3} := P_{wall.2}$	Point load - wall 3
$P_{wall.4} := A_{inner} \cdot \rho_c \cdot t_{wall.4} = 600.876\ kN$	Point load - wall 4

Created with PTC Mathcad Express. See www.mathcad.com for more information.

Attachment
C-2

Traffic load

$w := 11\ m$ Available width

$n_1 := 3$ for $9\ m < w < 12\ m$ Number of lanes, EC1-2 Cl. 4.2.3

$w - 3\ m \cdot n_1 = 2\ m$ Remaining width

Vertical loading is defined for Load Model 1 and 2.

For load model 1, the distributed loads for each lane is defined in Table 42 in EC 1-2 as shown below.

Location	Tandem system *TS*	*UDL* system
	Axle loads Q_{ik} (kN)	q_{ik} (or q_{ik}) (kN/m^2)
Lane Number 1	300	9
Lane Number 2	200	2,5
Lane Number 3	100	2,5
Other lanes	0	2,5
Remaining area (q_{rk})	0	2,5

For load model 2, the distributed load is given in EC1-2 Cl. 4.3.3, and is set to be:

$Q_{ak} := 400\ kN$

As a simplification, horozontal forces due to traffic is neglected

Created with PTC Mathcad Express. See www.mathcad.com for more information.

Attachment
C-3

Wind load

Wind load calculations are done after EC1-1-4

$L := 57\ m$ Largest span

$v_{b.0} := 22\ \frac{m}{s}$ Referance wind speed for Sør-Aurdal in Oppand EC1-1-4 NA.4(901.1)

$c_{dir} := 1.0$ EC1-1-4 NA.4.2(2)

$c_{season} := 1.0$ EC1-1-4 NA.4.2(2)

$H_0 := 900\ m$ EC-1-1-4 NA.4(901.2)

$H := 227\ m$ Kote height for Bagn bridge

$H_0 > H$ -> $c_{alt} := 1.0$ EC1-1-4 NA.4.2(2)

$c_{prob} := 1.0$

$v_b := c_{dir} \cdot c_{season} \cdot c_{prob} \cdot v_{b.0} = 22\ \frac{m}{s}$

$c_{0.z} := 1.0$ EC1-1-4 Cl. 4.3.1(1)

FROM EC1-1-4 Table NA.4.1 -> for terrain roughness category II

$k_r := 0.19$ Terrain roughness factor EC1-1-4 Table NA.4.1

$z_0 := 0.05\ m$ Roughness length EC1-1-4 Table NA.4.1

$z_{min} := 4\ m$ Minimum height EC1-1-4 Table NA.4.1

$z := 5\ m$ Height from superstructure to ground below

$z_{max} := 200\ m$ EC1-1-4 Cl. 4.3.2(1)

$c_{r.z} := k_r \cdot \ln\left(\frac{z}{z_0}\right) = 0.875$ for $z_{min} < z < z_{max}$ Roughness factor Cl. 4.3.2(1)

$v_{m.z} := c_{r.z} \cdot c_{0.z} \cdot v_b = 19.25\ \frac{m}{s}$ EC1-1-4 Cl. 4.3.1(1)

Created with PTC Mathcad Express. See www.mathcad.com for more information.

Attachment
C-3

Wind load

$k_l := 1.0$ Turbulens factor EC1-1-4 NA.4.4

$I_{v.z} := \frac{k_l}{c_{0.z} \cdot \ln\left(\frac{z}{z_0}\right)} = 0.217$ for $z_{min} < z < z_{max}$ Turbulens intensity EC1-1-4 Cl.4.4(1)

$\rho := 1.25 \ \frac{kg}{m^3}$ Air density

$k_p := 3.5$ Factor EC1-1-4 NA.4.5(1)

$q_{p.z} := 0.5 \cdot \rho \cdot {v_{m.z}}^2 \cdot (1 + 2 \ k_p \cdot I_{v.z}) = 583.619 \ Pa$ EC1-1-4 NA.4.5(1)

$q_b := \frac{1}{2} \ \rho \cdot {v_b}^2 = 302.5 \ Pa$ EC1-1-4 NA.4.5(1)

Created with PTC Mathcad Express. See www.mathcad.com for more information.

Attachment
C-3

Wind load

Wind - WITHOUT traffic

$L := 1\ \frac{m}{m}$ Unit length

$b_{tot} := 11.225\ m$ Bridge width

$d := 3.5\ m$ Bridge depth

$d_{tot} := d + 0.6\ m = 4.1\ m$ Heigth after EC1-1-4 Table 8.1

$A_{ref} := d_{tot} \cdot L = 4.1\ \frac{m^2}{m}$ Reference area EC1-1-4 Cl.8.3.1(3)

$c_{e.z} := \frac{q_{p.z}}{q_b} = 1.929$ Exposure factor, EC1-1-4 Cl.4.5(1)

$c_{fx.0} := 1.68$ for $\frac{b_{tot}}{d_{tot}} = 2.738$ Force facor, EC1-1-4 Figure 8.3

$c_{f.x} := c_{fx.0}$

$C := c_{e.z} \cdot c_{f.x} = 3.241$ Vind load factor, Cl 8.3.2(1)

$F_{w.x} := \frac{1}{2}\ \rho \cdot {v_b}^2 \cdot C \cdot A_{ref} = 4019.971\ \frac{N}{m}$ **Wind in x-direction**

$c_{f.z} := 0.9$ Force factor Cl.8.3.3(1)

$C := c_{e.z} \cdot c_{f.z} = 1.736$ Vind load factor, Cl 8.3.2(1)

$A_{ref.z} := b_{tot} \cdot L = 11.225\ m$

$F_{w.z} := \frac{1}{2} \cdot \rho \cdot {v_b}^2 \cdot C \cdot A_{ref.z} = 5896.016\ \frac{N}{m}$ **Wind in z-direction**

$e := \frac{b_{tot}}{4} = 2.806\ m$ Eccentricity for F(wz) CL 8.3.3(5)

$F_{w.y} := 0.25 \cdot F_{w.x} = 1004.993\ \frac{N}{m}$ **Wind in y-direction**

Created with PTC Mathcad Express. See www.mathcad.com for more information.

Attachment
C-3

Wind load

Wind - WITH traffic

$v_p := 35\ \frac{m}{s}$ Wind at highest point of the roadHB N400 5.4.3.3

$q_{b.t} := \frac{1}{2} \cdot \rho \cdot v_p^{\ 2} = 765.625\ Pa$

$d_{tot.t} := d + 2\ m = 5.5\ m$

$A_{ref.x.t} := d_{tot.t} \cdot L = 5.5\ \frac{m^2}{m}$

$c_{e.t.z} := \frac{q_{p.z}}{q_{b.t}} = 0.762$

$c_{x.f.t} := 1.89$ for $\frac{b_{tot}}{d_{tot.t}} = 2.041$ Force facor, EC1-1-4 Figure 8.3

$c_{fx.0} := c_{x.f.t}$

$F_{w.x.t} := \frac{1}{2}\ \rho \cdot v_b^{\ 2} \cdot C \cdot A_{ref.x.t} = 2888.916\ \frac{N}{m}$ **Wind in x-direction**

$c_{f.t.z} := 0.9$ Force factor Cl.8.3.3(1)

$C_t := c_{e.t.z} \cdot c_{f.t.z} = 0.686$ Vind load factor, Cl 8.3.2(1)

$A_{ref.z.t} := b_{tot} \cdot L = 11.225\ m$

$F_{w.z.t} := \frac{1}{2} \cdot \rho \cdot v_b^{\ 2} \cdot C_t \cdot A_{ref.z.t} = 2329.528\ \frac{N}{m}$ **Wind in z-direction**

$F_{w.y} := 0.25 \cdot F_{w.x.t} = 722.229\ \frac{N}{m}$ **Wind in y-direction**

Created with PTC Mathcad Express. See www.mathcad.com for more information.

Attachment
C-4

Determination of thermal load

Calculations done after EC1-1-5

Launching stages:

$\Delta T_{Mheat} := 10$ Table NA.6.1 + Table NA.6.2

$\Delta T_{Mcool} := 5$ Table NA.6.1 + Table NA.6.2

Input in NovaFrame: dT/N-width

$N_{width} := 3.5\ m$ Height of boc girder (N-direction)

$N_{over.poss} := \frac{\Delta T_{Mheat}}{N_{width}} = 2.86\ \frac{1}{m}$ Temperature gradient (over=positive)

$N_{over.neg} := \frac{\Delta T_{Mcool}}{N_{width}} = 1.43\ \frac{1}{m}$ Temperature gradient (over=negative)

Final construction

$T_{max.1} := 36$ Max temp in degrees(celcius) NA.A1

$T_{min.1} := -40$

EC1-1-5 NA.A.1(1): Values for Tmax and Tmin are to be adjusted for the structures height over the ocean by subtracting 0.3 degrees (celcius) pr. 100 meters height for minimum temp, and 0.65 degrees (celcius) for determination of maximum air temp.

$H := 227\ m$ Bridge - m.o.h

$\delta := \frac{H}{100\ m} = 2.27$

$\delta_{Tmax} := 0.65$

$\delta_{Tmin} := 0.3$

$T_{max} := T_{max.1} - \delta \cdot \delta_{Tmax} = 34.525$

$T_{min} := T_{min.1} - \delta \cdot \delta_{Tmin} = -40.681$

$T_{e.max} := T_{max} - 3 = 31.525$ Figure NA.6.1

$T_{e.min} := T_{min} + 8 = -32.681$ Figure NA.6.1

$T_0 := 10$

Created with PTC Mathcad Express. See www.mathcad.com for more information.

Determination of thermal load

$\Delta T_{N.exp} := T_{e.max} - T_0 = 21.525$

$\Delta T_{N.con} := T_{e.min} - T_0 = -42.681$

LOADCOMBINATIONS:

$\omega_N := 0.35$

$\omega_M := 0.75$

$LC_1 := \Delta T_{Mheat} + \omega_N \cdot \Delta T_{N.exp} = 17.534$

$LC_2 := \Delta T_{Mheat} + \omega_N \cdot \Delta T_{N.con} = -4.938$

$LC_3 := \Delta T_{Mcool} + \omega_N \cdot \Delta T_{N.exp} = 12.534$

$LC_4 := \Delta T_{Mcool} + \omega_N \cdot \Delta T_{N.con} = -9.938$

$LC_5 := \omega_M \cdot \Delta T_{Mheat} + \Delta T_{N.exp} = 29.025$

$LC_6 := \omega_M \cdot \Delta T_{Mheat} + \Delta T_{N.con} = -35.181$

$LC_5 := \omega_M \cdot \Delta T_{Mcool} + \Delta T_{N.exp} = 25.275$

$LC_5 := \omega_M \cdot \Delta T_{Mcool} + \Delta T_{N.con} = -38.931$

Created with PTC Mathcad Express. See www.mathcad.com for more information.

Attachment
C-5

Calculation of creep factor

$RH := 0.8$ Relative humidity

$A_c := 8.82\ m^2$ Cross-sectional area

$u := 27839.199\ mm$ Free circumference of the cross-section

$f_{cm} := 53\ MPa$

$t_0 := 7$ Age of the concrete at loading (in days)

$t_{100} := 100 \cdot 365 = 36500$ Age of concrete at 100 years (in days)

$t_{28} := 28$ Age of concrete after 28 days

$h_0 := \frac{2 \cdot A_c}{u \cdot mm} = 633.639$ The notional size of the member in mm

$\alpha_1 := \left(\frac{35\ MPa}{f_{cm}}\right)^{0.7} = 0.748$

$\alpha_2 := \left(\frac{35\ MPa}{f_{cm}}\right)^{0.2} = 0.92$

Coefficients to consider the influence of the concrete strength

$\alpha_3 := \left(\frac{35\ MPa}{f_{cm}}\right)^{0.5} = 0.813$

$\beta_H := 1.5 \left(1 + \left(0.012 \cdot RH\right)^{18}\right) \cdot h_0 + 250 \cdot \alpha_3 = 1153.617$ Coefficient depending on the relative humidity and h0

$\phi_{RH} := \left(1 + \frac{1 - RH}{0.1 \cdot \sqrt[3]{h_0}} \cdot \alpha_1\right) \cdot \alpha_2 = 1.081$ Factor to allow for the effect of humidity on the notional creep coefficient

$\beta_{fcm} := \frac{16.8}{\sqrt{\frac{f_{cm}}{MPa}}} = 2.308$ Factor to allow for the effect of concrete strength on the notional creep coefficient

$\beta_{t0} := \frac{1}{\left(0.1 + t_0^{0.20}\right)} = 0.635$ Factor to allow for the effect of concrete strength

$\phi_0 := \phi_{RH} \cdot \beta_{fcm} \cdot \beta_{t0} = 1.583$ Notional creep coefficient

Creep factor after 100 years

$\beta_{c.100.t0} := \left(\frac{\left(t_{100} - t_0\right)}{\beta_H + t_{100} - t_0}\right)^{0.3} = 0.991$

$\phi_{t.t0} := \phi_0 \cdot \beta_{c.100.t0} = 1.5679$

Creep factor after 28 days

$\beta_{c.28.t0} := \left(\frac{\left(t_{28} - t_0\right)}{\beta_H + t_{28} - t_0}\right)^{0.3} = 0.299$

$\phi_{28.t0} := \phi_0 \cdot \beta_{c.28.t0} = 0.4732$

Created with PTC Mathcad Express. See www.mathcad.com for more information.

Attachment
C-5

Calculation of creep factor

Creep strain

$E_{cm} := 36\ GPa$ Secant modulus of elasticity of concrete

$E_{c.eff} := \frac{E_{cm}}{1+\phi_{t.t0}} = 14019.466\ MPa$ Effective modulus

$A_{p.f} := 22 \cdot 2100\ mm^2 = 46200\ mm^2$ Total tendon area - FLANGE

$A_{p.w} := 4 \cdot 2100\ mm^2 = 8400\ mm^2$ Total tendon area - WEB

$f_{pk} := 1860\ MPa$ Characteristic tensile strength

$f_{p0.1k} := 1640\ MPa$ Characteristic 0.1% proof-stress

$\sigma_{p.max} := min\left(0.8\ f_{pk}, 0.9\ f_{p0.1k}\right) = 1476\ MPa$

$P_{max.f} := A_{p.f} \cdot \sigma_{p.max} = 68191.2\ kN$ Max prestressing force - DURING LAUNCH

$P_{max} := \left(A_{p.f} + A_{p.w}\right) \cdot \sigma_{p.max} = 80589.6\ kN$ Max prestressing force - DURING FINAL

$A_c := 8.82\ m^2$ Total concrete area

$I_{c.x} := 14.92\ m^4$ Second moment of area about x-axis

$y_{cog} := 2250.8\ mm$ Height from bottom to CoG

$H := 3.5\ m$ Height of box-girder

$y_t := H - y_{cog} = 1.249\ m$ Height from top to CoG

$y_b := y_{cog}$ Height from bottom to CoG

$e_1 := 1.06\ m \qquad e_2 := 2.06\ m$ Eccentricities

DURING LAUNCHING:

Over support:

$M_{support.NF} := 109039\ kN \cdot m$ Moment due to self-weight

$M_{support} := -P_{max.f} \cdot e_1 + M_{support.NF} = 36756.328\ kN \cdot m$ Moment due to self-weight +PS

$\varepsilon_{cc.support} := -\frac{P_{max.f}}{E_{c.eff} \cdot A_c} + \frac{M_{support} \cdot y_t}{E_{cm} \cdot I_{c.x}} = -4.66 \cdot 10^{-4}$

Span:

$M_{span.NF} := 59030\ kN \cdot m$ Moment due to self-weight

$M_{span} := -P_{max.f} \cdot e_2 + M_{span.NF} = -81443.872\ kN \cdot m$ Moment due to self-weight +PS

Created with PTC Mathcad Express. See www.mathcad.com for more information.

Calculation of creep factor

$$\varepsilon_{cc.span} := \frac{-P_{max.f}}{E_{c.eff} \cdot A_c} + \frac{M_{span} \cdot y_b}{E_{cm} \cdot I_{c.x}} = -8.928 \cdot 10^{-4}$$

Mean value

$$\varepsilon_{cc.mean} := \frac{\varepsilon_{cc.support} + \varepsilon_{cc.span}}{2} = -6.794 \cdot 10^{-4}$$

FINAL CONSTRUCTION:

Over support:

$M_{support.NF} := 59744\ kN \cdot m$ Moment due to self-weight

$M_{support} := -P_{max} \cdot e_1 + M_{support.NF} = -25680.976\ kN \cdot m$ Moment due to self-weight +PS

$$\varepsilon_{cc.support} := -\frac{P_{max}}{E_{c.eff} \cdot A_c} + \frac{M_{support} \cdot y_t}{E_{cm} \cdot I_{c.x}} = -7.115 \cdot 10^{-4}$$

Span:

$M_{span.NF} := 36662\ kN \cdot m$ Moment due to self-weight

$M_{span} := -P_{max} \cdot e_2 + M_{span.NF} = -129352.576\ kN \cdot m$ Moment due to self-weight +PS

$$\varepsilon_{cc.span} := \frac{-P_{max}}{E_{c.eff} \cdot A_c} + \frac{M_{span} \cdot y_b}{E_{cm} \cdot I_{c.x}} = -1.194 \cdot 10^{-3}$$

Mean value

$$\varepsilon_{cc.mean} := \frac{\varepsilon_{cc.support} + \varepsilon_{cc.span}}{2} = -9.526 \cdot 10^{-4}$$

Created with PTC Mathcad Express. See www.mathcad.com for more information.

Attachment
C-6

General calculation of shrincage

CALCULATIONS DONE AFTER ANNEX B IN EUROCODE 2

$RH := 0.8$ Relative humidity

$A_c := 8.82\ m^2$ Cross-sectional area

$u := 27839.199\ mm$ Free circumference of the cross-section

$f_{ck} := 45\ MPa$ Characteristic compressive strength

$f_{cm} := 53\ MPa$ Mean value of concrete compressive strength

$t := 28$ Age of the concrete at loading (in days)

$t_s := 100 \cdot 365 = 3.65 \cdot 10^4$ Age of concrete at calculation (in days)

$h_0 := \frac{2 \cdot A_c}{u \cdot mm} = 633.6389$ Notonal size of the member in mm

$\beta_{RH} := 1.55\ \left(1 - RH^3\right) = 0.7564$

ASSUMING CEMENT CLASS N

$\alpha_{ds1} := 4$ Coefficient, depending on cement class

$\alpha_{ds2} := 0.12$

$\varepsilon_{cd.0} := 0.85 \left(\left(220 + 110\ \alpha_{ds1}\right) \cdot \exp\left(-\alpha_{ds2} \cdot \frac{f_{cm}}{10\ MPa}\right)\right) \cdot 10^{-6} \cdot \beta_{RH} = 2.2465 \cdot 10^{-4}$

$\beta_{ds.t.ts} := \frac{t - t_s}{\left(t - t_s\right) + 0.04 \cdot \sqrt{h_0{}^3}} = 1.0178$ 100 years

$\beta_{ds.t.t} := \frac{t - t}{\left(t - t_s\right) + 0.04 \cdot \sqrt{h_0{}^3}} = 0$ 28 days

$k_h := 0.70$ EC2 Table 3.3 --> for h0>500

$\varepsilon_{cd.ts} := \beta_{ds.t.ts} \cdot k_h \cdot \varepsilon_{cd.0} = 1.6005 \cdot 10^{-4}$ Drying shrinkage strain after 100years

$\varepsilon_{cd.t} := \beta_{ds.t.t} \cdot k_h \cdot \varepsilon_{cd.0} = 0$ Drying shrinkage strain after 28 days

$\beta_{as.t} := 1 - \exp\left(-0.2 \cdot t^{0.5}\right) = 0.653$

$\varepsilon_{ca.\infty} := 2.5 \left(\frac{f_{ck}}{MPa} - 10\right) \cdot 10^{-6} = 8.75 \cdot 10^{-5}$

Created with PTC Mathcad Express. See www.mathcad.com for more information.

General calculation of shrincage

$\varepsilon_{ca.t} := \beta_{as.t} \cdot \varepsilon_{ca.\infty} = 5.7134 \cdot 10^{-5}$ Autogenous shrinkage strain (100 years)

$\varepsilon_{cs.100} := \varepsilon_{cd.ts} + \varepsilon_{ca.t} = 2.1719 \cdot 10^{-4}$ Total shrinkage strain after 100 years

$\varepsilon_{cs.28} := \varepsilon_{cd.t} + \varepsilon_{ca.t} = 5.7134 \cdot 10^{-5}$ Total shrinkage strain after 28 days

Calculation of total shrinkage strain after reinforcement is bonded

$\phi_{t.t0} := 1.568$

$E_p := 195\ GPa$ Elastic modulus for prestressing steel

$A_p := (4+22) \cdot 1680\ mm^2 = 43680\ mm^2$ Total prestressing area

$N_s := \varepsilon_{cs.100} \cdot E_p \cdot A_p = 1849.9133\ kN$

$I_{c.x} := 14.92\ m^4$ Second moment of area

$e_1 := 1.06\ m$ $e_2 := 2.06\ m$ Eccentricities

$E_{cm} := 36\ GPa$ Secant modulus of elasticity of concrete

$E_{cl.100year} := \dfrac{E_{cm}}{1+\phi_{t.t0}} = (1.4019 \cdot 10^4)\ MPa$

$\eta_p := \dfrac{E_p}{E_{cl.100year}} = 13.91$

$A_t := A_c + (\eta_p - 1) \cdot A_p = 9.3839\ m^2$ Transformed cross-secttional area

$y_{t.support} := \dfrac{(\eta_p - 1)\ A_p \cdot e_1}{A_t} = 63.6988\ mm$ Distance from transformed CoG to regular CoG

$y_{t.span} := \dfrac{(\eta_p - 1)\ A_p \cdot e_2}{A_t} = 123.7919\ mm$ Distance from transformed CoG to regular CoG

$I_{t.support} := I_{c.x} + (\eta_p - 1) \cdot A_p \cdot (e_1 - y_{t.support})^2 = (1.548 \cdot 10^{13})\ mm^4$

$I_{t.span} := I_{c.x} + (\eta_p - 1) \cdot A_p \cdot (e_2 - y_{t.span})^2 = (1.7034 \cdot 10^{13})\ mm^4$

$I_t := min(I_{t.support}, I_{t.span}) = (1.548 \cdot 10^{13})\ mm^4$ Support --> use e1

$\Delta\varepsilon_{p.shrinkage} := \varepsilon_{cs.100} + \dfrac{N_s}{E_{cl.100year} \cdot A_t} + \dfrac{N_s \cdot (e_1 - y_{t.support})^2}{E_{cl.100year} \cdot I_t} = 2.3971 \cdot 10^{-4}$

Created with PTC Mathcad Express. See www.mathcad.com for more information.

Appendix D

Loss of time-dependent prestressing force

Calculation of loss of prestressing force after EC2

This appendix is divided into the following parts:

D-1: Time-dependent losses for final construction

D-2: Time-dependent losses for launching stages

D-3: Overall effect

Attachment
D-1

Loss of prestressing force

$E_{cm} := 36\ GPa$ Secant modulus of elasticity of concrete

$\phi_{t.t0} := 1.5679$ Creep 100 years

$E_{c.eff} := \frac{E_{cm}}{1+\phi_{t.t0}} = 14.019\ GPa$

$A_c := 8.82\ m^2$ Concrete area

$I_x := 14.92\ m^4$ Second moment of area

$y_{cog} := 2250.8\ mm$ Distance from bottom to CoG

$E_p := 195\ GPa$ Elastic modulus for prestressing steel

$A_p := 2100\ mm^2$ Area pr tendon

$n := 26$ Total nr of tendons

$A_{tot} := n \cdot A_p = 54600\ mm^2$ Total tendon area

$\eta_{short} := \frac{E_p}{E_{cm}} = 5.417$

$\eta_{long} := \frac{E_p}{E_{c.eff}} = 13.909$

Area of transformed section

$A_{t.short} := A_c + (\eta_{short} - 1)\ A_{tot} = (9.061 \cdot 10^6)\ mm^2$

$A_{t.long} := A_c + (\eta_{long} - 1)\ A_{tot} = (9.525 \cdot 10^6)\ mm^2$

Eccentricities

$e_1 := 1.06\ m$ $e_2 := 2.06\ m$

The distance from CoG of the transformed section to CoG of the normal concrete section is calculated:

Short-term:

$y_{t.s.span} := \frac{(\eta_{short} - 1) \cdot A_{tot} \cdot e_2}{A_{t.short}} = 54.824\ mm$

$y_{t.s.support} := \frac{(\eta_{short} - 1) \cdot A_{tot} \cdot e_1}{A_{t.short}} = 28.21\ mm$

$I_{s.span} := I_x + A_c \cdot y_{t.s.span}^2 + (\eta_{short} - 1) \cdot A_{tot} \cdot (e_2 - y_{t.s.span})^2 = 15.916\ m^4$

$I_{s.support} := I_x + A_c \cdot y_{t.s.support}^2 + (\eta_{short} - 1) \cdot A_{tot} \cdot (e_1 - y_{t.s.support})^2 = 15.184\ m^4$

Created with PTC Mathcad Express. See www.mathcad.com for more information.

Loss of prestressing force

Long-term:

$$y_{t.l.span} := \frac{(\eta_{long} - 1) \cdot A_{tot} \cdot e_2}{A_{t.long}} = 152.444 \ mm$$

$$y_{t.l.support} := \frac{(\eta_{long} - 1) \cdot A_{tot} \cdot e_1}{A_{t.long}} = 78.442 \ mm$$

$$I_{l.span} := I_x + A_c \cdot y_{t.l.span}^{\ 2} + (\eta_{long} - 1) \cdot A_{tot} \cdot (e_2 - y_{t.l.span})^2 = 17.69 \ m^4$$

$$I_{l.support} := I_x + A_c \cdot y_{t.l.support}^{\ 2} + (\eta_{long} - 1) \cdot A_{tot} \cdot (e_1 - y_{t.l.support})^2 = 15.653 \ m^4$$

Created with PTC Mathcad Express. See www.mathcad.com for more information.

Loss of prestressing force

Creep - FINAL

Moments due to self-weight from NovaFrame:

$M_{support.NF} := 59108.36\ kN \cdot m$ $M_{span.NF} := 35851.8\ kN \cdot m$

$f_{pk} := 1860\ MPa$

$f_{p0.1k} := 1640\ MPa$

$\sigma_{p.max} := min\left(0.8\ f_{pk}, 0.9\ f_{p0.1k}\right) = \left(1.476 \cdot 10^{3}\right)\ MPa$

$P_{max} := A_p \cdot \sigma_{p.max} = 3099.6\ kN$

$N_t := -P_{max} \cdot n = -80589.6\ kN$

$M_{span} := N_t \cdot e_2 = -166014.576\ kN \cdot m$

$M_{support} := N_t \cdot e_1 = -85424.976\ kN \cdot m$

Long-term:

$M_{t.l.span} := M_{span} - N_t \cdot y_{t.l.span} + M_{span.NF} = -117877.4\ kN \cdot m$

$\sigma_{c.l} := -\frac{N_t}{A_{t.long}} + \frac{M_{t.l.span} \cdot \left(y_{cog} - y_{t.l.span}\right)}{I_{l.span}} = -5.522\ MPa$

$\Delta\varepsilon_{pl} := \frac{\sigma_{c.l}}{E_{c.eff}} = -3.939 \cdot 10^{-4}$

$\Delta\sigma_{pl} := \Delta\varepsilon_{pl} \cdot E_p = -76.803\ MPa$

Short-term:

$M_{t.s.span} := M_{span} - N_t \cdot y_{t.s.span} + M_{span.NF} = -125744.527\ kN \cdot m$

$\sigma_{c.s} := -\frac{N_t}{A_{t.short}} + \frac{M_{t.s.span} \cdot \left(y_{cog} - y_{t.s.span}\right)}{I_{s.span}} = -8.455\ MPa$

$\Delta\varepsilon_{ps} := \frac{\sigma_{c.s}}{E_{cm}} = -2.349 \cdot 10^{-4}$

$\Delta\sigma_{ps} := \Delta\varepsilon_{ps} \cdot E_p = -45.799\ MPa$

Created with PTC Mathcad Express. See www.mathcad.com for more information.

Loss of prestressing force

$$\frac{\text{abs}\left(\Delta\sigma_{ps}\right)}{\sigma_{p.max}}\cdot 100 = 3.103$$ Loss due to creep (short term) in %

Total loss due to creep:

$$\Delta\sigma_{pc} := \Delta\sigma_{pl} + \Delta\sigma_{ps} = -122.602\ \textit{MPa}$$

$$loss_c := \frac{\text{abs}\left(\Delta\sigma_{pc}\right)}{\sigma_{p.max}}\cdot 100 = 8.306$$ Total loss due to creep in %

Shrinkage

$$\varepsilon_{cs.100} := -2.1719\cdot 10^{-4}$$

$$N_s := \text{abs}\left(\varepsilon_{cs.100}\right)\cdot A_{tot}\cdot E_p = 2312.422\ \textit{kN}$$

$$\Delta\varepsilon_{p.shrinkage} := \varepsilon_{cs.100} + \frac{N_s}{E_{c.eff}\cdot A_{t.long}} + \frac{N_s\cdot\left(e_2 - y_{t.l.span}\right)^2}{E_{c.eff}\cdot I_{l.span}} = -1.659\cdot 10^{-4}$$

$$\Delta\sigma_{p.shrinkage} := \Delta\varepsilon_{p.shrinkage}\cdot E_p = -32.359\ \textit{MPa}$$

$$loss_l := \frac{\text{abs}\left(\Delta\sigma_{p.shrinkage}\right)}{\sigma_{p.max}}\cdot 100 = 2.192$$ Shrinkage loss in %

Relaxation

$$\rho_{1000} := 0.025$$

$$\sigma_{pm0} := min\left(0.75\ f_{pk}, 0.85\ f_{p0.1k}\right) = 1394\ \textit{MPa}$$

$$\sigma_{pi} := \frac{\text{abs}\left(N_t\right)}{A_{tot}} = 1476\ \textit{MPa}$$

$$\mu := \frac{\sigma_{pi}}{f_{pk}} = 0.794$$

Long term: final construction

$$t_{100} := 100\cdot 365\cdot 24 = 8.76\cdot 10^5$$ 100 years in hours

$$\frac{\Delta\sigma_{pr}}{\sigma_{pi}} = 0.66\cdot\rho_{1000}\cdot\exp\left(9.1\cdot\mu\cdot\left(\frac{t_{100}}{1000}\right)^{0.75\cdot(1-\mu)}\cdot 10^{-5}\right) = 0.017$$

Created with PTC Mathcad Express. See www.mathcad.com for more information.

Attachment
D- 1

Loss of prestressing force

$\Delta\sigma_{pr} := 0.017 \cdot \sigma_{pi} = 25.092\ \boldsymbol{MPa}$

$\frac{\Delta\sigma_{pr}}{\sigma_{pm0}} \cdot 100 = 1.8$ Loss in percentage from force in prestressing tendons in %

EC2 states that for relaxation, a reduction factor of 0,8 is to be used

$loss_r := \frac{\Delta\sigma_{pr}}{\sigma_{pm0}} \cdot 100 \cdot 0.8 = 1.44$ Adjusted loss, EC2 5.10.6(1)

Created with PTC Mathcad Express. See www.mathcad.com for more information.

Loss of prestressing force

Creep - Launching

$n_f := 22$ Total nr of tendons - flanges

$A_{p.f} := n_f \cdot A_p = 0.046\ m^2$ Total tendon area - flanges

Area of transformed section

$A_{t.short.l} := A_c + (\eta_{short} - 1)\ A_{p.f} = (9.024 \cdot 10^6)\ mm^2$

$A_{t.long.l} := A_c + (\eta_{long} - 1)\ A_{p.f} = (9.416 \cdot 10^6)\ mm^2$

Eccentricities

$e_1 := 1.06\ m$ $e_2 := 2.06\ m$

The distance from CoG of the transformed section to CoG of the normal concrete section is calculated:

$$y_{t.s.span.l} := \frac{(\eta_{short} - 1) \cdot A_{p.f} \cdot e_2}{A_{t.short.l}} = 46.58\ mm$$

$$y_{t.s.support.l} := \frac{(\eta_{short} - 1) \cdot A_{p.f} \cdot e_1}{A_{t.short.l}} = 23.969\ mm$$

$$I_{s.span.l} := I_x + A_c \cdot y_{t.s.span.l}^2 + (\eta_{short} - 1) \cdot A_{p.f} \cdot (e_2 - y_{t.s.span.l})^2 = 15.766\ m^4$$

$$I_{s.support.l} := I_x + A_c \cdot y_{t.s.support.l}^2 + (\eta_{short} - 1) \cdot A_{p.f} \cdot (e_1 - y_{t.s.support.l})^2 = 15.144\ m^4$$

Moments due to self-weight from NovaFrame:

$M_{support.NF} := 109039\ kN \cdot m$ $M_{span.NF} := 59030\ kN \cdot m$

$P_{max} := A_p \cdot \sigma_{p.max} = 3099.6\ kN$

$N_t := -P_{max} \cdot n_f = -68191.2\ kN$

$M_{span} := N_t \cdot e_2 = -140473.872\ kN \cdot m$

$M_{support} := N_t \cdot e_1 = -72282.672\ kN \cdot m$

$M_{t.s.span} := M_{span} - N_t \cdot y_{t.s.span.l} + M_{span.NF} = -78267.505\ kN \cdot m$

$$\sigma_{c.s} := -\frac{N_t}{A_{t.short.l}} + \frac{M_{t.s.span} \cdot (y_{cog} - y_{t.s.span.l})}{I_{s.span.l}} = -3.386\ MPa$$

$$\Delta\varepsilon_{ps} := \frac{\sigma_{c.s}}{E_{cm}} = -9.405 \cdot 10^{-5}$$

Created with PTC Mathcad Express. See www.mathcad.com for more information.

Loss of prestressing force

$\Delta\sigma_{ps} := \Delta\varepsilon_{ps} \cdot E_p = -18.339\ \mathit{MPa}$

$\frac{\mathrm{abs}\left(\Delta\sigma_{ps}\right)}{\sigma_{p.max}} \cdot 100 = 1.242$ Loss due to creep (short term) in %

Shrinkage

$\varepsilon_{cs.28} := 5.7134 \cdot 10^{-5}$

$N_s := \mathrm{abs}\left(\varepsilon_{cs.28}\right) \cdot A_{p.f} \cdot E_p = 514.72\ \mathit{kN}$

$\Delta\varepsilon_{p.shrinkage} := \varepsilon_{cs.28} + \frac{N_s}{E_{c.eff} \cdot A_{t.long}} + \frac{N_s \cdot \left(e_2 - y_{t.l.span}\right)^2}{E_{c.eff} \cdot I_{l.span}} = 6.854 \cdot 10^{-5}$

$\Delta\sigma_{p.shrinkage} := \Delta\varepsilon_{p.shrinkage} \cdot E_p = 13.365\ \mathit{MPa}$

$loss_{s.l} := \frac{\mathrm{abs}\left(\Delta\sigma_{p.shrinkage}\right)}{\sigma_{p.max}} \cdot 100 = 0.906$ Shrinkage loss in %

Relaxation

$t_{28} := 28 \cdot 24 = 672$ 28 days in hours

$\frac{\Delta\sigma_{pr}}{\sigma_{pi}} = 0.66 \cdot \rho_{1000} \cdot \exp\left(9.1 \cdot \mu \cdot \left(\frac{t_{28}}{1000}\right)^{0.75 \cdot (1-\mu)} \cdot 10^{-5}\right) = 0.017$

$\Delta\sigma_{pr} := 0.017 \cdot \sigma_{pi} = 25.092\ \mathit{MPa}$

$\frac{\Delta\sigma_{pr}}{\sigma_{pm0}} \cdot 100 = 1.8$ Loss in percentage from force in prestressing tendons in %

EC2 states that for relaxation, a reduction factor of 0,8 is to be used

$loss_{r.l} := \frac{\Delta\sigma_{pr}}{\sigma_{pm0}} \cdot 100 \cdot 0.8 = 1.44$ Adjusted loss, EC2 5.10.6(1)

Created with PTC Mathcad Express. See www.mathcad.com for more information.

Loss of prestressing force

Overall effect from creep, shrinkage and relaxation:

$loss_{c.s.r} := loss_c + loss_{s.l} + loss_r = 10.652$ Loss in %

Simplified method for determination of loss of prestress:

$$\sigma_{c.QP} := \frac{N_t}{A_{t.long}} + \frac{M_{t.l.span} \cdot \left(e_2 - y_{t.l.span}\right)}{I_{l.span}} = -19.87 \ \textit{MPa}$$

$$\Delta\sigma_{p.c.s.r} := \frac{\varepsilon_{cs.100} \cdot E_p + 0.8 \ \Delta\sigma_{pr} + \frac{E_p}{E_{cm}} \cdot \phi_{t.t0} \cdot \mathrm{abs}\left(\sigma_{c.QP}\right)}{1 + \frac{E_p}{E_{cm}} \cdot \frac{A_{tot}}{A_c} \cdot \left(1 + \frac{A_c}{I_x} \cdot {e_2}^2\right) \cdot \left(1 + 0.8 \cdot \phi_{t.t0}\right)} = 115.772 \ \textit{MPa}$$ EC2 5.10.6(2)

$\frac{\Delta\sigma_{p.c.s.r}}{\sigma_{pm0}} \cdot 100 = 8.305$ Total loss due to creep, shrinkage and relaxation in %

As the difference between the simplified method and the calculation of the time-dependent losses is so small, the losses for creep, shrinkage and relaxation from the time dependent losses are used in the model in NovaFrame.

Created with PTC Mathcad Express. See www.mathcad.com for more information.

Appendix E

Verification of model in NovaFrame

Verification calculations are done to ensure correct results from NovaFrame.

This appendix is divided into the following parts:

E-1: Verification of cross-sectional parameters

E-2: Verification of moments due to self-weight

Verification of results from NovaFrame

Cross-sectional properties (dimmensions from Figure 4.12)

$H := 3500\ mm$

$b_1 := 11225\ mm$ $t_1 := 400\ mm$ $A_1 := b_1 \cdot t_1 = 4.49\ m^2$

$b_2 := 5950\ mm$ $t_2 := 400\ mm$ $A_2 := b_2 \cdot t_2 = 2.38\ m^2$

$h_1 := 2700\ mm$ $t_3 := 400\ mm$ $A_3 := h_1 \cdot t_3 = 1.08\ m^2$

$h_2 := h_1$ $t_4 := t_3$ $A_4 := h_2 \cdot t_4 = 1.08\ m^2$

$A := A_1 + A_2 + A_3 + A_4 = 9.03\ m^2$

$y_{A1} := H - \frac{t_1}{2} = 3.3\ m$ $x_{A1} := 0$

$y_{A2} := \frac{t_2}{2} = 0.2\ m$ $x_{A2} := 0$

$y_{A3} := t_2 + \frac{h_1}{2} = 1.75\ m$ $x_{A3} := \frac{b_2}{2} - \frac{t_3}{2} = 2.775\ m$

$y_{A4} := y_{A3}$ $x_{A4} := x_{A3}$

$y_{cog} := \frac{\left(\left(A_1 \cdot y_{A1}\right) + \left(A_2 \cdot y_{A2}\right) + \left(A_3 \cdot y_{A3}\right) + \left(A_4 \cdot y_{A4}\right)\right)}{A} = 2.1122\ m$

$x_{cog} := 5612.5\ mm$ Symmetric cross-section in x-direction

Moment of inertia about x-axis:

$I_{xA1} := \frac{\left(b_1 \cdot {t_1}^3\right)}{12} + A_1 \cdot \left(y_{A1} - y_{cog}\right)^2 = 6.3949\ m^4$

$I_{xA2} := \frac{\left(b_2 \cdot {t_2}^3\right)}{12} + A_2 \cdot \left(y_{cog} - \frac{t_2}{2}\right)^2 = 8.7341\ m^4$

$I_{xA3} := \frac{\left(t_3 \cdot {h_1}^3\right)}{12} + A_3 \cdot \left(y_{cog} - y_{A3}\right)^2 = 0.7978\ m^4$

$I_{xA4} := I_{xA3}$

$I_x := I_{xA1} + I_{xA2} + I_{xA3} + I_{xA4} = 16.7245\ m^4$

Created with PTC Mathcad Express. See www.mathcad.com for more information.

Verification of results from NovaFrame

Moment of inertia about y-axis:

$$I_{yA1} := \frac{\left(t_1 \cdot {b_1}^3\right)}{12} = 47.1452\ m^4$$

$$I_{yA2} := \frac{\left(t_2 \cdot {b_2}^3\right)}{12} = 7.0215\ m^4$$

$$I_{yA3} := \frac{\left(h_1 \cdot {t_3}^3\right)}{12} + A_3 \cdot \left(\frac{b_2}{2} - \frac{t_3}{2}\right)^2 = 8.3311\ m^4$$

$$I_{yA4} := I_{yA3}$$

$$I_y := I_{yA1} + I_{yA2} + I_{yA3} + I_{yA4} = 70.8289\ m^4$$

Created with PTC Mathcad Express. See www.mathcad.com for more information.

Verification of results from NovaFrame

Moments from self-weight:

$q_c := 26\ \frac{kN}{m^3}$ Concrete self-weight

$A_c := 8.82\ m^2$ Area of concrete cross-section

$q := q_c \cdot A_c = 229.32\ \frac{kN}{m}$ Distributed load

$L := 138\ m$ Total length of bridge

$L_1 := 42\ m$ Length of span 1

$L_2 := 57\ m$ Length of span 2

$L_3 := 39\ m$ Length of span 3

When calculating the moments due to self-weight on the bridge, the moment-distribution method was used. This is because of the fact that the bridge is statically indeterment

The distribution factor is found by using the stiffness of the bridge.

Distribution factor				
Joint	Member	k	∑k	DF=k/∑k
2	2-1	$\frac{3EI}{L_1} = \frac{1}{14}EI$	$\frac{113}{798}EI$	0.504
	2-3	$\frac{4EI}{L_2} = \frac{4}{57}EI$		0.496
3	3-2	$\frac{4EI}{L_2} = \frac{4}{57}EI$	$\frac{109}{741}EI$	0.477
	3-4	$\frac{3EI}{L_3} = \frac{3}{39}EI$		0.523

Fixed-end moments are calculated to be distributed:

$FEM_{1.2} := -\frac{q \cdot {L_1}^2}{12} = -33710.04\ kN \cdot m$ $FEM_{2.1} := -FEM_{1.2}$

$FEM_{2.3} := -\frac{q \cdot {L_2}^2}{12} = -62088.39\ kN \cdot m$ $FEM_{3.2} := -FEM_{2.3}$

$FEM_{3.4} := -\frac{q \cdot {L_3}^2}{12} = -29066.31\ kN \cdot m$ $FEM_{4.3} := -FEM_{3.4}$

Created with PTC Mathcad Express. See www.mathcad.com for more information.

Attachment
E -2

Verification of results from NovaFrame

The distribution of moments are done in Excel, and are shown in the table below:

SUPPORT	1	2		3		4
Distribution factor		0.504	0.496	0.477	0.523	
FEM	-33710	33710	-62088	62088	-29066	29066
Release+carry over	33710	16855			-14533	-29066
Internal moments	0	50565	-62088	62088	-43599	0
Distribution		5807.592	5715.408	-8819.253	-9669.747	
Internal moments			-4409.6265	2857.704		
Distribution		2222.45176	2187.17474	-1363.1248	-1494.5792	
Internal moments			-681.5624	1093.58737		
Distribution		343.507452	338.054952	-521.64118	-571.9462	
Internal moments			-260.82059	169.027476		
Distribution		131.453576	129.367012	-80.626106	-88.40137	
Internal moments			-40.313053	64.6835059		
Distribution		20.3177787	19.9952743	-30.854032	-33.829474	
Internal moments			-15.427016	9.99763716		
Distribution		7.77521614	7.65180001	-4.7688729	-5.2287642	
Internal moments	0		-2.3844365	3.82590001		
Distribution		1.20175598	1.18268049	-1.8249543	-2.0009457	
TOTAL	0	59099.2995	-59099.3	55464.7329	-55464.733	0

$M_1 := 0\ kN \cdot m$ $M_{2.3} := -59099.3\ kN \cdot m$ $M_{3.4} := -55464.7\ kN \cdot m$

$M_{2.1} := 59099.3\ kN \cdot m$ $M_{3.2} := 55464.7\ kN \cdot m$ $M_4 := 0$

Reactions forces are calculated to find the maximum moments in span:

The reaction forces are found by looking at each fied element seperately

Span 1-2:

By taking the moment about support 1, the formula for R(2-1) is found:

$$R_{2.1} := \frac{M_{2.1} + \frac{q \cdot {L_1}^2}{2}}{L_1} = 6222.8462\ kN$$

Sum of all forces=0 gives:

$R_1 := q \cdot L_1 - R_{2.1} = 3408.5938\ kN$

Span 2-3:

By taking the moment about support 1, the formula for R(2-1) is found:

$$R_{3.1} := \frac{-M_{2.1} + M_{3.2} + \frac{q \cdot {L_2}^2}{2}}{L_2} = 6471.8551\ kN$$

Sum of all forces=0 gives:

$R_{2.2} := q \cdot L_2 - R_{3.1} = 6599.3849\ kN$

Created with PTC Mathcad Express. See www.mathcad.com for more information.

Verification of results from NovaFrame

Span 3-4:

By taking the moment about support 1, the formula for R(2-1) is found:

$$R_4 := \frac{-M_{3.2} + \frac{q \cdot L_3^{\,2}}{2}}{L_3} = 3049.5682\ \boldsymbol{kN}$$

Sum of all forces=0 gives:

$$R_{3.2} := q \cdot L_3 - R_4 = 5893.9118\ \boldsymbol{kN}$$

Total reactions:

$R_1 := R_1 = 3408593.8095\ \boldsymbol{N}$

$R_2 := R_{2.1} + R_{2.2} = 12822.2311\ \boldsymbol{kN}$

$R_3 := R_{3.1} + R_{3.2} = 12365.7669\ \boldsymbol{kN}$

$R_4 := R_4 = 3049568.2051\ \boldsymbol{N}$

Control to check that reactions are correct: R=q*L?

$R_1 + R_2 + R_3 + R_4 = 31646.16\ \boldsymbol{kN}$ = $q \cdot L = 31646.16\ \boldsymbol{kN}$ OK!

Moments in span

Max moment are found in the following distances (from support 1)

$x_{1.2} := 15\ \boldsymbol{m}$

$x_{2.3} := 71\ \boldsymbol{m}$

$x_{3.4} := 125\ \boldsymbol{m}$

$$M_{1.2} := -\frac{\left(q \cdot x_{1.2}^{\,2}\right)}{2} + R_1 \cdot x_{1.2} = 25330.4071\ \boldsymbol{kN \cdot m}$$

$$M_{2.3} := -\frac{\left(q \cdot x_{2.3}^{\,2}\right)}{2} + R_1 \cdot x_{2.3} + R_2 \cdot \left(x_{2.3} - L_1\right) = 35853.8025\ \boldsymbol{kN \cdot m}$$

$$M_{3.4} := -\frac{\left(q \cdot \left(L - x_{3.4}\right)^2\right)}{2} + R_4 \cdot \left(L - x_{3.4}\right) = 20266.8467\ \boldsymbol{kN \cdot m}$$

Created with PTC Mathcad Express. See www.mathcad.com for more information.

Appendix F

Design for launching stages

This appendix is divided into the following parts:

F-1: ULS – Ultimate moment capacity

F-2: ULS – Shear resistance

F-3: SLS – Analysis of cracked section

Attachment
F-1

Design for ULS - Construction stages

Cross-sectional properties

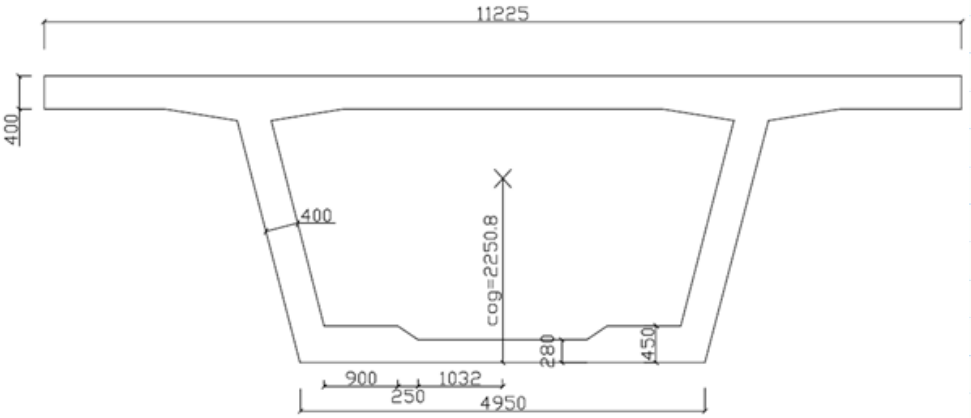

$h := 3500\ mm$ Height of box-girder

$h_{cog} := 2250.8\ mm$ Distance from bottom to CoG

$b_{top} := 11225\ mm$ Width of top flange

$t_{top} := 400\ mm$ Thickness of top flange

$b_{bottom} := 4950\ mm$ Width of bottom flange

$$t_{bottom} := \frac{0.9\ m \cdot 0.45\ m + 0.25\ m \cdot \left(\frac{0.45\ m - 0.28\ m}{2}\right) + 1.032\ m \cdot 0.28\ m}{0.9\ m + 0.25\ m + 1.032\ m}$$

$t_{bottom} = 327.78\ mm$ Average thickness of bottom flange

$t_{web} := 400\ mm$ Thickness of web

Concrete properties

$f_{ck} := 45\ MPa$ Characteristic compressive strength

$\alpha_{cc} := 0.85$ Factor

$\gamma_c := 1.5$ Safety factor

$f_{cd} := \alpha_{cc} \cdot \frac{f_{ck}}{\gamma_c} = 25.5\ MPa$ Design value of compressive strength

$f_{ctm} := 3.8\ MPa$ Mean value of axial tensile strength

Steel properties

$f_{yk} := 500\ MPa$ Characteristic yield strength

$\gamma_s := 1.15$ Safety factor

$f_{yd} := \frac{f_{yk}}{\gamma_s} = 434782608.7\ \frac{kg}{m \cdot s^2}$ Design yield strength

Created with PTC Mathcad Express. See www.mathcad.com for more information.

Design for ULS - Construction stages

Prestressing tendon

$A_p := 2100\ mm^2$ — Area pr tendon

$A_{p.top} := 14 \cdot A_p = 0.0294\ m^2$ — Total area of tendons in bottom flange

$A_{p.bottom} := 8 \cdot A_p = 0.0168\ m^2$ — Total area of tendons in top flange

$f_{pk} := 1860\ MPa$ — Characteristic tensile strength

$f_{p0.1k} := 1640\ MPa$ — Characteristic 0.1% proof-stress

$E_p := 195\ GPa$ — Elastic modulus

$f_{pd} := \frac{f_{p0.1k}}{\gamma_s} = 1426.09\ MPa$

$f_{ctk.0.05} := 2.7\ MPa$

$Ø_{duct} := 80\ mm$ — Outer diameter of duct

Capacity pr cable:

$t_{f.h} := 700\ \frac{mm}{\cos(15.54\ deg)} = 726.56\ mm$ — Horizontal measurement of flange

$d_{duct} := h - 150\ mm - \frac{Ø_{duct}}{2} = 3.31\ m$ — Distance from top/bottom to center duct

Created with PTC Mathcad Express. See www.mathcad.com for more information.

Design for ULS - Construction stages

ULTIMATE MOMENT CAPACITY

$\varepsilon_{cu} := 0.0035$ Ultimate compressive strain

$\sigma_{pm0} := min\left(0.85\ f_{pk}, 0.85\ f_{p0.1k}\right) = 1394000000\ \frac{kg}{m \cdot s^2}$ Stress in tendon immediately after post-tensioning

The following values are represented in Figure 5.4

$\varepsilon_{p0} := \frac{\sigma_{pm0}}{E_p} = 0.01$

$\Delta\varepsilon_{loss} := 0.15\ \varepsilon_{p0} = 0$

$\varepsilon`_{p0} := \varepsilon_{p0} - \Delta\varepsilon_{loss} = 0.01$

$\Delta\varepsilon_p := \frac{f_{pd}}{E_p} - \varepsilon`_{p0} = 0$

$\alpha_b := \frac{\varepsilon_{cu}}{\Delta\varepsilon_p + \varepsilon_{cu}} = 0.74$

Moment capacity at support

$A_{pb} := 0.8 \cdot \frac{f_{cd}}{f_{pd}}\ \alpha_b \cdot b_{bottom} \cdot d_{duct} = 0.17\ m^2$ $A_p \le A_{pb}$ ->under-reinforced

$\alpha := \frac{f_{pd} \cdot A_{p.top}}{0.8 \cdot f_{cd} \cdot b_{bottom} \cdot d_{duct}} = 0.13$

$M_{Rd.support} := 0.8 \cdot f_{cd} \cdot \alpha \cdot b_{bottom} \cdot (1 - 0.4 \cdot \alpha) \cdot {d_{duct}}^2 = 131814.99\ kN \cdot m$ Moment capacity

Largest moment is found in support 2

$M_{Ed} := 145993\ kN \cdot m$

$M_{Ed.red.support} := 0.9 \cdot M_{Ed} = 131393.7\ kN \cdot m$

Checking if:

$M_{Rd.support} < M_{Ed.red.support}$ OK! There is no need for extra reinforcement

Moment capacity at mid-span

$A_{pb} := 0.8 \cdot \frac{f_{cd}}{f_{pd}}\ \alpha_b \cdot b_{top} \cdot d_{duct} = 0.393\ m^2$ $A_p \le A_{pb}$ ->under-reinforced

$\alpha := \frac{f_{pd} \cdot A_{p.bottom}}{0.8\ f_{cd} \cdot b_{top} \cdot d_{duct}} = 0.03$

$M_{Rd.span} := 0.8 \cdot f_{cd} \cdot \alpha \cdot b_{top} \cdot (1 - 0.4 \cdot \alpha) \cdot {d_{duct}}^2 = 78299.18\ kN \cdot m$ Moment capacity

Largest moment is found in span2-3

$M_{Ed.span} := 92561\ kN \cdot m$

$M_{Rd.span} < M_{Ed}$ Not OK! There is a need for extra reinforcement

Created with PTC Mathcad Express. See www.mathcad.com for more information.

Design for ULS - Construction stages

Reinforcement at span

$C_{nom.LF} := 150\ mm$

$A`_s := \frac{M_{Ed.span} - M_{Rd.span}}{f_{yd} \cdot (d_{duct} - C_{nom.LF})} = 10380.44\ mm^2$

Using Ø25 for reinforcement

$A_{Ø25} := \pi \cdot \left(\frac{30\ mm}{2}\right)^2 = 706.86\ mm^2$

$n := \frac{A`_s}{A_{Ø25}} = 14.69$

$n := 15$

$Spacing := \frac{b_{bottom}}{n} = 330\ mm$

$A`_s := 7 \cdot A_{Ø25} = 4948.01\ mm^2$

Created with PTC Mathcad Express. See www.mathcad.com for more information.

Design for ULS - Construction stages

SHEAR RESISTANCE

$V_{Ed} := 8138\ kN$ Design shear forcce

$V_{Ed.red} := 0.9 \cdot V_{Ed} = 7324.2\ kN$ Reduced design shear force

$A_p := 22 \cdot A_p = 46200\ mm^2$ Total tendon area

$A_c := 8.82\ m^2$ Concrete area

Determination of design shear capacity

$k := 1 + \sqrt{\frac{200\ mm}{d_{duct}}} = 1.25$ $k \le 2.0$ OK!

$b_w := 2 \cdot t_{web} = 800\ mm$

$\rho_1 := \frac{A_p}{b_w \cdot d_{duct}} = 0.02$

$k_1 := 0.15$

$k_2 := 0.18$

$C_{Rd.c} := \frac{k_2}{\gamma_c} = 0.12$

$\sigma_{p.max} := min\left(0.8\ f_{pk}, 0.9\ f_{p0.1k}\right) = 1476\ MPa$

$P_{max} := A_p \cdot \sigma_{p.max} = 68191.2\ kN$

$P_s := P_{max} \cdot 0.75 = 51143.4\ kN$

$\sigma_{cp} := \frac{P_s}{A_c} = 5.8\ MPa$ $\sigma_{cp} \le 0.2\ f_{cd}$ =5.1MPa OK!

$v_{min} := 0.035 \cdot k^{\left(\frac{3}{2}\right)} \cdot \left(\frac{f_{ck}}{MPa}\right)^{0.5} = 0.33$

$V_{Rd.c} := \max\left(\left(\left(C_{Rd.c} \cdot k \cdot \left(100\ \rho_1 \cdot \frac{f_{ck}}{MPa}\right)^{\left(\frac{1}{3}\right)} \cdot MPa + k_1 \cdot \sigma_{cp}\right) \cdot b_w \cdot d_{duct}, \left(v_{min} \cdot MPa + k_1 \cdot \sigma_{cp}\right) \cdot b_w \cdot d_{duct}\right)\right)$

$V_{Rd.c} = 3998.3\ kN$

$V_{Ed} > V_{Rd.c}$ -> NOT OK!

It is required to calculate the required design shear reinforcement

Created with PTC Mathcad Express. See www.mathcad.com for more information.

Design for ULS - Construction stages

Determination of shear force capacity

$\alpha_{cw} := 1 + \frac{\sigma_{cp}}{f_{cd}} = 1.23$

During launching there are no ducts in the web of the cross-section, and therefore

$b_{w.nom} := t_{web}$ and $b_{nom} := b_w$ EC2 Cl. 6.2.3(6)

$\sigma_t := \sigma_{cp} = 5.8\ MPa$

$f_{ctk.0.05} = 2.7\ MPa$

EC2 NA6.2.3 states that for $\sigma_t > f_{ctk0.05}$ $\cot\theta$ is found to be within the following interval

$1 \le cot\theta \le 1.25$ Thus,

$\theta_{max} := 45\ deg$ $\theta_{min} := 38.66\ deg$

$z := 0.9\ d_{duct} = 2.98\ m$ Inner leaver arm, EC2 Cl.6.2.3(1)

$v_1 := 0.6$ EC2 (6.10.aN)

$V_{Rd.max.1} := \frac{\alpha_{cw} \cdot b_{nom} \cdot z \cdot v_1 \cdot f_{cd}}{\tan(\theta_{max}) + \cot(\theta_{max})} = 22377.23\ kN$ EC2 Cl. 6.2.3(3)

$V_{Rd.max.1.25} := \frac{\alpha_{cw} \cdot b_{nom} \cdot z \cdot v_1 \cdot f_{cd}}{\tan(\theta_{min}) + \cot(\theta_{min})} = 21831.47\ kN$

$V_{Rd.max} := min(V_{Rd.max.1}, V_{Rd.max.1.25}) = 21831.47\ kN$

As $V_{Rd.max}$ is larger than the design shear force, the required shear reinforcement may be calculated

Determination of shear reinforcement

$f_{ywd} := \frac{f_{yk}}{\gamma_s} = 434.78\ MPa$

Using Ø12 for shear reinforcement

$Ø_{12} := 15\ mm$ $A_{Ø12} := \pi \cdot \left(\frac{Ø_{12}}{2}\right)^2 = 176.71\ mm^2$

Using 8*Ø12 bars:

$n := 8$ $A_{sw} := n \cdot A_{Ø12} = 1413.72\ mm^2$

$s := \frac{A_{sw} \cdot z \cdot f_{ywd} \cdot \cot(\theta_{max})}{V_{Ed.red}} = 250\ mm$

8Ø12s250 is the required shear reinforcement

Created with PTC Mathcad Express. See www.mathcad.com for more information.

Attachment
F-3

Design for SLS - Construction stages

Cross-sectional properties

$H := 3.5\ m$ Height of box-girder

$h_{cog} := 2.2508\ m$ Height from bottom of cross-section to CoG

$A_c := 8.82\ m^2$ Concrete area of box-girder

$I_{c.x} := 14.92\ m^4$ Second moment of area about x-axis

Concrete properties

$f_{ck} := 45\ MPa$ Characteristic strength of concrete

$f_{ctm} := 3.8\ MPa$ Mean value of axial tensile strength of concrete

$E_{cm} := 36\ GPa$ Secant modulus of elasticity of concrete

Prestressing tendon

$A_p := 22 \cdot 2100\ mm^2 = 0.046\ m^2$ Total tendon area (top and bottom)

$Ø_{duct} := 80\ mm$ Outer diameter of duct

$f_{pk} := 1860\ MPa$ Char. tensile strength of prestressing steel

$f_{p0.1k} := 1640\ MPa$ 0.1% proof-stress of prestressing steel

$E_p := 195\ GPa$ Modulus of elasticity for prestressing steel

$\sigma_{p.max} := min\left(0.8\ f_{pk}, 0.9\ f_{p0.1k}\right) = 1476\ MPa$

$\sigma_{pm0} := min\left(0.75\ f_{pk}, 0.85\ f_{p0.1k}\right) = 1394\ MPa$

Prestressing force

$P_{max} := A_p \cdot \sigma_{p.max} = 68191.2\ kN$

$0.95 \cdot f_{p0.1k} \cdot A_p = 71979.6\ kN$

$P_s := P_{max} \cdot 0.75 = 51143.4\ kN$

$P_{m0} := A_p \cdot \sigma_{pm0} = 64402.8\ kN$

$P_t := P_{m0}$

$P_0 := P_{max}$

Created with PTC Mathcad Express. See www.mathcad.com for more information.

Design for SLS - Construction stages

ANALYSIS OF CRACKED SECTION

$y_{b.cog} := 2250.8\ mm$ Distance from bottom to cog

$y_{t.cog} := H - y_{b.cog} = 1249.2\ mm$ Distance from top to cog

$Z_t := \frac{I_{c.x}}{y_{t.cog}} = \left(1.194 \cdot 10^{10}\right)\ mm^3$ Resistance-moment in top

$Z_b := \frac{I_{c.x}}{y_{b.cog}} = \left(6.629 \cdot 10^{9}\right)\ mm^3$ Resistance moment in bottom

$e_1 := 1.06\ m$ Distance from upper prestress to CoG

$e_2 := 2.06\ m$ Distance from lower prestress to CoG

Transformed cross-section

$\eta_p := \frac{E_p}{E_{cm}} = 5.417$ Modular ratio of prestressing steel

$A_t := A_c + \left(\eta_p - 1\right)\ A_p = 9.024\ m^2$ Transformed cross-section

$y_{span} := \frac{\left(\eta_p - 1\right)\ A_p \cdot e_2}{A_t} = 46.58\ mm$ Distance from transformed CoG to regular CoG

$y_{support} := \frac{\left(\eta_p - 1\right)\ A_p \cdot e_1}{A_t} = 23.969\ mm$ Distance from transformed CoG to regular CoG

$y_{t.span.cog} := y_{t.cog} + y_{span} = 1295.78\ mm$ Distance from top to transformed CoG (Span)

$y_{b.span.cog} := y_{b.cog} - y_{span} = 2204.22\ mm$ Distance from bottom to transformed CoG (Span)

$y_{t.support.cog} := y_{t.cog} - y_{support} = 1225.231\ mm$ Distance from top to transformed CoG (Sup.)

$y_{b.support.cog} := y_{b.cog} + y_{support} = 2274.769\ mm$ Distance from bottom to transformed CoG (Sup.)

$I_{t.span} := I_{c.x} + A_c \cdot {y_{span}}^2 + \left(\eta_p - 1\right)\ A_p \cdot \left(e_2 - y_{span}\right)^2 = 15.766\ m^4$

$I_{t.support} := I_{c.x} + A_c \cdot {y_{support}}^2 + \left(\eta_p - 1\right)\ A_p \cdot \left(e_1 - y_{support}\right)^2 = 15.144\ m^4$

$W_{t.span} := \frac{I_{t.span}}{y_{t.span.cog}} = 12.167\ m^3$

$W_{b.span} := \frac{I_{t.span}}{y_{b.span.cog}} = 7.153\ m^3$

$W_{t.support} := \frac{I_{t.support}}{y_{t.support.cog}} = 12.36\ m^3$

$W_{b.support} := \frac{I_{t.support}}{y_{b.support.cog}} = 6.657\ m^3$

Created with PTC Mathcad Express. See www.mathcad.com for more information.

Design for SLS - Construction stages

Allowable stresses

$\sigma_{c.t.allow} := f_{ctm}$ Allowable stress in tension zone

$\sigma_{c.c.allow} := -(0.6\ f_{ck}) = -27\ \boldsymbol{MPa}$ Allowable stress in compression zone

Bending stresses at support at transfer (Model 62)

(Statically determinate)

$M_{0.support} := 109039\ \boldsymbol{kN \cdot m}$ Moment due to self-weight

$$\sigma_{t.0} := -\frac{P_0}{A_t} - \frac{P_0 \cdot (e_1 - y_{support}) \cdot y_{t.support.cog}}{I_{t.support}} + \frac{M_{0.support}}{W_{t.support}} = -4.451\ \boldsymbol{MPa}$$ < -27 MPa --> OK!

$$\sigma_{b.0} := -\frac{P_0}{A_t} + \frac{P_0 \cdot (e_1 - y_{support}) \cdot y_{b.support.cog}}{I_{t.support}} - \frac{M_{0.support}}{W_{b.support}} = -13.323\ \boldsymbol{MPa}$$ < -27 MPa --> OK!

Bending stresses at mid-span at transfer (Model 92):

(Statically indeterminate)

$M_{0.span} := 59030\ \boldsymbol{kN \cdot m}$ Moment due to self-weight

Finding moment-diagram for statically indeterminate system:
The secondary moment is found as following. Formulas from "Stålkonstruksjoner"[19] are used to determine the deflections and moments. In the calculations L is set as following:

$L_1 := 42\ \boldsymbol{m}$

$L_2 := 57\ \boldsymbol{m}$

$L := L_1 + L_2$

$M_0 = Pe$ Primary moment

$\delta_0 = \frac{Pe}{EI}\frac{L^2}{8}$ Deflection due to primary moment

As illustrated in Figure 5.10, one support is removed, and an imaginary force F is placed at the point of the support that will create a negative deflection.

$M_1 = \frac{FL_1L_2}{L} = \frac{266}{11} m * F$ Secondary moment

$\delta_1 = \frac{1}{48}\frac{PL}{EI}\left(3\frac{L_1}{L} - 4\left(\frac{L_1}{L}\right)^2\right) = 19553{,}625m^3\frac{F}{EI}$ Deflection due to the secondary moment

This deflection should be equal to the deflection from the primary moment to ensure no deflection at the point of the removed support. From setting these deflections equal to each other, the magnitude of the force F is found.

Created with PTC Mathcad Express. See www.mathcad.com for more information.

Design for SLS - Construction stages

$$\delta_1 = \delta_0 \rightarrow 19553{,}625m^3 \frac{F}{EI} = \frac{Pe}{EI}\frac{L^2}{8}$$

$$F = \frac{Pe}{8}\frac{(L_1 + L_2)^2}{19553{,}635m^3}$$ Imposed imaginary force

By inserting this in the formula for M_1, the secondary moment is found expressed by Pe.

$$M_1 = \frac{266}{11}m * \frac{Pe}{8}\frac{(L_1 + L_2)^2}{19553{,}635m^3} = 1{,}515Pe$$ Secondary moment

The total moment is found by subtracting the secondary moment from the primary moment.
Thus, the stresses are determined as following:

$$\sigma_{t.0} := \frac{-P_0}{A_t} + \frac{P_0 \cdot (e_2 - y_{span}) \cdot y_{t.span.cog}}{I_{t.span}} - \frac{1.515\ P_0 \cdot (e_2 - y_{span}) \cdot y_{t.span.cog}}{I_{t.span}} - \frac{M_{0.span}}{W_{t.span}}$$

$\sigma_{t.0} = -18.219\ \boldsymbol{MPa}$ < -27 MPa --> OK

$$\sigma_{b.0} := \frac{-P_0}{A_t} - \frac{P_0 \cdot (e_2 - y_{span}) \cdot y_{b.span.cog}}{I_{t.span}} + \frac{1.515\ P_0 \cdot (e_2 - y_{span}) \cdot y_{t.span.cog}}{I_{t.span}} + \frac{M_{0.span}}{W_{b.span}}$$

$\sigma_{b.0} = -1.404\ \boldsymbol{MPa}$ < -27 MPa --> OK!

The stresses due to prestressing do not exceed the allowable stresses, and the cross-section can therefore be considered un-cracked.

Created with PTC Mathcad Express. See www.mathcad.com for more information.

Appendix G

Design of final construction

This appendix is divided into the following parts:

G-1: ULS – Ultimate moment capacity

G2: ULS – Shear resistance

G-3: SLS – Stresses at transfer

G-4: SLS – Stresses due to characteristic load combination

G-5: SLS – Stresses due to quasi-permanent load combination

G-6: SLS – Deflection control

Attachment
G-1

Design for ULS - Final construction

Cross-sectional properties

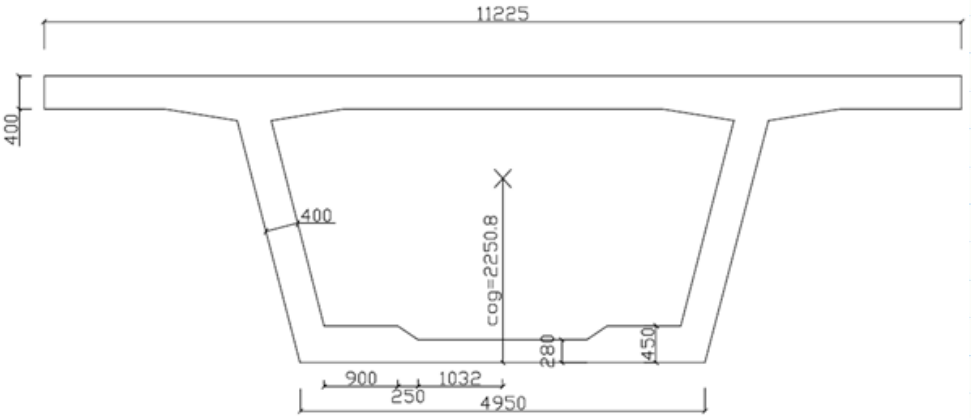

$h := 3500\ mm$ Height of box-girder

$h_{cog} := 2250.8\ mm$ Distance from bottom to CoG

$b_{top} := 11225\ mm$ Width of top flange

$t_{top} := 400\ mm$ Thickness of top flange

$b_{bottom} := 4950\ mm$ Width of bottom flange

$$t_{bottom} := \frac{0.9\ m \cdot 0.45\ m + 0.25\ m \cdot \left(\frac{0.45\ m - 0.28\ m}{2}\right) + 1.032\ m \cdot 0.28\ m}{0.9\ m + 0.25\ m + 1.032\ m}$$

$t_{bottom} = 327.777\ mm$ Average thickness of bottom flange

$t_{web} := 400\ mm$ Thickness of web

Concrete properties

$f_{ck} := 45\ MPa$ Characteristic compressive strength

$\alpha_{cc} := 0.85$ Factor

$\gamma_c := 1.5$ Safety factor

$f_{cd} := \alpha_{cc} \cdot \frac{f_{ck}}{\gamma_c} = 25.5\ MPa$ Design value of compressive strength

$f_{ctm} := 3.8\ MPa$ Mean value of axial tensile strength

Steel properties

$f_{yk} := 500\ MPa$ Characteristic yield strength

$\gamma_s := 1.15$ Safety factor

$f_{yd} := \frac{f_{yk}}{\gamma_s} = \left(4.348 \cdot 10^8\right)\ Pa$ Design yield strength

Created with PTC Mathcad Express. See www.mathcad.com for more information.

Design for ULS - Final construction

Prestressing tendon

$A_p := 2100\ mm^2$ — Area pr tendon

$A_{p.bottom} := 8 \cdot A_p = 0.0168\ m^2$ — Total area of tendons in bottom flange

$A_{p.top} := 14 \cdot A_p = 0.0294\ m^2$ — Total area of tendons in top flange

$A_{p.web} := 4 \cdot A_p = 0.008\ m^2$ — Total area of tendons in web

$f_{pk} := 1860\ MPa$ — Characteristic tensile strength

$f_{p0.1k} := 1640\ MPa$ — Characteristic 0.1% proof-stress

$E_p := 195\ GPa$ — Elastic modulus

$f_{pd} := \frac{f_{p0.1k}}{\gamma_s} = (1.426 \cdot 10^3)\ MPa$

$f_{ctk.0.05} := 2.7\ MPa$

$Ø_{duct} := 80\ mm$ — Outer diameter of duct

$C_{nom.UF} := 150\ mm$ — Nomial cover upper flange

$C_{nom.LF} := C_{nom.UF}$ — Nomial cover lower flange

$d_{duct} := h - C_{nom.UF} - \frac{Ø_{duct}}{2} = 3.31\ m$ — Distance from top/bottom to center duct

Created with PTC Mathcad Express. See www.mathcad.com for more information.

Design for ULS - Final construction

ULTIMATE MOMENT CAPACITY

$\varepsilon_{cu} := 0.0035$

$\sigma_{pm0} := min\left(0.85\ f_{pk}, 0.85\ f_{p0.1k}\right) = \left(1.394 \cdot 10^{9}\right)\ \boldsymbol{Pa}$

$loss_{15} := 0.15$

$\varepsilon_{p0} := \frac{\sigma_{pm0}}{E_p} = 0.007$

$\Delta\varepsilon_{loss} := 0.15\ \varepsilon_{p0} = 0.00107$

$\varepsilon`_{p0} := \varepsilon_{p0} - \Delta\varepsilon_{loss} = 0.006$

$\Delta\varepsilon_p := \frac{f_{pd}}{E_p} - \varepsilon`_{p0} = 0.001$

$\alpha_b := \frac{\varepsilon_{cu}}{\Delta\varepsilon_p + \varepsilon_{cu}} = 0.739$

Moment capacity at mid-span

$A_{pb} := 0.8 \cdot \frac{f_{cd}}{f_{pd}}\ \alpha_b \cdot b_{top} \cdot d_{duct}^{\,2} = 0.393\ \boldsymbol{m}^2$ $\quad A_p \le A_{pb}$ under-reinforced

$\alpha := \frac{f_{pd} \cdot \left(A_{p.bottom} + A_{p.web}\right)}{0.8\ f_{cd} \cdot b_{top} \cdot d_{duct}} = 0.047$

$M_{Rd.span} := 0.8 \cdot f_{cd} \cdot \alpha \cdot b_{top} \cdot \left(1 - 0.4 \cdot \alpha\right) \cdot d_{duct}^{\,2} = 116696.778\ \boldsymbol{kN \cdot m}$

Largest moment is found in span2-3

$M_{Ed.span} := 148654\ \boldsymbol{kN \cdot m}$

$M_{Rd.span} < M_{Ed.span}$ **NOT OK! There is a need for extra reinforcement in span**

Reinforcement at span

$C_{nom.LF} := 95\ \boldsymbol{mm}$

$A`_s := \frac{M_{Ed.span} - M_{Rd.span}}{f_{yd} \cdot \left(d_{duct} - C_{nom.LF}\right)} = \left(2.286 \cdot 10^{4}\right)\ \boldsymbol{mm}^2$

Using Ø25 for reinforcement

$A_{Ø25} := \pi \cdot \left(\frac{30\ \boldsymbol{mm}}{2}\right)^2 = 706.858\ \boldsymbol{mm}^2$

$n := \frac{A`_s}{A_{Ø25}} = 32.343$

$n := 33$

$Spacing := \frac{b_{bottom}}{n} = 150\ \boldsymbol{mm}$

$A`_s := 7 \cdot A_{Ø25} = \left(4.948 \cdot 10^{3}\right)\ \boldsymbol{mm}^2$

Created with PTC Mathcad Express. See www.mathcad.com for more information.

Design for ULS - Final construction

Moment capacity at support

$A_{pb} := 0.8 \cdot \frac{f_{cd}}{f_{pd}} \alpha_b \cdot b_{bottom} \cdot d_{duct} = 0.173\ m^2$ $A_p \le A_{pb}$ under-reinforced

$\alpha := \frac{f_{pd} \cdot \langle A_{p.top} + A_{p.web} \rangle}{0.8 \cdot f_{cd} \cdot b_{bottom} \cdot d_{duct}} = 0.1613$

$M_{Rd.support} := 0.8 \cdot f_{cd} \cdot \alpha \cdot b_{bottom} \cdot (1 - 0.4 \cdot \alpha) \cdot d_{duct}^{\ 2} = 166918.487\ kN \cdot m$

Largest moment is found at support 2

$A_{p.top} = 0.0294\ m^2$

$M_{Ed.support} := 132303\ kN \cdot m$

$M_{Ed.red.support} := M_{Ed.support} \cdot 0.9 = 119072.7\ kN \cdot m$

Checking if:

$M_{Rd.support} > M_{Ed.red.support}$ **OK! No need for extra reinforcement**

Created with PTC Mathcad Express. See www.mathcad.com for more information.

Design for ULS - Final construction

SHEAR RESISTANCE

$V_{Ed} := 14053\ kN$

$V_{Ed.red} := 0.9 \cdot V_{Ed} = 12647.7\ kN$

$A_{p.flange} := 22 \cdot A_p = (4.62 \cdot 10^4)\ mm^2$ Total tendon are (top and bottom flange)

$A_{p.web} := 4 \cdot A_p = (8.4 \cdot 10^3)\ mm^2$

$A_{p.tot} := A_{p.flange} + A_{p.web} = 54600\ mm^2$

$A_c := 8.82\ m^2$

Determination of design shear capacity

$k := 1 + \sqrt{\frac{200\ mm}{d_{duct}}} = 1.246$ $k \leq 2.0$ OK!

$b_w := 2 \cdot t_{web} = 800\ mm$

$\rho_1 := \frac{A_p}{b_w \cdot d_{duct}} = 7.931 \cdot 10^{-4}$

$k_1 := 0.15$

$k_2 := 0.18$

$C_{Rd.c} := \frac{k_2}{\gamma_c} = 0.12$

$\sigma_{p.max} := min(0.8\ f_{pk}, 0.9\ f_{p0.1k}) = 1476\ MPa$

$P_{max} := A_{p.tot} \cdot \sigma_{p.max} = 80589.6\ kN$

$0.95 \cdot f_{p0.1k} \cdot A_{p.tot} = 85066.8\ kN$

$P_s := P_{max} \cdot 0.75 = 60442.2\ kN$

$\sigma_{cp} := \frac{P_s}{A_c} = 6.853\ MPa$

$v_{min} := 0.035 \cdot k^{\left(\frac{3}{2}\right)} \cdot \left(\frac{f_{ck}}{MPa}\right)^{0.5} = 0.326$

$V_{Rd.c} := \max\left(\left(\left(C_{Rd.c} \cdot k \cdot \left(100\ \rho_1 \cdot \frac{f_{ck}}{MPa}\right)^{\left(\frac{1}{3}\right)} \cdot MPa + k_1 \cdot \sigma_{cp}\right) \cdot b_w \cdot d_{duct}, \left(v_{min} \cdot MPa + k_1 \cdot \sigma_{cp}\right) \cdot b_w \cdot d_{duct}\right)\right)$

$V_{Rd.c} = 3586.466\ kN$

$V_{Ed} > V_{Rd.c}$ -> NOT OK! **It is required to calculate the required design shear reinforcement**

Created with PTC Mathcad Express. See www.mathcad.com for more information.

Design for ULS - Final construction

Determination of shear force capacity

$\alpha_{cw} := 1 + \frac{\sigma_{cp}}{f_{cd}} = 1.269$

During launching there are no ducts in the web of the cross-section, and therefore

$b_{w.nom} := t_{web}$ and $b_{nom} := b_w$ EC2 Cl. 6.2.3(6)

$\sigma_t := \sigma_{cp} = 6.853\ MPa$

$f_{ctk.0.05} = 2.7\ MPa$

EC2 NA6.2.3 states that for $\sigma_t > f_{ctk0.05}$ $\cot\theta$ is found to be within the following interval

$1 \le cot\theta \le 1.25$ Thus,

$\theta_{max} := 45\ deg$ $\theta_{min} := 38.66\ deg$

$z := 0.9\ d_{duct} = 2.979\ m$ Inner leaver arm, EC2 Cl.6.2.3(1)

$v_1 := 0.6$ EC2 (6.10.aN)

$V_{Rd.max.1} := \frac{\alpha_{cw} \cdot b_{nom} \cdot z \cdot v_1 \cdot f_{cd}}{\tan(\theta_{max}) + \cot(\theta_{max})} = 23130.999\ kN$ EC2 Cl. 6.2.3(3)

$V_{Rd.max.1.25} := \frac{\alpha_{cw} \cdot b_{nom} \cdot z \cdot v_1 \cdot f_{cd}}{\tan(\theta_{min}) + \cot(\theta_{min})} = 22566.862\ kN$

$V_{Rd.max} := min(V_{Rd.max.1}, V_{Rd.max.1.25}) = 22566.862\ kN$

As $V_{Rd.max}$ is larger than the design shear force, the required shear reinforcement may be calculated

Determination of shear reinforcement

$f_{ywd} := \frac{f_{yk}}{\gamma_s} = 434.783\ MPa$

Using Ø12 for shear reinforcement

$Ø_{12} := 15\ mm$ $A_{Ø12} := \pi \cdot \left(\frac{Ø_{12}}{2}\right)^2 = 176.715\ mm^2$

Using 12*Ø12 bars:

$n := 12$ $A_{sw} := n \cdot A_{Ø12} = (2.121 \cdot 10^3)\ mm^2$

$s := \frac{A_{sw} \cdot z \cdot f_{ywd} \cdot \cot(\theta_{max})}{V_{Ed.red}} = 217.162\ mm$

12Ø12s220 is the required shear reinforcement

Created with PTC Mathcad Express. See www.mathcad.com for more information.

G-3

Stresses in top and bottom for TRANSFER
STRESSES DUE TO PRESTRESS AND SELF-WEIGHT
Description:
This listing consists of calculated elastic stresses for the upper face
and the lower face of the cross-section associatied with the selected elements.
Upper and lower face are defined by using the SECTFACE command.

Sort. Line No:	Element No:	X/L:	Upper	Lower
300	3	0	-6.944	-8.769
300	3	1	-7.089	-8.669
300	4	0	-7.089	-8.669
300	4	1	-7.213	-8.615
300	5	0	-7.213	-8.615
300	5	1	-7.315	-8.604
300	6	0	-7.315	-8.605
300	6	1	-7.399	-8.635
300	7	0	-7.399	-8.635
300	7	1	-7.464	-8.704
300	8	0	-7.464	-8.705
300	8	1	-7.514	-8.809
300	9	0	-7.514	-8.81
300	9	1	-7.548	-8.947
300	10	0	-7.548	-8.948
300	10	1	-7.57	-9.115
300	11	0	-7.57	-9.116
300	11	1	-7.58	-9.31
300	12	0	-7.58	-9.311
300	12	1	-7.581	-9.529
300	13	0	-7.581	-9.53
300	13	1	-7.574	-9.769
300	14	0	-7.574	-9.769
300	14	1	-7.566	-9.97
300	15	0	-7.566	-9.971
300	15	1	-7.562	-10.121
300	16	0	-7.562	-10.121
300	16	1	-7.455	-10.144
300	17	0	-7.455	-10.145
300	17	1	-7.338	-10.148
300	18	0	-7.338	-10.148
300	18	1	-7.226	-10.143
300	19	0	-7.226	-10.144
300	19	1	-7.119	-10.127
300	20	0	-7.104	-10.155
300	20	1	-7.036	-10.049
300	21	0	-7.036	-10.049
300	21	1	-6.968	-9.964
300	22	0	-6.968	-9.964
300	22	1	-6.901	-9.878
300	23	0	-6.901	-9.878

300	23	1	-6.833	-9.795
300	24	0	-6.833	-9.794
300	24	1	-6.762	-9.718
300	25	0	-6.762	-9.717
300	25	1	-6.686	-9.65
300	26	0	-6.686	-9.649
300	26	1	-6.605	-9.594
300	27	0	-6.605	-9.594
300	27	1	-6.515	-9.555
300	28	0	-6.515	-9.554
300	28	1	-6.417	-9.533
300	29	0	-6.417	-9.533
300	29	1	-6.307	-9.533
300	30	0	-6.307	-9.533
300	30	1	-6.185	-9.557
300	31	0	-6.185	-9.556
300	31	1	-6.049	-9.607
300	32	0	-6.049	-9.607
300	32	1	-5.899	-9.686
300	33	0	-5.899	-9.686
300	33	1	-5.732	-9.796
300	34	0	-5.732	-9.796
300	34	1	-5.547	-9.94
300	35	0	-5.547	-9.94
300	35	1	-5.343	-10.119
300	36	0	-5.343	-10.119
300	36	1	-5.12	-10.337
300	37	0	-5.12	-10.336
300	37	1	-4.876	-10.594
300	38	0	-4.876	-10.593
300	38	1	-4.609	-10.892
300	39	0	-4.609	-10.892
300	39	1	-4.319	-11.235
300	40	0	-4.599	-10.773
300	40	1	-3.966	-11.504
300	41	0	-3.965	-11.504
300	41	1	-3.477	-12.156
300	42	0	-3.477	-12.156
300	42	1	-3.018	-12.786
300	43	0	-3.018	-12.786
300	43	1	-2.538	-13.464
300	44	0	-2.539	-13.464
300	44	1	-1.979	-14.263
300	45	0	-2.036	-14.168
300	45	1	-2.419	-13.096
300	46	0	-2.417	-13.097
300	46	1	-2.754	-12.237
300	47	0	-2.753	-12.237
300	47	1	-3.074	-11.47
300	48	0	-3.074	-11.471
300	48	1	-3.401	-10.674

300	49	0	-3.32	-10.81
300	49	1	-3.631	-10.048
300	50	0	-3.631	-10.048
300	50	1	-3.934	-9.328
300	51	0	-3.934	-9.328
300	51	1	-4.218	-8.644
300	52	0	-4.218	-8.644
300	52	1	-4.482	-7.996
300	53	0	-4.482	-7.996
300	53	1	-4.727	-7.381
300	54	0	-4.727	-7.382
300	54	1	-4.954	-6.8
300	55	0	-4.954	-6.8
300	55	1	-5.164	-6.251
300	56	0	-5.164	-6.251
300	56	1	-5.357	-5.733
300	57	0	-5.357	-5.733
300	57	1	-5.533	-5.246
300	58	0	-5.533	-5.246
300	58	1	-5.694	-4.787
300	59	0	-5.694	-4.787
300	59	1	-5.839	-4.357
300	60	0	-5.839	-4.357
300	60	1	-5.969	-3.954
300	61	0	-5.969	-3.955
300	61	1	-6.085	-3.578
300	62	0	-6.084	-3.578
300	62	1	-6.186	-3.227
300	63	0	-6.186	-3.228
300	63	1	-6.274	-2.902
300	64	0	-6.274	-2.902
300	64	1	-6.348	-2.6
300	65	0	-6.348	-2.6
300	65	1	-6.41	-2.321
300	66	0	-6.41	-2.321
300	66	1	-6.454	-2.059
300	67	0	-6.454	-2.059
300	67	1	-6.485	-1.818
300	68	0	-6.485	-1.818
300	68	1	-6.504	-1.598
300	69	0	-6.504	-1.598
300	69	1	-6.512	-1.399
300	70	0	-6.512	-1.399
300	70	1	-6.51	-1.221
300	71	0	-6.51	-1.221
300	71	1	-6.496	-1.062
300	72	0	-6.489	-1.073
300	72	1	-6.568	-1.118
300	73	0	-6.568	-1.118
300	73	1	-6.637	-1.179
300	74	0	-6.637	-1.179

300	74	1	-6.695	-1.26
300	75	0	-6.695	-1.26
300	75	1	-6.742	-1.36
300	76	0	-6.742	-1.36
300	76	1	-6.778	-1.481
300	77	0	-6.778	-1.481
300	77	1	-6.802	-1.622
300	78	0	-6.802	-1.622
300	78	1	-6.809	-1.779
300	79	0	-6.809	-1.779
300	79	1	-6.803	-1.958
300	80	0	-6.803	-1.958
300	80	1	-6.784	-2.16
300	81	0	-6.784	-2.16
300	81	1	-6.752	-2.386
300	82	0	-6.752	-2.386
300	82	1	-6.707	-2.637
300	83	0	-6.707	-2.637
300	83	1	-6.647	-2.913
300	84	0	-6.647	-2.913
300	84	1	-6.573	-3.216
300	85	0	-6.573	-3.216
300	85	1	-6.484	-3.546
300	86	0	-6.484	-3.545
300	86	1	-6.38	-3.903
300	87	0	-6.38	-3.903
300	87	1	-6.259	-4.29
300	88	0	-6.259	-4.29
300	88	1	-6.123	-4.707
300	89	0	-6.123	-4.707
300	89	1	-5.969	-5.155
300	90	0	-5.969	-5.155
300	90	1	-5.797	-5.635
300	91	0	-5.797	-5.635
300	91	1	-5.608	-6.148
300	92	0	-5.608	-6.148
300	92	1	-5.4	-6.695
300	93	0	-5.4	-6.695
300	93	1	-5.173	-7.278
300	94	0	-5.173	-7.278
300	94	1	-4.926	-7.897
300	95	0	-5.121	-7.572
300	95	1	-4.791	-8.525
300	96	0	-4.791	-8.525
300	96	1	-4.421	-9.397
300	97	0	-4.421	-9.397
300	97	1	-4.06	-10.242
300	98	0	-4.06	-10.241
300	98	1	-3.69	-11.091
300	99	0	-3.69	-11.09
300	99	1	-3.301	-11.978

300	100	0	-3.302	-11.978
300	100	1	-2.883	-12.937
300	101	0	-2.884	-12.936
300	101	1	-2.417	-13.999
300	102	0	-1.806	-13.287
300	102	1	-2.453	-12.432
300	103	0	-2.451	-12.432
300	103	1	-2.902	-11.829
300	104	0	-2.902	-11.829
300	104	1	-3.278	-11.341
300	105	0	-3.278	-11.341
300	105	1	-3.689	-10.84
300	106	0	-3.597	-10.98
300	106	1	-3.921	-10.639
300	107	0	-3.921	-10.639
300	107	1	-4.189	-10.337
300	108	0	-4.189	-10.337
300	108	1	-4.434	-10.078
300	109	0	-4.434	-10.078
300	109	1	-4.657	-9.862
300	110	0	-4.657	-9.862
300	110	1	-4.858	-9.686
300	111	0	-4.858	-9.686
300	111	1	-5.038	-9.549
300	112	0	-5.038	-9.549
300	112	1	-5.199	-9.448
300	113	0	-5.199	-9.448
300	113	1	-5.342	-9.383
300	114	0	-5.342	-9.383
300	114	1	-5.467	-9.35
300	115	0	-5.467	-9.35
300	115	1	-5.576	-9.348
300	116	0	-5.576	-9.349
300	116	1	-5.67	-9.375
300	117	0	-5.67	-9.376
300	117	1	-5.75	-9.429
300	118	0	-5.75	-9.43
300	118	1	-5.817	-9.507
300	119	0	-5.817	-9.508
300	119	1	-5.873	-9.607
300	120	0	-5.873	-9.608
300	120	1	-5.919	-9.726
300	121	0	-5.919	-9.727
300	121	1	-5.956	-9.862
300	122	0	-5.956	-9.863
300	122	1	-5.987	-10.013
300	123	0	-5.987	-10.013
300	123	1	-6.011	-10.174
300	124	0	-6.011	-10.174
300	124	1	-6.032	-10.344
300	125	0	-6.032	-10.344

300	125	1	-6.05	-10.519
300	126	0	-6.05	-10.52
300	126	1	-6.068	-10.697
300	127	0	-6.055	-10.721
300	127	1	-6.094	-10.855
300	128	0	-6.094	-10.854
300	128	1	-6.056	-10.794
300	129	0	-6.056	-10.793
300	129	1	-6.043	-10.688
300	130	0	-6.044	-10.687
300	130	1	-6.058	-10.486
300	131	0	-6.058	-10.485
300	131	1	-6.095	-10.181
300	132	0	-6.095	-10.18
300	132	1	-6.138	-9.873
300	133	0	-6.138	-9.872
300	133	1	-6.183	-9.57
300	134	0	-6.183	-9.569
300	134	1	-6.227	-9.277
300	135	0	-6.227	-9.276
300	135	1	-6.266	-9.002
300	136	0	-6.266	-9.002
300	136	1	-6.296	-8.751
300	137	0	-6.296	-8.751
300	137	1	-6.314	-8.53
300	138	0	-6.315	-8.529
300	138	1	-6.318	-8.343
300	139	0	-6.318	-8.343
300	139	1	-6.304	-8.197
300	140	0	-6.305	-8.196
300	140	1	-6.27	-8.095

G-4

Stresses due to characteristic load combination
Description:
This listing consists of calculated elastic stresses for the upper face
and the lower face of the cross-section associatied with the selected elements.
Upper and lower face are defined by using the SECTFACE command.

Sort. Line No:	Element No:	X/L:	Upper Min:	Lower Min:
102	3	0	-12.365	-14.19
102	3	1	-12.513	-14.087
102	4	0	-12.513	-14.087
102	4	1	-12.638	-14.029
102	5	0	-12.638	-14.03
102	5	1	-12.743	-14.016
102	6	0	-12.742	-14.016
102	6	1	-12.828	-14.044
102	7	0	-12.827	-14.045
102	7	1	-12.895	-14.111
102	8	0	-12.895	-14.111
102	8	1	-12.945	-14.214
102	9	0	-12.945	-14.214
102	9	1	-12.981	-14.349
102	10	0	-12.981	-14.35
102	10	1	-13.004	-14.516
102	11	0	-13.004	-14.516
102	11	1	-13.015	-14.709
102	12	0	-13.015	-14.71
102	12	1	-13.016	-14.927
102	13	0	-13.016	-14.928
102	13	1	-13.01	-15.166
102	14	0	-13.01	-15.166
102	14	1	-13.002	-15.366
102	15	0	-13.002	-15.367
102	15	1	-12.999	-15.516
102	16	0	-12.999	-15.517
102	16	1	-12.892	-15.539
102	17	0	-12.892	-15.54
102	17	1	-12.776	-15.543
102	18	0	-12.776	-15.544
102	18	1	-12.664	-15.539
102	19	0	-12.663	-15.539
102	19	1	-12.557	-15.523
102	20	0	-12.541	-15.551
102	20	1	-12.473	-15.446
102	21	0	-12.473	-15.445
102	21	1	-12.405	-15.361
102	22	0	-12.405	-15.361
102	22	1	-12.337	-15.277

102	23	0	-12.337	-15.276
102	23	1	-12.268	-15.195
102	24	0	-12.268	-15.195
102	24	1	-12.196	-15.119
102	25	0	-12.196	-15.119
102	25	1	-12.12	-15.054
102	26	0	-12.12	-15.053
102	26	1	-12.037	-15
102	27	0	-12.037	-15
102	27	1	-11.946	-14.963
102	28	0	-11.946	-14.962
102	28	1	-11.846	-14.944
102	29	0	-11.846	-14.944
102	29	1	-11.735	-14.947
102	30	0	-11.735	-14.947
102	30	1	-11.611	-14.974
102	31	0	-11.611	-14.973
102	31	1	-11.474	-15.028
102	32	0	-11.474	-15.027
102	32	1	-11.321	-15.11
102	33	0	-11.321	-15.11
102	33	1	-11.152	-15.224
102	34	0	-11.152	-15.224
102	34	1	-10.965	-15.372
102	35	0	-10.965	-15.372
102	35	1	-10.759	-15.556
102	36	0	-10.759	-15.556
102	36	1	-10.534	-15.778
102	37	0	-10.534	-15.778
102	37	1	-10.286	-16.04
102	38	0	-10.287	-16.04
102	38	1	-10.017	-16.344
102	39	0	-10.017	-16.343
102	39	1	-9.724	-16.691
102	40	0	-10.005	-16.23
102	40	1	-9.368	-16.966
102	41	0	-9.368	-16.966
102	41	1	-8.876	-17.624
102	42	0	-8.876	-17.624
102	42	1	-8.414	-18.261
102	43	0	-8.414	-18.26
102	43	1	-7.931	-18.945
102	44	0	-7.931	-18.945
102	44	1	-7.368	-19.756
102	45	0	-7.425	-19.655
102	45	1	-7.811	-18.577
102	46	0	-7.81	-18.577
102	46	1	-8.15	-17.71
102	47	0	-8.15	-17.711
102	47	1	-8.474	-16.938
102	48	0	-8.474	-16.938

102	48	1	-8.804	-16.135
102	49	0	-8.724	-16.271
102	49	1	-9.038	-15.503
102	50	0	-9.038	-15.503
102	50	1	-9.344	-14.777
102	51	0	-9.344	-14.778
102	51	1	-9.631	-14.088
102	52	0	-9.631	-14.088
102	52	1	-9.877	-13.473
102	53	0	-9.877	-13.473
102	53	1	-10.132	-12.841
102	54	0	-10.132	-12.841
102	54	1	-10.369	-12.243
102	55	0	-10.369	-12.243
102	55	1	-10.588	-11.677
102	56	0	-10.588	-11.678
102	56	1	-10.789	-11.144
102	57	0	-10.789	-11.144
102	57	1	-10.974	-10.642
102	58	0	-10.974	-10.642
102	58	1	-11.142	-10.17
102	59	0	-11.142	-10.171
102	59	1	-11.294	-9.728
102	60	0	-11.294	-9.728
102	60	1	-11.431	-9.313
102	61	0	-11.431	-9.313
102	61	1	-11.553	-8.926
102	62	0	-11.553	-8.926
102	62	1	-11.669	-8.565
102	63	0	-11.669	-8.566
102	63	1	-11.838	-8.231
102	64	0	-11.838	-8.231
102	64	1	-11.987	-7.921
102	65	0	-11.986	-7.921
102	65	1	-12.114	-7.635
102	66	0	-12.114	-7.635
102	66	1	-12.215	-7.366
102	67	0	-12.215	-7.366
102	67	1	-12.297	-7.12
102	68	0	-12.297	-7.12
102	68	1	-12.358	-6.896
102	69	0	-12.358	-6.896
102	69	1	-12.4	-6.693
102	70	0	-12.4	-6.693
102	70	1	-12.421	-6.511
102	71	0	-12.421	-6.512
102	71	1	-12.424	-6.351
102	72	0	-12.417	-6.362
102	72	1	-12.504	-6.406
102	73	0	-12.504	-6.406
102	73	1	-12.57	-6.467

102	74	0	-12.57	-6.467
102	74	1	-12.617	-6.548
102	75	0	-12.617	-6.548
102	75	1	-12.644	-6.65
102	76	0	-12.644	-6.65
102	76	1	-12.651	-6.774
102	77	0	-12.651	-6.773
102	77	1	-12.638	-6.919
102	78	0	-12.638	-6.918
102	78	1	-12.599	-7.08
102	79	0	-12.599	-7.079
102	79	1	-12.539	-7.264
102	80	0	-12.539	-7.264
102	80	1	-12.458	-7.472
102	81	0	-12.458	-7.472
102	81	1	-12.357	-7.705
102	82	0	-12.357	-7.705
102	82	1	-12.234	-7.964
102	83	0	-12.234	-7.963
102	83	1	-12.126	-8.249
102	84	0	-12.126	-8.248
102	84	1	-12.047	-8.561
102	85	0	-12.047	-8.561
102	85	1	-11.953	-8.901
102	86	0	-11.953	-8.901
102	86	1	-11.842	-9.27
102	87	0	-11.842	-9.27
102	87	1	-11.715	-9.67
102	88	0	-11.715	-9.669
102	88	1	-11.571	-10.1
102	89	0	-11.571	-10.099
102	89	1	-11.409	-10.562
102	90	0	-11.41	-10.561
102	90	1	-11.23	-11.056
102	91	0	-11.23	-11.056
102	91	1	-11.032	-11.585
102	92	0	-11.032	-11.585
102	92	1	-10.815	-12.15
102	93	0	-10.815	-12.149
102	93	1	-10.579	-12.75
102	94	0	-10.579	-12.75
102	94	1	-10.322	-13.387
102	95	0	-10.517	-13.062
102	95	1	-10.176	-14.035
102	96	0	-10.175	-14.034
102	96	1	-9.794	-14.928
102	97	0	-9.794	-14.927
102	97	1	-9.422	-15.793
102	98	0	-9.422	-15.793
102	98	1	-9.04	-16.664
102	99	0	-9.04	-16.664

102	99	1	-8.639	-17.575
102	100	0	-8.639	-17.575
102	100	1	-8.208	-18.557
102	101	0	-8.208	-18.557
102	101	1	-7.728	-19.644
102	102	0	-7.198	-18.769
102	102	1	-7.847	-17.907
102	103	0	-7.846	-17.907
102	103	1	-8.3	-17.299
102	104	0	-8.3	-17.299
102	104	1	-8.679	-16.805
102	105	0	-8.679	-16.805
102	105	1	-9.093	-16.299
102	106	0	-9.002	-16.439
102	106	1	-9.328	-16.092
102	107	0	-9.328	-16.093
102	107	1	-9.599	-15.785
102	108	0	-9.599	-15.785
102	108	1	-9.847	-15.522
102	109	0	-9.847	-15.522
102	109	1	-10.072	-15.301
102	110	0	-10.072	-15.302
102	110	1	-10.275	-15.121
102	111	0	-10.275	-15.121
102	111	1	-10.458	-14.98
102	112	0	-10.458	-14.98
102	112	1	-10.621	-14.876
102	113	0	-10.621	-14.876
102	113	1	-10.766	-14.807
102	114	0	-10.766	-14.807
102	114	1	-10.893	-14.771
102	115	0	-10.893	-14.772
102	115	1	-11.003	-14.767
102	116	0	-11.003	-14.767
102	116	1	-11.099	-14.791
102	117	0	-11.099	-14.792
102	117	1	-11.18	-14.842
102	118	0	-11.18	-14.843
102	118	1	-11.249	-14.918
102	119	0	-11.249	-14.919
102	119	1	-11.306	-15.016
102	120	0	-11.306	-15.017
102	120	1	-11.353	-15.134
102	121	0	-11.353	-15.134
102	121	1	-11.417	-15.222
102	122	0	-11.417	-15.222
102	122	1	-11.45	-15.368
102	123	0	-11.45	-15.368
102	123	1	-11.477	-15.526
102	124	0	-11.477	-15.526
102	124	1	-11.499	-15.693

102	125	0	-11.499	-15.693
102	125	1	-11.518	-15.866
102	126	0	-11.518	-15.867
102	126	1	-11.537	-16.043
102	127	0	-11.524	-16.067
102	127	1	-11.563	-16.201
102	128	0	-11.563	-16.201
102	128	1	-11.525	-16.141
102	129	0	-11.525	-16.14
102	129	1	-11.511	-16.037
102	130	0	-11.511	-16.036
102	130	1	-11.525	-15.838
102	131	0	-11.525	-15.836
102	131	1	-11.559	-15.536
102	132	0	-11.56	-15.535
102	132	1	-11.6	-15.233
102	133	0	-11.6	-15.232
102	133	1	-11.643	-14.934
102	134	0	-11.643	-14.933
102	134	1	-11.683	-14.648
102	135	0	-11.683	-14.647
102	135	1	-11.718	-14.38
102	136	0	-11.718	-14.379
102	136	1	-11.744	-14.137
102	137	0	-11.745	-14.136
102	137	1	-11.758	-13.924
102	138	0	-11.758	-13.924
102	138	1	-11.757	-13.748
102	139	0	-11.757	-13.747
102	139	1	-11.737	-13.612
102	140	0	-11.737	-13.611
102	140	1	-11.696	-13.522

G-5

Stresses due to Quasi-permanent load combination
Description:
This listing consists of calculated elastic stresses for the upper face
and the lower face of the cross-section associatied with the selected elements.
Upper and lower face are defined by using the SECTFACE command.

Sort. Line No:	Element No:	X/L:	Upper Min:	Lower Min:
104	3	0	-10.539	-11.451
104	3	1	-10.767	-11.12
104	4	0	-10.767	-11.12
104	4	1	-10.973	-10.832
104	5	0	-10.973	-10.832
104	5	1	-11.158	-10.587
104	6	0	-11.158	-10.587
104	6	1	-11.32	-10.384
104	7	0	-11.32	-10.384
104	7	1	-11.463	-10.221
104	8	0	-11.463	-10.221
104	8	1	-11.585	-10.096
104	9	0	-11.585	-10.096
104	9	1	-11.689	-10.009
104	10	0	-11.689	-10.009
104	10	1	-11.774	-9.957
104	11	0	-11.774	-9.957
104	11	1	-11.842	-9.94
104	12	0	-11.842	-9.94
104	12	1	-11.893	-9.955
104	13	0	-11.893	-9.955
104	13	1	-11.929	-10.001
104	14	0	-11.929	-10.001
104	14	1	-11.953	-10.05
104	15	0	-11.953	-10.05
104	15	1	-11.968	-10.138
104	16	0	-11.968	-10.139
104	16	1	-11.919	-10.162
104	17	0	-11.919	-10.163
104	17	1	-11.854	-10.166
104	18	0	-11.854	-10.166
104	18	1	-11.779	-10.161
104	19	0	-11.779	-10.161
104	19	1	-11.695	-10.183
104	20	0	-11.688	-10.197
104	20	1	-11.611	-10.22
104	21	0	-11.611	-10.22
104	21	1	-11.523	-10.276
104	22	0	-11.523	-10.276
104	22	1	-11.423	-10.352
104	23	0	-11.423	-10.352
104	23	1	-11.312	-10.452

104	24	0	-11.312	-10.452
104	24	1	-11.187	-10.575
104	25	0	-11.187	-10.575
104	25	1	-11.048	-10.725
104	26	0	-11.048	-10.725
104	26	1	-10.894	-10.902
104	27	0	-10.894	-10.902
104	27	1	-10.725	-11.108
104	28	0	-10.725	-11.108
104	28	1	-10.54	-11.344
104	29	0	-10.54	-11.344
104	29	1	-10.338	-11.611
104	30	0	-10.338	-11.611
104	30	1	-10.119	-11.911
104	31	0	-10.119	-11.911
104	31	1	-9.88	-12.245
104	32	0	-9.88	-12.245
104	32	1	-9.623	-12.615
104	33	0	-9.623	-12.615
104	33	1	-9.346	-13.021
104	34	0	-9.346	-13.021
104	34	1	-9.048	-13.464
104	35	0	-9.048	-13.464
104	35	1	-8.73	-13.946
104	36	0	-8.73	-13.946
104	36	1	-8.389	-14.468
104	37	0	-8.389	-14.468
104	37	1	-8.027	-15.031
104	38	0	-8.027	-15.031
104	38	1	-7.642	-15.635
104	39	0	-7.642	-15.635
104	39	1	-7.233	-16.283
104	40	0	-7.363	-16.047
104	40	1	-6.772	-16.912
104	41	0	-6.772	-16.912
104	41	1	-6.242	-17.759
104	42	0	-6.242	-17.759
104	42	1	-5.714	-18.615
104	43	0	-5.714	-18.615
104	43	1	-5.162	-19.516
104	44	0	-5.162	-19.516
104	44	1	-4.556	-20.499
104	45	0	-4.582	-20.452
104	45	1	-5.111	-19.315
104	46	0	-5.111	-19.315
104	46	1	-5.605	-18.306
104	47	0	-5.605	-18.306
104	47	1	-6.073	-17.366
104	48	0	-6.073	-17.366
104	48	1	-6.529	-16.431
104	49	0	-6.49	-16.5

104	49	1	-6.931	-15.604
104	50	0	-6.931	-15.604
104	50	1	-7.356	-14.751
104	51	0	-7.356	-14.751
104	51	1	-7.76	-13.936
104	52	0	-7.76	-13.936
104	52	1	-8.142	-13.16
104	53	0	-8.142	-13.16
104	53	1	-8.503	-12.422
104	54	0	-8.503	-12.422
104	54	1	-8.843	-11.722
104	55	0	-8.843	-11.722
104	55	1	-9.163	-11.059
104	56	0	-9.163	-11.059
104	56	1	-9.462	-10.432
104	57	0	-9.462	-10.432
104	57	1	-9.742	-9.842
104	58	0	-9.742	-9.842
104	58	1	-10.003	-9.287
104	59	0	-10.003	-9.287
104	59	1	-10.244	-8.768
104	60	0	-10.244	-8.768
104	60	1	-10.466	-8.283
104	61	0	-10.466	-8.283
104	61	1	-10.669	-7.833
104	62	0	-10.669	-7.833
104	62	1	-10.854	-7.416
104	63	0	-10.854	-7.416
104	63	1	-11.02	-7.033
104	64	0	-11.02	-7.033
104	64	1	-11.167	-6.683
104	65	0	-11.167	-6.682
104	65	1	-11.297	-6.365
104	66	0	-11.297	-6.365
104	66	1	-11.405	-6.077
104	67	0	-11.405	-6.077
104	67	1	-11.496	-5.821
104	68	0	-11.496	-5.821
104	68	1	-11.569	-5.596
104	69	0	-11.569	-5.596
104	69	1	-11.625	-5.403
104	70	0	-11.625	-5.403
104	70	1	-11.663	-5.242
104	71	0	-11.663	-5.242
104	71	1	-11.685	-5.111
104	72	0	-11.682	-5.117
104	72	1	-11.737	-5.11
104	73	0	-11.737	-5.11
104	73	1	-11.776	-5.133
104	74	0	-11.776	-5.133
104	74	1	-11.798	-5.186

104	75	0	-11.798	-5.186
104	75	1	-11.803	-5.271
104	76	0	-11.803	-5.271
104	76	1	-11.79	-5.387
104	77	0	-11.79	-5.387
104	77	1	-11.76	-5.535
104	78	0	-11.76	-5.535
104	78	1	-11.709	-5.711
104	79	0	-11.709	-5.711
104	79	1	-11.64	-5.92
104	80	0	-11.64	-5.92
104	80	1	-11.553	-6.162
104	81	0	-11.553	-6.162
104	81	1	-11.448	-6.436
104	82	0	-11.448	-6.436
104	82	1	-11.324	-6.744
104	83	0	-11.324	-6.744
104	83	1	-11.181	-7.086
104	84	0	-11.181	-7.086
104	84	1	-11.02	-7.461
104	85	0	-11.02	-7.461
104	85	1	-10.84	-7.872
104	86	0	-10.84	-7.872
104	86	1	-10.64	-8.317
104	87	0	-10.64	-8.317
104	87	1	-10.42	-8.798
104	88	0	-10.42	-8.798
104	88	1	-10.181	-9.315
104	89	0	-10.181	-9.315
104	89	1	-9.921	-9.869
104	90	0	-9.921	-9.869
104	90	1	-9.641	-10.459
104	91	0	-9.641	-10.459
104	91	1	-9.341	-11.088
104	92	0	-9.341	-11.088
104	92	1	-9.02	-11.754
104	93	0	-9.02	-11.754
104	93	1	-8.677	-12.459
104	94	0	-8.677	-12.459
104	94	1	-8.313	-13.204
104	95	0	-8.405	-13.038
104	95	1	-7.987	-13.972
104	96	0	-7.987	-13.972
104	96	1	-7.539	-14.887
104	97	0	-7.539	-14.887
104	97	1	-7.083	-15.808
104	98	0	-7.083	-15.808
104	98	1	-6.611	-16.752
104	99	0	-6.611	-16.752
104	99	1	-6.116	-17.737
104	100	0	-6.116	-17.737

104	100	1	-5.594	-18.779
104	101	0	-5.594	-18.779
104	101	1	-5.035	-19.895
104	102	0	-5.054	-19.862
104	102	1	-5.686	-18.882
104	103	0	-5.686	-18.882
104	103	1	-6.21	-18.05
104	104	0	-6.21	-18.05
104	104	1	-6.679	-17.298
104	105	0	-6.679	-17.298
104	105	1	-7.15	-16.56
104	106	0	-7.111	-16.632
104	106	1	-7.53	-15.996
104	107	0	-7.53	-15.996
104	107	1	-7.911	-15.401
104	108	0	-7.911	-15.401
104	108	1	-8.267	-14.848
104	109	0	-8.267	-14.848
104	109	1	-8.601	-14.338
104	110	0	-8.601	-14.338
104	110	1	-8.912	-13.869
104	111	0	-8.912	-13.869
104	111	1	-9.202	-13.441
104	112	0	-9.202	-13.441
104	112	1	-9.469	-13.051
104	113	0	-9.469	-13.051
104	113	1	-9.716	-12.7
104	114	0	-9.716	-12.7
104	114	1	-9.943	-12.386
104	115	0	-9.943	-12.386
104	115	1	-10.15	-12.109
104	116	0	-10.15	-12.109
104	116	1	-10.338	-11.867
104	117	0	-10.338	-11.867
104	117	1	-10.507	-11.659
104	118	0	-10.507	-11.659
104	118	1	-10.659	-11.484
104	119	0	-10.659	-11.484
104	119	1	-10.793	-11.34
104	120	0	-10.793	-11.34
104	120	1	-10.91	-11.228
104	121	0	-10.91	-11.228
104	121	1	-11.012	-11.145
104	122	0	-11.012	-11.145
104	122	1	-11.099	-11.09
104	123	0	-11.099	-11.09
104	123	1	-11.171	-11.062
104	124	0	-11.171	-11.062
104	124	1	-11.229	-11.06
104	125	0	-11.229	-11.06
104	125	1	-11.274	-11.081

104	126	0	-11.274	-11.081
104	126	1	-11.307	-11.126
104	127	0	-11.301	-11.137
104	127	1	-11.333	-11.182
104	128	0	-11.333	-11.182
104	128	1	-11.315	-11.153
104	129	0	-11.315	-11.153
104	129	1	-11.297	-11.123
104	130	0	-11.297	-11.123
104	130	1	-11.281	-11.067
104	131	0	-11.281	-11.067
104	131	1	-11.265	-10.98
104	132	0	-11.265	-10.98
104	132	1	-11.241	-10.913
104	133	0	-11.241	-10.913
104	133	1	-11.207	-10.868
104	134	0	-11.207	-10.868
104	134	1	-11.16	-10.848
104	135	0	-11.16	-10.848
104	135	1	-11.1	-10.858
104	136	0	-11.1	-10.858
104	136	1	-11.024	-10.9
104	137	0	-11.024	-10.9
104	137	1	-10.93	-10.976
104	138	0	-10.93	-10.976
104	138	1	-10.818	-11.09
104	139	0	-10.818	-11.09
104	139	1	-10.685	-11.245
104	140	0	-10.685	-11.245
104	140	1	-10.531	-11.443

Attachment
G-6

Deflection control

Cross-sectional properties

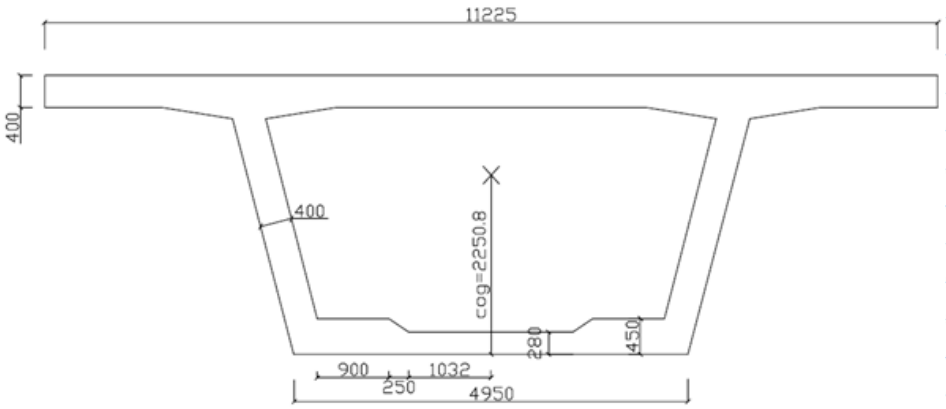

$H := 3500\ mm$ Height of box-girder

$h_{cog} := 2250.8\ mm$ Distance from bottom to CoG

$b_{top} := 11225\ mm$ Width of top flange

$t_{top} := 400\ mm$ Thickness of top flange

$b_{bottom} := 4950\ mm$ Width of bottom flange

$$t_{bottom} := \frac{0.9\ m \cdot 0.45\ m + 0.25\ m \cdot \left(\frac{0.45\ m - 0.28\ m}{2}\right) + 1.032\ m \cdot 0.28\ m}{0.9\ m + 0.25\ m + 1.032\ m}$$

$t_{bottom} = 327.777\ mm$ Average thickness of bottom flange

$t_{web} := 400\ mm$ Thickness of web

$I_{c.x} := 14.92\ m^4$ Second moment of area about x-axis

Concrete properties

$f_{ck} := 45\ MPa$ Characteristic compressive strength

$\alpha_{cc} := 0.85$ Factor

$\gamma_c := 1.5$ Safety factor

$f_{cd} := \alpha_{cc} \cdot \frac{f_{ck}}{\gamma_c} = 25.5\ MPa$ Design value of compressive strength

$f_{ctm} := 3.8\ MPa$ Mean value of axial tensile strength

$E_{cm} := 36\ GPa$ Secant modulus of elasticity of concrete

$A_c := 8.82\ m^2$

Created with PTC Mathcad Express. See www.mathcad.com for more information.

Attachment
G-6

Deflection control

Steel properties

$f_{yk} := 500\ MPa$ Characteristic yield strength

$\gamma_s := 1.15$ Safety factor

$f_{yd} := \frac{f_{yk}}{\gamma_s} = (4.348 \cdot 10^8)\ Pa$ Design yield strength

Prestressing tendon

$A_p := 2100\ mm^2$ Area pr tendon

$A_{p.bottom} := 8 \cdot A_p = 0.0168\ m^2$ Total area of tendons in bottom flange

$A_{p.top} := 14 \cdot A_p = 0.0294\ m^2$ Total area of tendons in top flange

$A_{p.web} := 4 \cdot A_p = 0.008\ m^2$ Total area of tendons in web

$A_p := A_{p.top} + A_{p.bottom} + A_{p.web} = 0.0546\ m^2$ Total tendon area (top and bottom flange +web)

$f_{pk} := 1860\ MPa$ Characteristic tensile strength

$f_{p0.1k} := 1640\ MPa$ Characteristic 0.1% proof-stress

$E_p := 195\ GPa$ Elastic modulus

$f_{pd} := \frac{f_{p0.1k}}{\gamma_s} = (1.426 \cdot 10^3)\ MPa$

$f_{ctk.0.05} := 2.7\ MPa$

$Ø_{duct} := 80\ mm$ Outer diameter of duct

$C_{nom.UF} := 150\ mm$

$C_{nom.LF} := C_{nom.UF}$

$d_{duct} := H - C_{nom.UF} - \frac{Ø_{duct}}{2} = 3.31\ m$

$\sigma_{p.max} := min(0.8\ f_{pk}, 0.9\ f_{p0.1k}) = 1476\ MPa$

$\sigma_{pm0} := min(0.75\ f_{pk}, 0.85\ f_{p0.1k}) = 1394\ MPa$

$P_{max.1} := A_{p.web} \cdot \sigma_{p.max} = 12398.4\ kN$

Prestressing force

$P_{max} := A_p \cdot \sigma_{p.max} = 80589.6\ kN$ $P_{max.2} := (A_{p.top} + A_{p.bottom}) \cdot \sigma_{p.max} = 68191.2\ kN$

$0.95 \cdot f_{p0.1k} \cdot A_p = 85066.8\ kN$

$P_s := P_{max} \cdot 0.75 = 60442.2\ kN$

Created with PTC Mathcad Express. See www.mathcad.com for more information.

Deflection control

$P_{m0} := A_p \cdot \sigma_{pm0} = 76112.4\ kN$

$P_t := P_{m0}$

$P_0 := P_{max}$

ANALYSIS OF CRACKED SECTION

$y_{b.cog} := 2250.8\ mm$ Distance from bottom to cog

$y_{t.cog} := H - y_{b.cog} = 1249.2\ mm$ Distance from top to cog

$e_1 := 1.06\ m$ Distance from upper prestress to CoG

$e_2 := 2.06\ m$ Distance from lower prestress to CoG

Transformed cross-section

$\eta_p := \frac{E_p}{E_{cm}} = 5.417$ Modular ratio of prestressing steel

$A_t := A_c + (\eta_p - 1)\ A_p = 9.061\ m^2$ Transformed cross-section

$y_{span} := \frac{(\eta_p - 1)\ A_p \cdot e_2}{A_t} = 54.824\ mm$ Distance from transformed CoG to regular CoG

$y_{support} := \frac{(\eta_p - 1)\ A_p \cdot e_1}{A_t} = 28.21\ mm$ Distance from transformed CoG to regular CoG

$y_{t.span.cog} := y_{t.cog} + y_{span} = (1.304 \cdot 10^3)\ mm$ Distance from top to transformed CoG (Span)

$y_{b.span.cog} := y_{b.cog} - y_{span} = (2.196 \cdot 10^3)\ mm$ Distance from bottom to transformed CoG (Span)

$y_{t.support.cog} := y_{t.cog} - y_{support} = (1.221 \cdot 10^3)\ mm$ Distance from top to transformed CoG (Sup.)

$y_{b.support.cog} := y_{b.cog} + y_{support} = (2.279 \cdot 10^3)\ mm$ Distance from bottom to transformed CoG (Sup.)

$I_{t.span} := I_{c.x} + A_c \cdot y_{span}^2 + (\eta_p - 1)\ A_p \cdot (e_2 - y_{span})^2 = 15.916\ m^4$

$I_{t.support} := I_{c.x} + A_c \cdot y_{support}^2 + (\eta_p - 1)\ A_p \cdot (e_1 - y_{support})^2 = 15.184\ m^4$

Created with PTC Mathcad Express. See www.mathcad.com for more information.

Deflection

$\delta_{SW.NF} := 18.784\ mm$ Largest deflection due to SW from NovaFrame analysis, found at span 2-3

$Q_{LM1} := 600\ kN$

$q_{LM1} := 33.54\ \frac{kN}{m}$

$L_2 := 57\ m$

$\rho_c := 26\ \frac{kN}{m^3}$

$EI_{span} := E_{cm} \cdot I_{t.span} = \left(5.73 \cdot 10^8\right)\ kN \cdot m^2$

$EI_{support} := E_{cm} \cdot I_{t.support} = \left(5.466 \cdot 10^8\right)\ kN \cdot m^2$

$\delta_{allow.N400} := \frac{L_2}{350} = 162.857\ mm$

UNCRACKED SECTION:

Statically determinate system

Checking deflections due to traffic load

$\delta_{QLM1} := \frac{Q_{LM1} \cdot {L_2}^3}{48 \cdot EI_{span}} = 4.04\ mm$

$\delta_{qLM1} := \frac{5}{384} \cdot \frac{q_{LM1} \cdot {L_2}^4}{EI_{span}} = 8.046\ mm$

$\delta_{TR} := \delta_{QLM1} + \delta_{qLM1} = 12.086\ mm$ $\delta_{TR} < \delta_{allow.N400}$ -> OK!

Deflection due to traffic with selfweight:

$\delta_{SW.23} := \frac{5}{384} \cdot \frac{\rho_c \cdot A_c \cdot {L_2}^4}{E_{cm} \cdot I_{t.span}} = 55.01\ mm$

$\delta_{tot} := \delta_{TR} + \delta_{SW.23} = 67.096\ mm$ $\delta_{tot} < \delta_{allow.N400}$ -> OK!

Checking deflections due to traffic load (statically indeterminate system):

$I_{t.span} := I_{c.x} + A_c \cdot {y_{span}}^2 + \left(\eta_p - 1\right) A_p \cdot \left(e_2 - y_{span}\right)^2 = 15.916\ m^4$

$\delta_{QLM1} := \frac{Q_{LM1} \cdot {L_2}^3}{192 \cdot EI_{span}} = 1.01\ mm$

Created with PTC Mathcad Express. See www.mathcad.com for more information.

Attachment
G-6

Deflection control

$$\delta_{qLM1} := \frac{1}{384} \cdot \frac{q_{LM1} \cdot L_2^{\,4}}{EI_{span}} = 1.609\ mm$$

$$\delta_{TR} := \delta_{QLM1} + \delta_{qLM1} = 2.619\ mm \qquad \delta_{TR} < \delta_{allow.N400}$$ -> OK!

$$\delta_{SW.23} := \frac{1 \cdot \rho_c \cdot A_c \cdot L_2^{\,4}}{384 \cdot E_{cm} \cdot I_{t.span}} = 11.002\ mm$$

$$\delta_{tot} := \delta_{TR} + \delta_{SW.23} = 13.621\ mm \qquad \delta_{tot} < \delta_{allow.N400}$$ -> OK!

Created with PTC Mathcad Express. See www.mathcad.com for more information.